12-4-2018

Empirical Validation and Comparison of the Hybrid Coordinate Ocean Model (HYCOM) Between the Gulf of Mexico and the Tongue of the Ocean

Cynthia A. Cleveland
Nova Southeastern University, cynthia.cleveland@gmail.com

Thesis of
Cynthia A. Cleveland

Submitted in Partial Fulfillment of the Requirements for the Degree of

Master of Science

M.S. Marine Environmental Sciences

M.S. Coastal Zone Management

Nova Southeastern University
Halmos College of Natural Sciences and Oceanography

December 2018

Approved:
Thesis Committee

Major Professor: Matthew Johnston, Ph.D.

Committee Member: Bernard Riegl, Ph.D.

Committee Member: Adam Akif

HALMOS COLLEGE OF NATURAL SCIENCES AND OCEANOGRAPHY

EMPIRICAL VALIDATION AND COMPARISON OF THE HYBRID COORDINATE OCEAN MODEL (HYCOM) BETWEEN THE GULF OF MEXICO AND THE TONGUE OF THE OCEAN

By:

Cynthia A. Cleveland

Submitted to the Faculty of
Halmos College of Natural Sciences and Oceanography
In partial fulfillment of the requirements for
the degree of Master of Science with specialties in:

Marine Environmental Sciences and Coastal Zone Management

Nova Southeastern University

December 2018

List of Tables

List of Figures

Table of Contents

Abstract

Ocean models are increasingly able to synthesize a large temporal domain with fine spatial resolution. With this increase in functionality and availability, ocean models are in high demand by researchers, establishing a critical need for validating a model's ability to represent interior ocean dynamics. Satellite measurements are typically used for validation, however these measurements are limited to the upper layers of the ocean and therefore satellite measurements of sea surface height and sea surface temperature are the most validated output parameters of three-dimensional ocean models. Unfortunately there is a paucity of model validation studies for the interior ocean. This study fills a knowledge gap by contrasting model data from the Hybrid Coordinate Ocean Model (HYCOM) for the interior ocean in the Tongue of the Ocean (TOTO), Bahamas and the Gulf of Mexico (GoM) against observational (i.e., *in situ*) data collected in both locations. Conductivity temperature and depth (CTD) data in the GoM were collected during five research cruises by the DEEPEND Consortium between May of 2015 and May 2017. These data were collected as part of the investigation into the impact of oil spills on faunal communities in deep water of the GoM. CTD and expendable CTD (XCTD) data in the TOTO were collected by the Naval Undersea Warfare Center (NUWC) detachment Atlantic Undersea Test and Evaluation Center (AUTEC) in support of U.S. Navy acoustic testing between 1997 and 2017 to characterize the sound velocity profile of the water column. The global 1/12° HYCOM configuration (GLBu0.08) was found to be a better fit in the upper 400 and 250 meters of the TOTO for temperature and salinity, respectively, than the GoM 1/25° HYCOM configuration (GOMI0.04 1/25°) fit the GoM *in situ* data for the same depths. The GoM 1/25° HYCOM configuration (GOMI0.04 1/25°) provided a better fit in the GoM for depths of 500 and 300 meters and deeper for temperature and salinity, respectively, than the global 1/12° HYCOM configuration (GLBu0.08) fit the TOTO *in situ* data at the same depths. A comprehensive comparison of the vertical profile between the model and observational data for each of the regions of interest provides insight into using HYCOM forecast data for future applications.

Keywords: HYCOM, Model Validation, Tongue of the Ocean, AUTEC, Gulf of Mexico, DEEPEND Consortium

1.0 Introduction

A near real-time forecast of the ocean's physical characteristics (i.e., geostrophic water flow, salinity, temperature, etc.) is invaluable for a wide range of oceanographic studies. Insight into these physical characteristics provides oceanographers and biologists, for example, with information to assess potential oceanic distribution of contaminates, model connectivity of native and invasive species, predict El Nino Southern Oscillation events, and project future levels of ocean acidification (Liu et al., 2001; Luo et al., 2008; Steinacher et al., 2009; Robinson et al., 2011).

An accurate picture of the physical ocean environment can be obtained through a variety of resources, but each has its limitations. For example, satellite imagery can provide empirical measurements of the ocean's surface characteristics at a specific location and for a point in time, but cannot acquire data for the entire earth contemporaneously. Satellite measurements of reflectance are also limited to the upper layers of the ocean due to attenuation of light in deep water (Kantha & Clayson, 2000) and satellites cannot measure temperature at depth. On the other hand, empirical measurements from buoys, floats, and conductivity temperature and depth (CTD) sensors provide accurate and instantaneous information regarding interior ocean (i.e., the portion of the ocean which excludes the surface mixing layer and boundaries) dynamics, but are limited in horizontal coverage and are only able to capture a relatively short time series (Chassignet et al., 2006; Kara & Hurlburt, 2006; Chassignet et al., 2007; Sandvik, et al., 2016). Obtaining empirical measurements is optimal, but due to the cost of collection, limited spatial and temporal scope, field measurements do not lend themselves to studies and experiments that require full ocean coverage at a fine scale, such as biophysical modeling (Kantha & Clayson, 2000).

One solution to the limitations of relying on *in situ* ocean measurements is the use of synthetic ocean models. Ocean models utilize atmospheric forcing algorithms to synthesize complete, near real-time physical ocean data for a region of interest, in addition to the ability to produce forecasts and hindcasts. While these data are typically of high spatial and temporal resolution, it is important that ocean models make accurate predictions

in order to be a reliable information source regarding ocean dynamics (Kara & Hurlburt, 2006). By their nature however data derived from numerical models are estimates and therefore have an associated amount of error introduced by atmospheric forcing conditions, resolution, and finite spatial precision, for example (Kantha & Clayson, 2000; Sandvik et al., 2016). By characterizing this error, the value of a model for a given situation can be determined and perhaps corrected for to increase accuracy of the model output.

1.1 Types/Examples of Ocean Models

Bryan (1969) formulated the first numerical comprehensive ocean model in the late 1960's for studying ocean circulation while integrating irregular coastlines and variable bottom topography (Kantha & Clayson, 2000). This model was the first suitable for global simulations, yet constraints in available computing power limited it to regional applications (Semtner, 1986). Since that time, advances in computation have given way to Ocean General Circulation Models (OGCM) as important tools in the field of ocean dynamics. OGCMs integrate the environmental factors which influence the general circulation of the ocean and have been utilized to study various physical scenarios, such as thermohaline circulation, eddy turbulence, and heat flux (Madec et al., 1997).

Ocean models can be generally classified by the type of vertical coordinate system they utilize: isopycnal, z-level, and sigma level. Isopycnal models delineate layers based on water density (i.e., isopycnals) and are best suited for the deep stratified ocean because mixing occurs primarily along and not across isopcynals in the deep ocean (Kantha & Clayson, 2000). In the mixed layer (0-200 m), z-levels are the best coordinate choice as they provide high vertical resolution by using constant fixed depths. In unstratified or shallow coastal regions, sigma levels are the best choice for a coordinate layer as they follow the terrain (Chassignet et al., 2003; Wallcraft et al., 2005; Chassignet et al., 2006; Chassignet et al., 2007).

Many OGCMs have been developed which utilize one of these vertical coordinate systems, such as the Regional Ocean Modeling System (ROMS), which utilizes topography following (i.e., sigma) coordinates, and the Miami Isopycnic Coordinate Ocean Model (MICOM), which is isopycnal (Bleck et al., 1995; Shchepetkin & McWilliams,

2005). HYCOM, the Hybrid Coordinate Ocean Model, was developed to maintain many of the properties of the MICOM while improving on it vertical coordinate selection. This ability allows the model to be optimized for different portions of the ocean including shallow coastal regions, the stratified open ocean, or the mixed layers (Castellanos et al., 2016). The global HYCOM is publicly available from 1992 to present at a 1/12° spatial resolution and is divided into multiple experiments. The HYCOM is also available at finer spatial resolutions for regional and basin configurations (Additional information can be found in Sections 2.1 and 3.1.1).

1.2 Model Validation and Assimilation

As an ocean circulation model is developed, designers take care in the application of the theory and equations utilized, but tend not to validate the model outputs with observational data as part of the initial design process. This responsibility typically falls back to the end user, as he or she is most interested in the quality of the model output (Dee, 1995). A typical approach to quantitatively evaluating an ocean model's performance in the ocean interior, from a user perspective, is to compare the model outputs with unassimilated observational data from expendable bathythermograph (XBT), CTD and Argo floats at a given spatial-temporal location (Chassignet et al., 2006; Kara & Hurlburt 2006; She et al., 2006; Chassignet et al., 2007; Castellanos et al., 2016). Understandably, the goal of end user validation is to determine a model's accuracy in its given application (Dee, 1995). Due to an overall deficiency in observational data of quality and duration however most ocean models have not been thoroughly evaluated for accuracy against *in situ* measurements (Kara & Hurlbert, 2006; She et al., 2006), especially in the deep ocean. What observational data is available is concentrated at the ocean surface, therefore sea surface height and sea surface temperature are the most validated model outputs for 3D ocean models (She et al., 2006)

Ocean models are estimates of true ocean conditions and therefore are subject to atmospheric forcing errors or imperfect parameterizations of physical processes, which may cause the model to deviate from the actual ocean conditions during a forecast (Kantha & Clayson, 2000). Developers of some ocean models, such as the HYCOM, attempt to

integrate primitive model validation into their predictive algorithms, producing 'assimilated models'. An assimilated model is one in which observational data is incorporated into the model to perform a real-time correction of the model. Data assimilation is a method of combining observed data taken from different locations and different points in time with that produced by the model to yield the best estimation of the true state of the ocean throughout the model domain. Assimilated models are generally thought to be more accurate than unassimilated models, because even if a model could parameterize the ocean's physical processes correctly, it would be unable to correctly account for the nature of instability processes (Kantha & Clayson, 2000).

1.3 Study Motivation and Purpose

As computational capacity increases, ocean models are increasingly able to synthesize larger domains with increased spatial resolution, establishing a need for further model versus *in situ* data comparison studies to characterize a model's ability to represent ocean dynamics (Castellanos et al., 2016). Given the lack of model validation studies for the interior ocean, the purpose of this study was to validate HYCOM data against unassimilated (i.e., not integrated into HYCOM) CTD and expendable CTD (XCTD) data sets collected *in situ* by two different organizations, the Deep-Pelagic Nekton Dynamics of the Gulf of Mexico Consortium (DEEPEND) and the Naval Undersea Warfare Center (NUWC) detachment Atlantic Undersea Test and Evaluation Center (NUWC det. AUTEC), in the GoM and Tongue of the Ocean (TOTO), respectively. In addition to the validation performed, a correction factor was formulated that can be applied to correct the HYCOM for applications in each region. Each organization has a vested interest in the validation of the HYCOM for their respective experiments and operations. Validation of the model in the GoM provides the DEEPEND Consortium with an accurate representation of the physical oceanographic characteristics which will aid community analysis of deep pelagic fauna. Validation of the HYCOM in the TOTO has implications for the NUWC det. AUTEC, improving predictions of the sound velocity profile and increasing in-water accuracy during Navy operations. The results of this study can also be used by other organizations which conduct experiments in the GoM and TOTO that may use HYCOM data.

2.0 Background

2.1 The Hybrid Coordinate Ocean Model

The HYCOM is the basis for the Global Ocean Forecast System (GOFS) and provides a near real time, three-dimensional assimilated model of the water conditions with global, basin and regional resolution. The present horizontal resolution of water conditions for the global HYCOM is 1/12°, while a 1/25° horizontal resolution global model is scheduled for operation in 2018. Basin-scale resolution can be as fine as 1/50°, while regional configurations have been developed to a horizontal resolution as fine as 1/100° (Chassignet & Wallcraft, 2016). For broad application throughout Earth's oceans, the HYCOM combines the three vertical coordinate systems and smoothly transitions as determined by a hybrid vertical coordinate generator, a decision made at each time iteration (Chassignet et. al., 2003; Chassignet et al., 2006; Chassignet et al., 2007). This unique hybridization extends the range of previous OGCMs and allows the HYCOM to achieve the optimum simulation of open-ocean and coastal circulation features (Chassignet et al., 2009).

The isopycnal coordinate model is the default for HYCOM. In areas where isopycnals provide diminished vertical resolution, HYCOM allows for deviation of the coordinate surface by identifying grid points that do not lie within their reference isopycnal layer. The model then attempts to move the point vertically to the appropriate reference isopycnal. Constraints are in place to prohibit the crowding of points in shallow water and keep the grid points at a fixed depth (Chassignet et al., 2007; HYCOM 2017b). HYCOM uses atmospheric forcing conditions provided by empirically-derived surface wind stress, air temperature, specific humidity, shortwave radiation and longwave radiation (Chassignet, et al., 2006; Chassignet, et al., 2007). The Navy Coupled Ocean Data Assimilation (NCODA) is responsible for assimilating these observational data from satellites, ships, buoys, XBTs, CTDs, gliders and ARGO floats into the HYCOM to predict ocean dynamics and characterize mesoscale variability (Chassignet, et al., 2006; Chassignet, et al., 2007; Kelly et al., 2007; HYCOM, 2017b; U.S. Naval Research Laboratory, 2017).

2.2 The DEEPEND Consortium and the GoM

The DEEPEND Consortium is a member of the Gulf of Mexico Research Initiative, the latter whose mission is to investigate the impact of oil spills on GoM ecosystems in addition to expanding the knowledge of the GoM in order to increase preparedness for future oil spills. (Gulf of Mexico Research Initiative, 2013). The DEEPEND Consortium's goal is to characterize and establish baseline conditions for the pelagic ecosystems in the northern GoM so that anthropogenic and natural changes over time can be detected and monitored (DEEPEND, 2017a). In prior DEEPEND work (Johnston et al., in review), waters of the GoM were classified into three separate categories: 1) Gulf Common Water (GCW), described by cooler water (approximately 5°C to 25°C, <1000m) where salinity ranges between 34.9 and 36.5 PSU, 2) Loop Current Origin Water (LCOW), which is warm (6°C to 30°C) to a depth of approximately 1000 meters with a higher salinity maximum between 19°C and 26°C, and 3) mixed waters (MIX), which are frontal regions of the LC and a mixture of LCOW and GCW with a temperature range between 5°C to 30°C and a salinity range between 34.9 and 37 PSU (Johnston et al., in review). As these mesoscale features in the GoM may dramatically impact the native biology, understanding ocean dynamics will help DEEPEND assess their influence on deep water faunal communities (DEEPEND, 2017b). DEEPEND relies upon GoM HYCOM model data for many phases of their work, therefore validating HYCOM against empirical measurements is valuable in understanding discrepancies between HYCOM model and *in situ* ocean conditions.

2.3 Atlantic Undersea Test and Evaluation Center and the TOTO

The NUWC det. AUTEC is located on Andros Island in the Bahamas, proximal to the TOTO. The TOTO is a deep-water basin approximately 20 miles wide and 150 miles long, with a maximum depth of 2000 meters. The deep basin is surrounded on three sides by shallow banks, reefs, and other islands, with its only connection to the open ocean at the north end, through the Northeast Providence Channel. This isolated geography with limited shipping traffic results in low acoustic ambient noise, making it the ideal ocean environment for acoustic measurements, detection and tracking. The water temperature and salinity of the TOTO varies little over the year with a seasonal thermocline centered at

approximately 180 meters and a maximum salinity at 150 meters spanning the length of the TOTO (Shonting, 1970; U.S. Navy, 1967). Due to the TOTO's location and surrounding topography, it is greatly influenced by evaporation and precipitation. In fact, the monthly salinity profile varies greatly near the surface and is dependent on rainfall and the wind and tidal flushing of bank water of varying salinities (Shonting, 1970). TOTO water deeper than 400 meters is characterized as North Atlantic Central Water (NACW) and North Atlantic Depp Water (NADW), bathing the bottom between 1500 and 2000 meters. These waters closely resemble and are in free circulation with the Sargasso Sea, which lies west of the Bahamas (Ridley, 1962; Shonting, 1970).

AUTEC's primary mission is to provide a deep-water range for the testing, calibration and evaluation of U.S. Navy assets with high positional accuracy through underwater, surface, and in-air tracking (Cecil, 1992). The velocity of sound through sea water during acoustic testing is affected by three parameters; temperature, salinity and pressure. For applications like those at NUWC det. AUTEC which require accurate depth or distance, precise knowledge of the sound velocity is required (Urick, 1983). Although the TOTO is a relatively stable basin, seasonal fluctuations in solar radiation and wind stress impact the surface mixing layer which in turn affect the accuracy of acoustic operations (Shonting, 1970; Metzger et al., 2017). To adjust for this, different sound velocity profiles are utilized throughout the year at NUWC det. AUTEC based on historical *in situ* observational data. NUWC det. AUTEC does not currently utilize the HYCOM or other OGCMs for forecasting the environmental conditions of the TOTO, however the ability of the NUWC det. AUTEC to utilize an ocean circulation model, such as the HYCOM, could provide an early indication of annual and decadal trends in the TOTO's oceanographic characteristics as well as seasonal variability. With up-to-date knowledge of the TOTO's internal parameters through the HYCOM, sound velocity profiles which best characterize the current conditions can be implemented, resulting in improved accuracy for naval acoustic operations.

3.0 Methods

3.1 Data Collection

3.1.1 HYCOM

The publicly-available, assimilated configurations of both the global 1/12° and GoM 1/25° HYCOM were used for this study (available for download at www.hycom.org). The HYCOM+NCODA GoM 1/25° resolution configuration GOMI0.04 (hereafter "GOMI0.04 configuration") provides an hourly snapshot in Coordinated Universal Time (UTC) of GoM conditions, interpolated to 40 standard vertical layers, and was used in this study to compare against the CTD cast data (hereafter "observational data") collected by the DEEPEND Consortium in the GoM. The GOMI0.04 configuration was selected because its resolution in the GoM is finer than the GLUb0.08 1/12° HYCOM configuration and the GOMI0.04 configuration spans the period of time in which CTD observational data was collected.

In the TOTO, the global GOFS 3.0 HYCOM+NCODA Global 1/12° resolution configuration GLBu0.08 (hereafter "GLUb0.08 configuration") was utilized, which provides a daily snapshot at zero hours UTC beginning in October 1992 (HYCOM, 2017a). The GLBu0.08 configuration was selected over the GLBa0.08 configuration as it has a higher spatial resolution in the upper ocean and 40 standard z levels, while the GLBa0.08 configuration has fewer (33) z levels with low spatial resolution in the upper ocean. In addition, the GLBu0.08 configuration includes in-situ temperature, while the GLBa0.08 configuration only includes potential temperature (Wallcraft, 2014). Due to the extended time series covered by the observational data in the TOTO, both the global 1/12° "analysis" and "reanalysis" experimental runs of the GLBu0.08 configuration were utilized to provide historical coverage from 1992. The HYCOM analysis runs (hereafter "analysis") are snapshots in time produced from either real-time runs or real-time run simulated by a hindcast. Over time, the results are typically broken into different experiments based on upgrades to the model version, data assimilation version, or changes in the available atmospheric forcing (Wallcraft, 2015). For its duration, the reanalysis run (hereafter "reanalysis") uses a constant software system maintaining the same version of the HYCOM, the same atmospheric forcing source (Climate Forecast System Reanalysis), and

the same data assimilation version (NCODA 3DVAR). In addition, the bathymetry in the reanalysis follows the coastline more closely. The observational data in the TOTO spanned four experiments during the analysis and one experiment during the reanalysis (Table 1). The analysis and reanalysis overlap for approximately eight months, during which time six CTD casts were collected.

Both the HYCOM configurations used in this study (GOMI0.04 1/25° and the GLBu0.08 1/12°) are available with 40 standard vertical layers, although the vertical layers utilized by the two configurations differed in the upper ocean (See Appendix 1). In addition, the NetCDF file for each model configuration had a slightly different format, with five variables (time, depth, latitude, longitude, and temperature) defined differently and two variables (time and longitude) formatted differently. In addition, time and longitude were also formatted differently between the analysis and reanalysis in the GLBu0.08 configuration.

Table 1: The HYCOM configurations and experiments utilized during this study

Model Configuration	Experiment	Extent	Resolution	Output Frequency	Experiment Date Range
GOM10.04	Expt 32.5	GoM	1/25°	Hourly	4/1/2014 - Present
GOFS 3.0 Analysis GLBu0.08	Expt 91.2	Global	1/12°	Daily	4/18/2016 - Present
GOFS 3.0 Analysis GLBu0.08	Expt 91.1	Global	1/12°	Daily	4/5/2014 - 4/18/2016
GOFS 3.0 Analysis GLBu0.08	Expt 91.0	Global	1/12°	Daily	8/21/2013 - 4/4/2014
GOFS 3.0 Analysis GLBu0.08	Expt 90.9	Global	1/12°	Daily	1/3/2012 - 8/20/2013
GOFS 3.0 Reanalysis GLBu0.08	Expt 19.1	Global	1/12°	Daily	8/1/1995 - 12/31/2012

3.1.2 DEEPEND and the GoM

CTD sensor data in the GoM were obtained by the DEEPEND Consortium over five research cruises between 2015 and 2017, for a total of 85 casts (Sutton, 2015; Sutton, 2016; Sutton, 2017, Sutton, 2018 a; Sutton, 2018 b). Research cruise DP01 took place in May of 2015, DP02 in August 2015, DP03 in May of 2016, DP04 in August 2016, and

cruise DP05 in May of 2017. The casts span the latitudes between 26.85 North and 29.07 North and between longitudes 85.99 West and 89.99 West at 23 stations (Figure 1). The deepest cast was 2002 meters, with the average deepest depth across all casts of 1385 meters. Two casts were not utilized in this study; one was noted to be a duplicate cast, while the other was corrupt. The CTD system included two temperature and two conductivity sensors, while fourteen casts used only one salinity sensor. For casts which two temperature and conductivity measurements were taken, the mean of the two measurements was calculated after data quality checks were performed, but prior to analysis. The GoM cast data included only the downcast (i.e., data collected while the instrument was lowered through the water column) which were binned using medians into one-meter depth intervals using custom MATLAB scripts and functions (English, D., unpublished data logs).

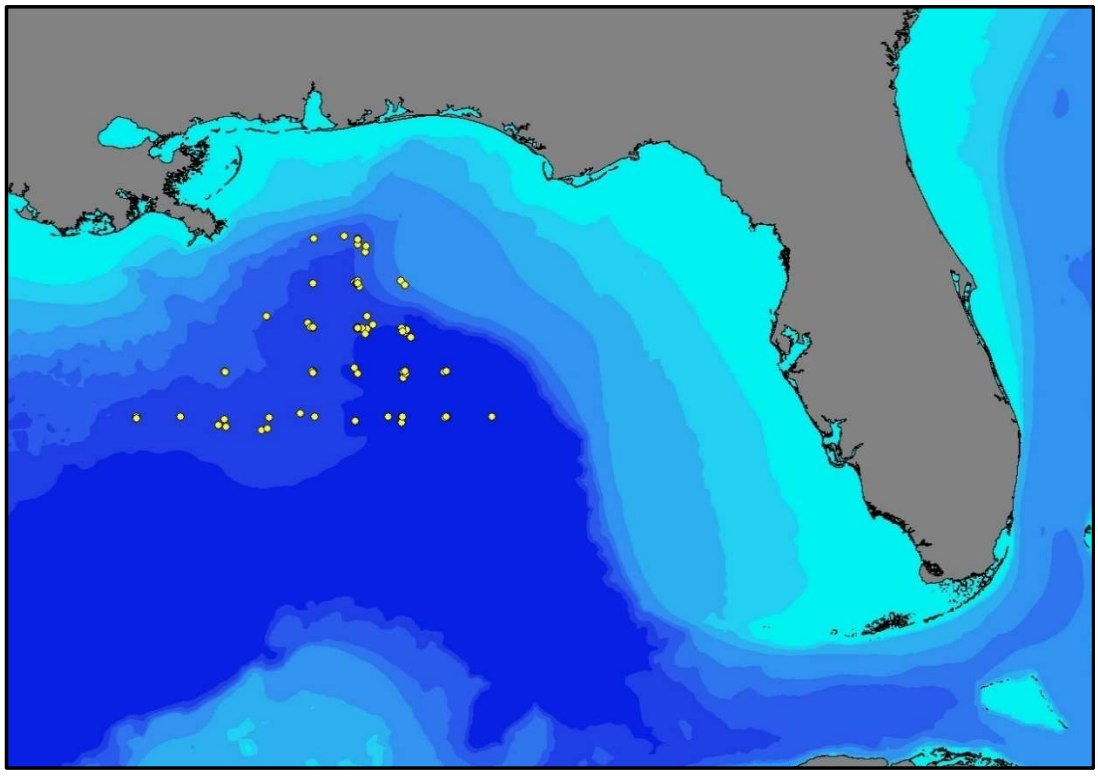

Figure 1: GoM Observational CTD Cast Collection Locations

3.1.3 AUTEC and the TOTO

371 CTD and XCTD sensor data casts were collected between 1997 and 2017 by the NUWC det. AUTEC between latitudes 23.834 degrees North and 24.962 degrees North and between longitudes 76.862 degrees West and 77.822 degrees West (Figure 2). The deepest cast was to 1903 meters, with the average deepest depth across all casts of 1243 meters. The long-time series and changes in data formatting of the TOTO data left many gaps and inconsistencies between data sets, requiring tedious review by hand. For datasets after 2005, the time, date, and location were corrected by hand using cast logs. Unfortunately, for datasets prior to 2004, this information was not available and 123 CTD casts were unusable due to a lack of position or units documentation. Of the remaining 22 casts, the depths were limited to less than 200 meters and were in non-consistent formats, and therefore all casts prior to 2005 were omitted from the analysis. There were 226 AUTEC CTD and XCTD casts between 2005 and 2017 and two casts were omitted because of suspect data or a lack of HYCOM data in the vicinity of the cast for comparison.

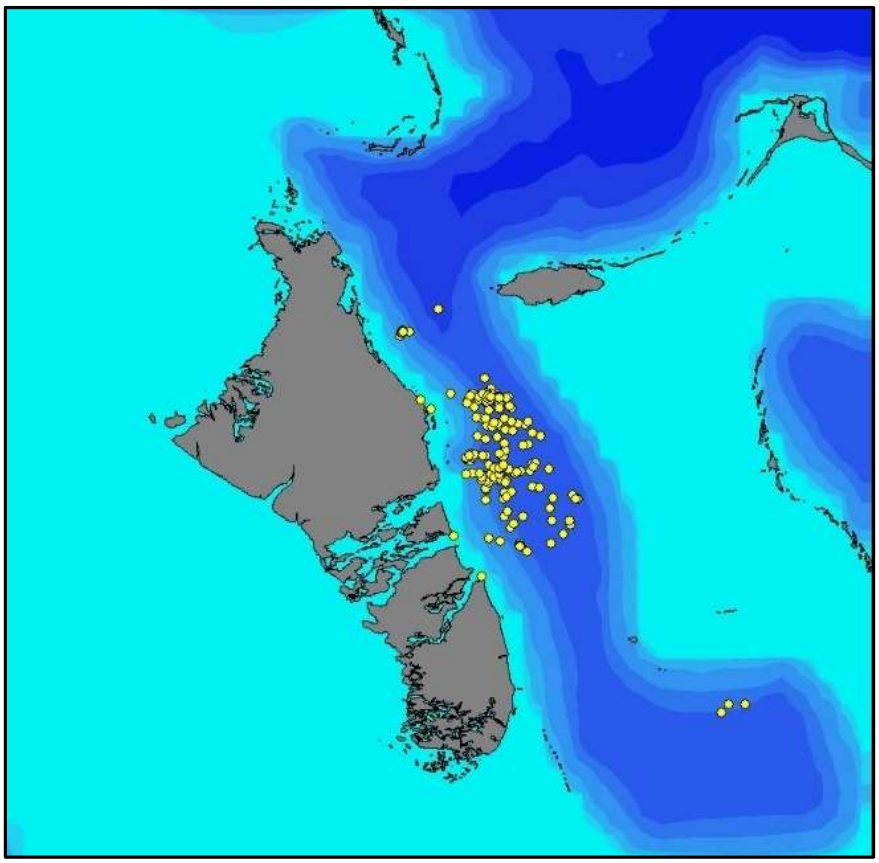

Figure 2: TOTO Observational CTD Cast Collection Locations

Of the 224 casts retained for this study, format of the time, date, and location were inconsistent among the data therefore MATLAB was used to standardize the format of the data. Time was documented in both local and UTC time throughout the AUTEC casts and a majority of the data were in local time. Remaining entries were converted to local time to standardize. Raw cast data in the TOTO were provided in English Engineering units and included both the downcast and upcast (i.e., data collected while the instrument is raised from the bottom to the surface). The upcast was manually removed from the data set as it may contain contaminated sensor data from disturbances to the water column caused by the instrument's initial decent (R. Bolin, pers. communication 2018). The data was converted to scientific units using MATLAB to ensure all datasets were consistent.

3.2 Code development

MATLAB was used to extract the HYCOM netCDF data (i.e., latitude, longitude, day, time, depth, salinity and temperature), analyze the raw CTD casts, check data quality, perform interpolation, analyze the HYCOM and the CTD data, calculate statistics and plot the study results. Due to the differences between both the HYCOM and observational data, separate MATLAB m files were composed for extracting and analyzing the data for each basin. Additionally, the XCTD data collected in the TOTO were in a different format than the CTD data, requiring a separate code.

3.2.1 Quality Control Procedures

Prior to analysis, the raw observational CTD data were vetted through control procedures to identify outliers and erroneous measurements following Boyer & Levitus (1994) and Johnson et al. (2013). For each observational data point, the data were checked for depth duplications, depth inversions, excessive temperature and salinity gradients and inversions, and to ensure temperature and salinity measurements were within an acceptable range. All measurements which were flagged during quality control were omitted from the CTD interpolation to standard levels. Depth duplication occurred when a depth reading was identical to the reading immediately preceding it. Depth duplications were eliminated from the data set. A depth inversion occurred when an observation was at a depth shallower than the depth immediately before it. When found, the second observation was flagged. The temperature and salinity data were also verified to be within an acceptable range of values based on the geographic location of data collection to eliminate outliers. As both the GoM and the TOTO fall within the North Atlantic geographic boundary as defined by the World Ocean Database User's Manual (Appendix 2) (Johnson et al., 2013), the ranges were established based on frequency distributions, statistical analysis, literature values, and atlases and are broad enough to account for variations by season and year (Boyer & Levitus, 1994; Johnson et al., 2013). Measurements which fell outside of the acceptable ranges were flagged. For both temperature and salinity, gradients checks were performed to verify measurements did not excessively increase or decrease over a depth range. A gradient is

the change in the value of a variable between two depths divided by the change in depth, defined by Johnson et al. (2013) as

$$gradient = \frac{\Delta v}{\Delta z} = \frac{v_2 - v_1}{z_2 - z_1}$$

where

v_1= the value of the variable at the current depth level

v_2= the value of the variable at the next depth level

z_1= the depth of the current depth level

z_2= the depth of the next depth level

Acceptable maximum gradient (MGV) and inversion (MIV) values were obtained from Johnson et al. (2013) and utilized for this check (Table 2). A negative (or excessive) gradient was one in which the measurement decreases over depth at a rate higher than the MGV, while a positive gradient (or excessive inversion) occurred where the measurement increases over depth at a rate higher than the MIV. Measurements which did not meet the gradient checks were flagged in the CTD file.

Table 2: Maximum Acceptable Inversion and Gradient Values for Temperature and Salinity (Johnson et al., 2013)

Variable	**Maximum Inversion Value (Depths<400m)**	**Maximum Gradient Value (Depths<400m)**	**Maximum Inversion Value (Depths>400m)**	**Maximum Gradient Value (Depths>400m)**
Temperature	0.300	0.700	0.300	0.700
Salinity	9.000	9.000	0.050	0.050

3.2.2 HYCOM Interpolation

The HYCOM data were selected for the date, time and locations associated with each CTD cast. The HYCOM data are available only on the prescribed grid (1/25° in the GoM and 1/12° in the TOTO) and at the defined time increment (1 hour in the GoM and 1

day in the TOTO). In order to calculate the HYCOM estimation at the exact location and time (in the GoM) of the CTD cast, two types of interpolation were required.

The hourly snapshots available from the GOMI0.04 configuration allowed for a direct comparison in the GoM between the model and CTD data at the exact time of the cast at each depth level and each latitude-longitude pair using spline interpolation. Spline interpolation was selected over other interpolation methods as it resulted in a better fit for the HYCOM hourly temperature and salinity fluctuations observed over the course of a day.

The HYCOM data were isolated using the four nearest latitude-longitude pairs surrounding the CTD cast location. The HYCOM data from the surrounding grid were interpolated to the exact location of the CTD cast using bilinear interpolation, or linear interpolation when a cast fell on the HYCOM grid. For CTD casts that occurred near the boundary of the basin, the HYCOM data were not always available at the four surrounding grid points for the full depth of the cast. In the GoM, the HYCOM grid surrounding one data point was not complete due to its proximity to the Continental Shelf. Due to the narrowness of the TOTO and the 1/12° resolution HYCOM grid, the grid was typically incomplete for CTD casts which took place on the western side of the basin off of Central Andros. When the entire HYCOM grid was not available at a particular depth, linear or bilinear interpolation was performed on the remaining grid points and the interpolated data point was flagged as less certain. In the GoM, the required HYCOM grid was unavailable for 0.04% of the data. In the TOTO, 6.47% and 6.51% of the required temperature and salinity data were missing.

3.2.3 Lagrangian Interpolation of CTD data

The HYCOM model outputs were interpolated to 40 standard depth levels. As the raw observational CTD/XCTD data captured the entire water column, the CTD data were interpolated to HYCOM's standard depth levels to compare the two. Data flagged during the quality control steps were not used for interpolation to standard levels. The standard depth level interpolation was based on that described by Boyer and Levitus (1994) and Johnson et al. (2013) and consisted of conducting two three-point Lagrangian

interpolations on the four observational data points surrounding the standard depth level after which an average of the two interpolated values was taken as the value for the standard depth. Linear interpolation was performed in cases where there were not enough data points to perform Lagrangian interpolation, such as near the surface and when a cast began or ended near a standard depth level. If an observed measurement was collected exactly at a standard depth level, a direct substitution was made. When observed values occurred within 5 meters of the surface, the shallowest value was taken as the surface value. Data used for interpolation had to fall within a reasonable distance from the standard level, otherwise measurements too far from the standard depth could adversely influence the interpolated value. Documentation in other studies regarding the maximum distance used for vertical interpolation was poor, so a distance of 25 meters was selected for this study.

3.2.4 Comparison to HYCOM

After the CTD cast was interpolated to the standard depth levels, the interpolated CTD data was compared to the HYCOM estimation at each depth level. For all data points, the CTD measurement was subtracted from the HYCOM estimate. The differences were plotted along with the raw data for verification as well as saved to an output file for statistical analysis.

The statistical analyses done in this study included descriptive statistics and regression analysis, primarily evaluating the error, mean error and root mean square error (RMS error). The error is the difference between an observational data point at a particular location (latitude, longitude, and depth) and time the corresponding HYCOM estimate. The mean error is the mean of the error between the HYCOM estimate and observational data using the full set of comparisons and can be analyzed for a particular criteria (depth, month, year, experiment, cruise in this study) and over the entire data set. The RMS error measures the amount of error between two data sets, or as presented here, the fit of the HYCOM model's estimation to the observed CTD data. RMS error is extensively used at NUWC det. AUTEC for determining accuracy.

Ocean condition data from the HYCOM are estimations of the true ocean, and as such are subject to input condition errors and the very nature of trying to emulate imperfect

physical processes. Some level of error in the estimation of the ocean parameters in the GoM and the TOTO was therefore expected, while this study quantifies that error. The validation of the HYCOM model was taken a step further by determining a correction factor for the model for more accurate application of the model in the regions presented. The depth levels of the GLBu0.08 1/12° HYCOM configuration used in this study were focused near the surface, while the depth levels in the GOMI0.04 1/25° HYCOM configuration were distributed more through the water column. This discrepancy between experiments in combination with the variability in mean error values made a non-linear regression fit impractical (Mean error data available in Table 10). Due to the complexity of the mean error as a function of the standard depth levels, Generalized Additive Models (GAM) were required to find the optimal fit of the mean error data as a function of depth in each region. A GAM is an optimized spline-fitting model in which the model is defined in terms of smoothing functions which are additive (Wood, 2006).

4.0 Results

4.1 Observational Measurements

The observational measurements through the entire water column were analyzed to characterize and identify trends when compared to the HYCOM data (Table 3). For temperature and over all CTD and XCTD casts, the GoM and the TOTO had approximately the same range in values at the surface (Figure 3 and Figure 4). With increasing depth, the CTD temperature profiles had more variability in the GoM than in the TOTO. The salinity profiles were similar in the two regions (Figure 5 and Figure 6). The minimum salinity was at the surface in both regions, with a minimum in the GoM that was 2.13 PSU lower than in the TOTO, likely due to the larger fresh water influences from the Gulf Coast and evaporation that exceeds precipitation in the TOTO (Ridley, 1962). Depending on the season, both regions reached their maximum salinity between 100 and 200 meters, with higher readings in the TOTO than in the GoM. At depths deeper than 1000 meters, the salinity in both regions was stable at approximately 35 PSU.

Table 3: Observational Data Summary by Region

	TOTO	GoM
Maximum Temperature (°C)	30.66	31.49
Minimum Temperature (°C)	3.40	4.27
Maximum Salinity (PSU)	37.23	37.55
Minimum Salinity (PSU)	29.60	27.47
Maximum Depth (meters)	1903.8	2001.5
Mean Max Depth (meters)	1060.4	1396.8

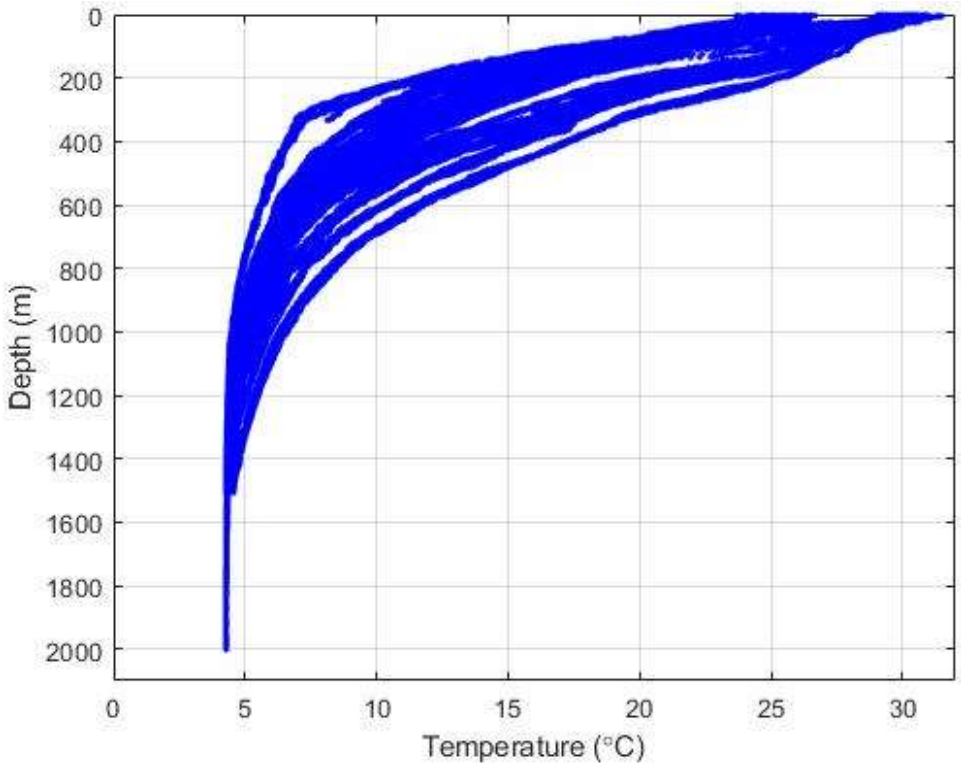

Figure 3: Temperature vs Depth for Observational Cast Data in the GoM

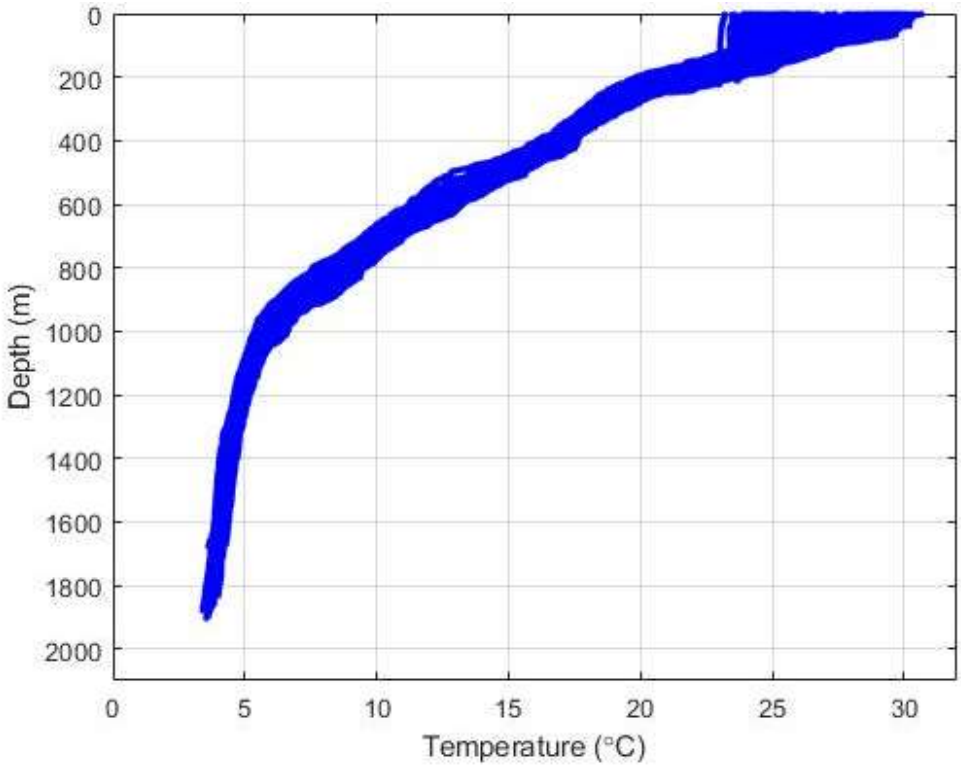

Figure 4: Temperature vs Depth for Observational Cast Data in the TOTO

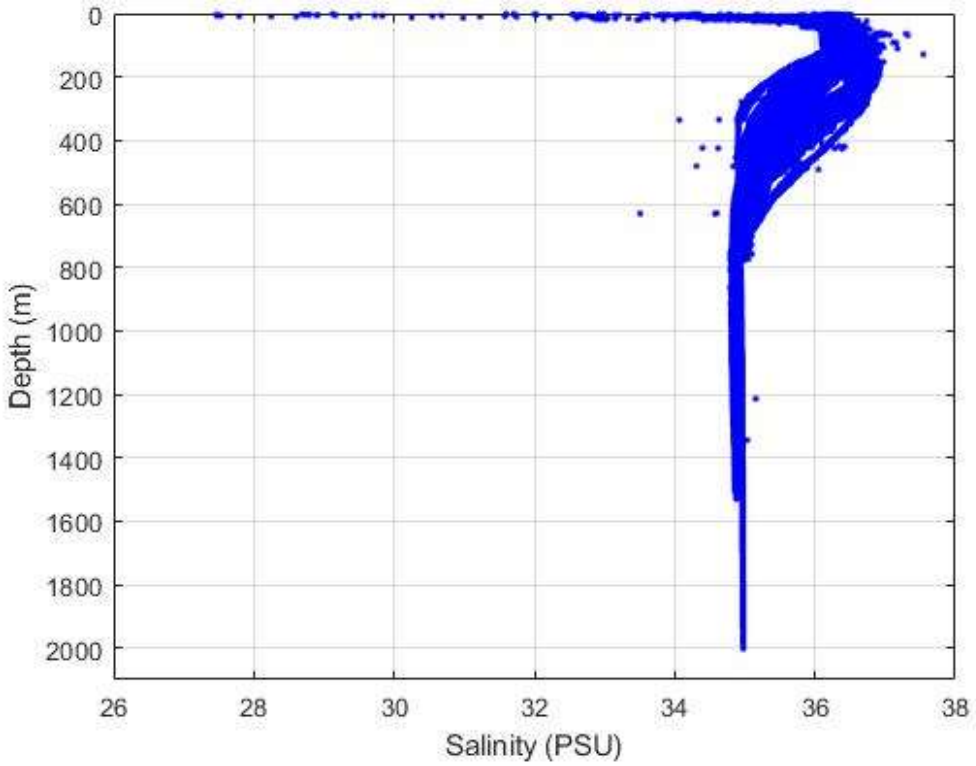

Figure 5: Salinity vs Depth for Observational Cast Data in the GoM

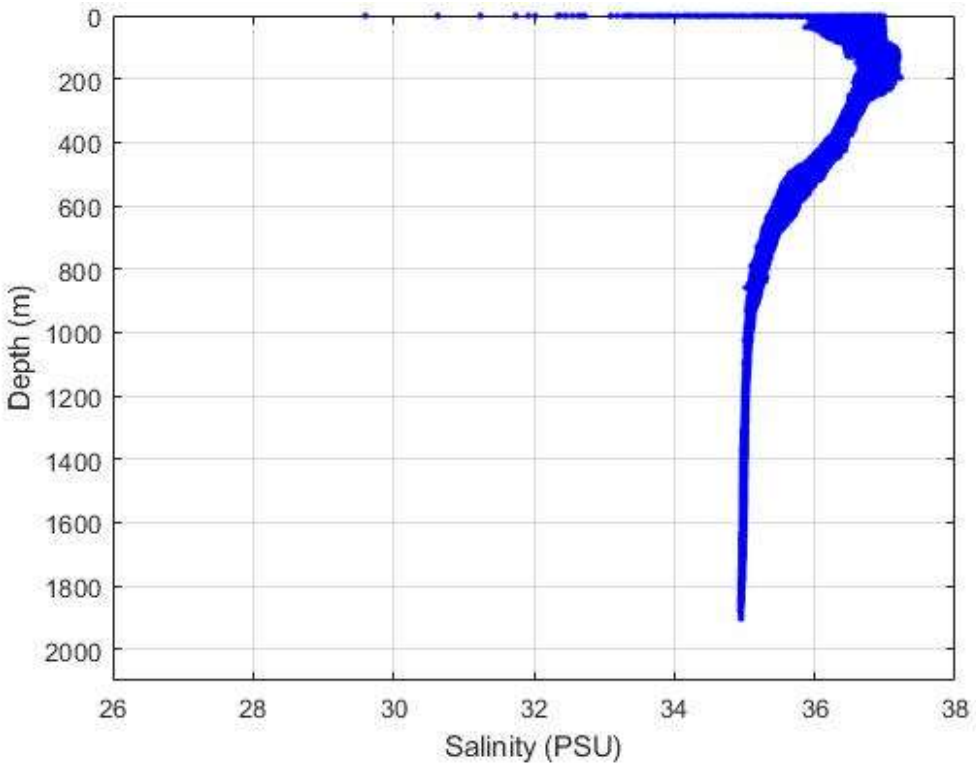

Figure 6: Salinity vs Depth for Observational Cast Data in the TOTO

Although the GoM observational data were only measured during two months, the temporal resolution within each month was high, allowing for three successive comparisons in the month of May and two in August. Observational data collected in August 2015 (DP02) and August 2016 (DP04) plotted a similar profile, whereas both the temperature and salinity show more variability over the course of each cruise. The temperature and salinity profiles in May of 2015 (cruise DP01) and 2017 (DP05) however were fairly consistent over the course of each cruise. Interestingly, the data from the May 2016 (DP03) cruise more closely resembled that taken during the two August cruises rather than the May 2015 and 2017 cruises.

The variability between the cruises in the GoM was observed in the upper 200 meters in the CTD casts. In May 2015 the thermocline was between 20 to 40 meters, while the water temperature in the surface layer ranged between 24.22°C and 26.29°C (Appendix 3). The surface salinity during May 2015 ranged from 33.61 PSU to 36.39 PSU (Appendix 4). In August 2015 the thermocline was sometimes present between 20 and 40 meters,

with surface temperatures between 29.07°C and 31.49°C (Appendix 5). In August 2015 the surface salinity was between 29.13 PSU and 36.31 PSU (Appendix 6). In May 2016 the temperature data showed more variability than the other two May cruises (Appendix 7). The temperature in the surface layer during May 2016 presented with two distinct profiles. The first had a thermocline between 20 and 40 meters with surface temperatures between 24.65°C and 25.92°C. Three CTD casts followed the second profile with surface temperatures between 26.31°C and 26.67°C and two thermoclines, the first between 60 and 80 meters and the second between 130 and 140 meters. May 2016 had the most variability in salinity measurements of the five cruises, predominately in depths 50 to 125 meters and 400 to 800 meters (Appendix 8), although the surface salinity had the least variability with a range of 0.33 PSU. In August 2016, the thermocline was present for most CTD casts between 20 and 30 meters, while for two casts the thermocline was between 125 and 150 meters (Appendix 9). The surface temperatures range in August 2016 between 29.25°C and 31.39°C. The salinity in August 2016 ranged between 27.47 PSU and 36.37 PSU (Appendix 10). In May 2017 the thermocline was predominately present between 50 and 70 meters, with a few CTD casts presenting a thermocline between 20 and 30 meters (Appendix 11). The range in surface temperatures in May 2017 was between 23.7°C and 25.32°C. The surface salinities in May 2017 were between 36.3 PSU and 36.48 PSU (Appendix 12).

The coldest surface temperature in the GoM occurred in May 2017 (23.7°C), while the warmest surface temperature occurred in August 2015 (31.49°C). The greatest range in surface temperatures occurred in August 2015 (2.42°C), while the smallest range was in May 2016 (1.27°C). The maximum salinity of all casts occurs at a depth between 80 and 200 meters, with the shallowest occurring in May 2015, while the deepest occurred during one cast in August 2016. The greatest range in surface salinities occurred in August 2016 (8.9 PSU).

In the TOTO, the temperature remained warm (between 23.19°C and 30.66°C for all casts) for the first 100-150 meters before beginning a gradual decrease with depth, reaching its minimum temperature at the deepest depth of each cast. The range in salinity values in the TOTO was highest between the surface and 250 meters, after which the range

of values decreased at each depth, reaching a consistent salinity at approximately 1100 meters.

Seasonal variation in the TOTO was observed in the upper 150 meters in the CTD casts. Between the months of February and April the thermocline was at a constant depth of 150 meters with a surface layer that warmed over the period. The temperatures in the surface layer ranged between 23.37°C and 25.38°C (Appendix 14 through Appendix 16). As the surface layer continued to warm in May, the observational data indicated two thermoclines, one at 70 meters and one at 150 meters with a surface layer between 23.99°C and 26.67°C (Appendix 17). During the summer months (June through August), the thermocline was shallow (20-40 meters) or not present in the observational data and the surface layer ranged in temperatures between 25.89 °C and 30.13°C (Appendix 18 through Appendix 20). By September and October, the thermocline reestablished itself at a depth of 50 meters with a surface layer between 28.62°C and 30.65°C (Appendix 21 and Appendix 22). During November and December, the thermocline deepened to between 60 and 120 meters, with temperatures in the surface layer ranging between 25.46°C and 28.94°C, cooling predominately during November (Appendix 23 and Appendix 24). The warmest surface layer was found in September when the temperatures were between 29.02°C and 30.65°C, while the coolest layer occurred during February (23.37°C to 24.62°C).

The observational data from the TOTO had the lowest surface salinities in May (31.74 PSU) through September (29.6 PSU), while the highest surface salinities occurred in July (36.97 PSU) and between January and April (the highest in February and March with 36.93 PSU each). The greatest variability in TOTO salinity occurred in the upper 2 meters of the water column. September and July had the greatest range in values (7.15 PSU and 6.35 PSU, respectively), while November and October had the smallest range in the top 2 meters (0.45 PSU and 0.51 PSU). The maximum salinity of all casts occurred at a depth between 120 and 180 meters. The shallowest occurred in October and November (120 meters), while the deepest occurred between February and June (between 160 and 180 meters) (Appendix 25 through Appendix 36).

4.2 HYCOM Estimated Variables

In general, the HYCOM estimations were consistent with observational CTD data in each region. In the GoM, the HYCOM temperature estimations and variability of the temperatures decreased quickly with depth, consistent with the observational data (Figure 7). In the TOTO, the temperature remained warm until approximately 100 meters before slowly decreasing with depth in both the HYCOM estimate and observational data (Figure 9). Notably, in the TOTO the range of temperature extremes at each depth and variability in values was narrower than in the GoM. The HYCOM's minimum estimation of salinity in the GoM was approximately 3 PSU higher than the minimum observational data point (Figure 8). Both the HYCOM estimations and the observational data for salinity in the GoM had the most variability at depths between 100 to 700 meters. At depths greater than 700 meters the range in salinity values decreased, becoming more consistent through the remainder of the water column. The HYCOM estimation for salinity in the TOTO varied less than 1 PSU in the first 100 meters while the observational salinity data had a range of 7.63 PSU (Figure 10). Below 100 meters the HYCOM estimates had more variability in salinity range than the observational data. In the TOTO, the HYCOM data were only available for the upper 1250 meters of water for all but one station, yet 59% of the TOTO casts extend deeper than 1250 meters.

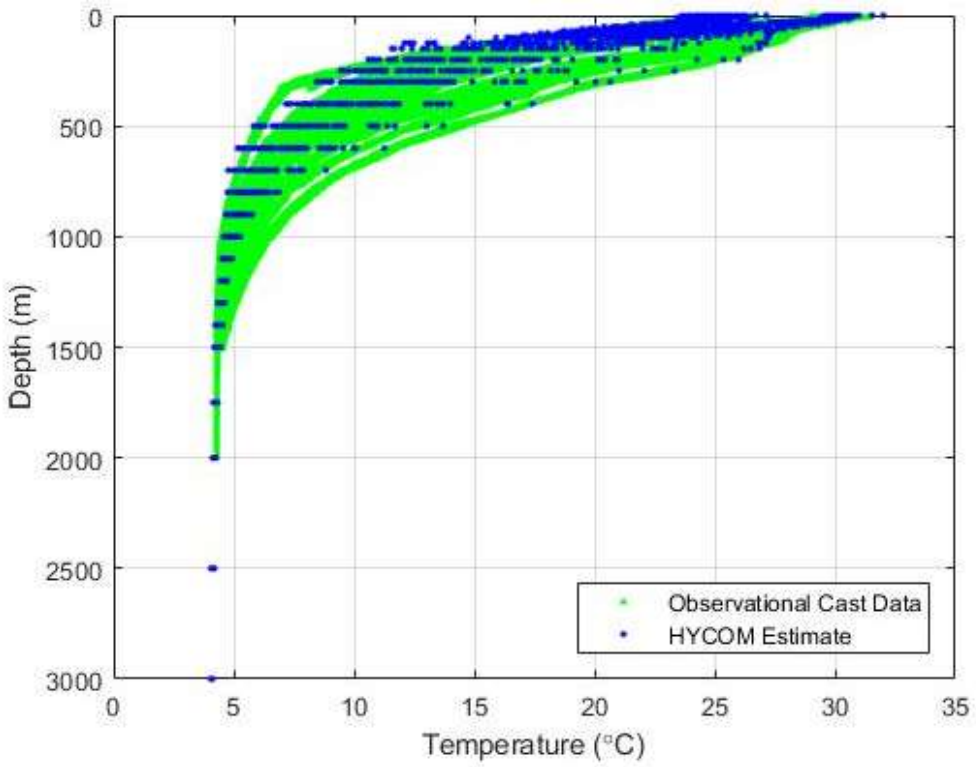

Figure 7: Observational CTD and HYCOM Model Temperature Data in the GoM

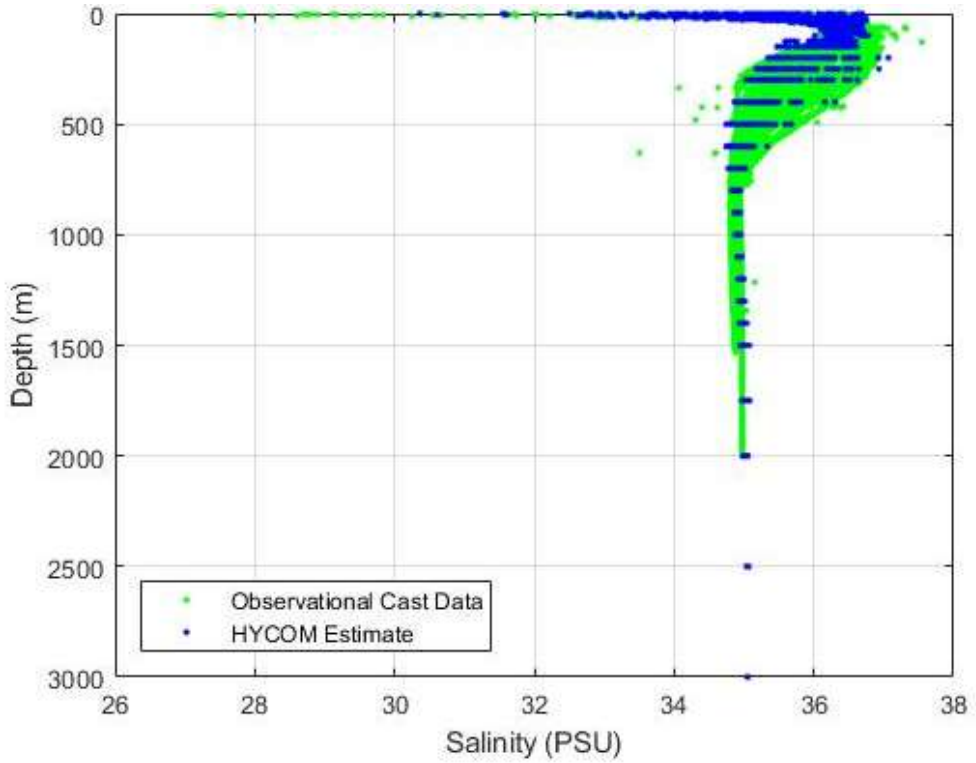

Figure 8: Observational CTD and HYCOM Model Salinity Data in the GoM

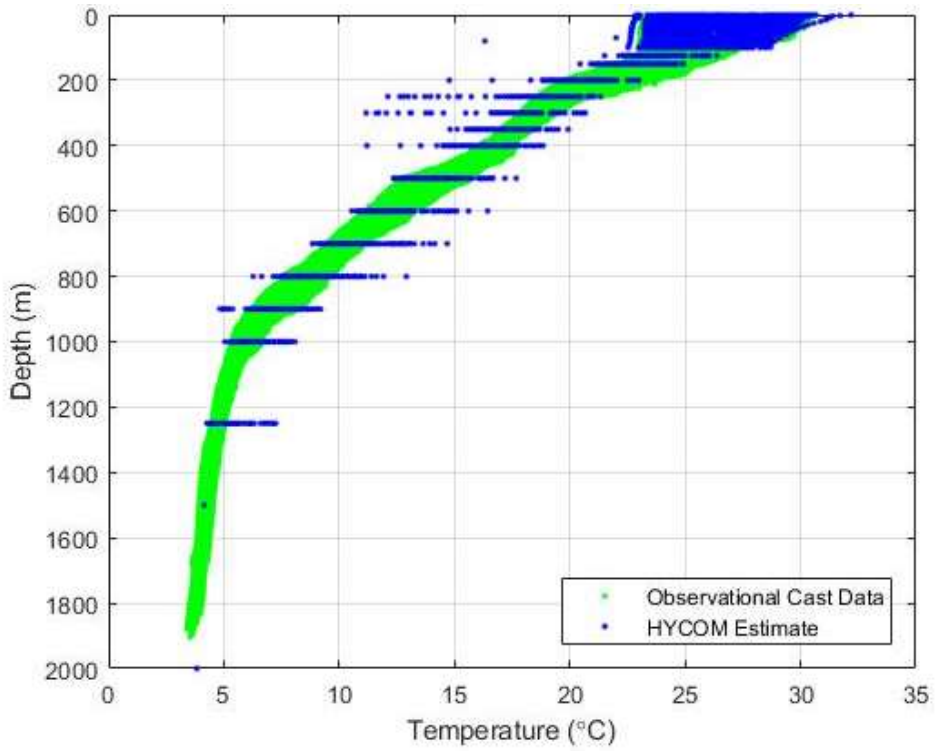

Figure 9: Observational CTD and HYCOM Model Temperature data in the TOTO

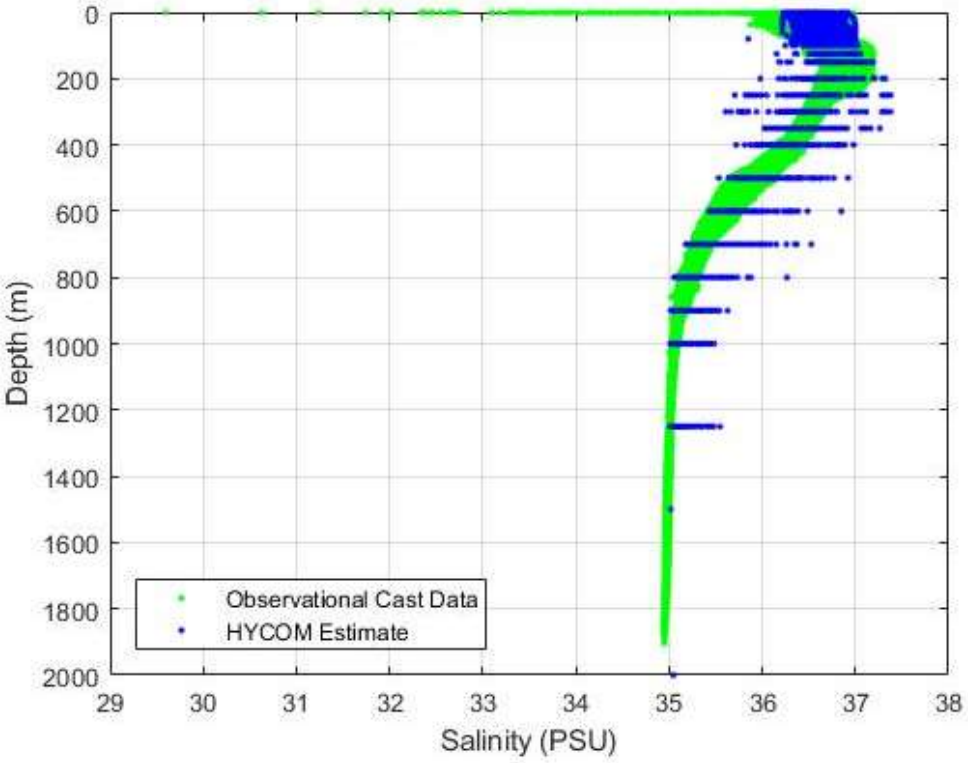

Figure 10: Observational CTD and HYCOM Model Salinity Data in the TOTO

4.3 Summary of the HYCOM Estimation and Observational CTD Data Comparison

The long timespan of the observational data collected in the TOTO allowed for several comparisons both within the region as well as against the results in the GoM, including the month, year, experiment, and between individual GoM cruises. Still, trends were only noted between the two basins and between the different depth levels. The collection dates of CTD casts in the two regions did not correspond, and therefore a direct comparison of HYCOM's performance between the two could not be made for a given moment in time. Except where noted (Section 4.10), the results presented do not include the HYCOM data that were flagged during the bilinear interpolation or observational data that failed the quality control check.

The mean error between the HYCOM and observational data through the entire water column was characterized to evaluate the performance of the HYCOM in each region. The mean error between the HYCOM temperature estimation and observational data in the GoM was higher than in the TOTO, indicating that the HYCOM predicted the temperature in the TOTO better than in the GoM (Table 4). The HYCOM also predicted salinity better in the TOTO than in the GoM, as the mean error between the HYCOM salinity estimation and the observational data was also smaller than in the GoM (Table 5). Although the HYCOM predicted the ocean conditions in the TOTO better than in the GoM, for both variables the range between the minimum and maximum error was higher in the TOTO than in the GoM. Because the standard deviation was lower in the TOTO for both temperature and salinity, the variability in the HYCOM's ability to estimate the conditions was lower in this region.

Table 4: Summary of Statistics of the Error between the HYCOM and Observational Temperature by Region

	GoM	TOTO
Mean	-0.6690	-0.2798
Standard Deviation	1.2851	0.8491
RMS Error	1.4486	0.8939
Maximum	3.3746	4.4187
Minimum	-6.8053	-8.0386

Table 5: Summary of Statistics for the Error between the HYCOM and Observational Salinity by Region

	GoM	TOTO
Mean	-0.2100	-0.0152
Standard Deviation	0.6121	0.2531
RMS Error	0.6470	0.2535
Maximum	7.7979	4.2197
Minimum	-5.9452	-1.2424

4.4 Error between the HYCOM Estimation and Observational CTD Data

In this study, the HYCOM was more likely to underestimate the ocean conditions than over estimate them in both the TOTO and the GoM (Table 6 and Table 7). When plotting the error between the HYCOM estimation and the observational data at the standards depth levels in the GoM (Figure 11), the HYCOM underestimated temperature more often than overestimated at each depth, with the most variability in the upper 400 meters. Not only was temperature underestimated more often than overestimated in the GoM, but the HYCOM also underestimated by a greater magnitude than it overestimated. Although the HYCOM also underestimated the temperature in the TOTO more often than it overestimated, between the depths of 2 meters and 100 meters the mean error was close to zero (Figure 12). The HYCOM underestimated the temperature more often between 125 and 500 meters in the TOTO, while deeper than 600 meters the HYCOM overestimated more often. In the GoM, there was a strong tendency for HYCOM to underestimate the salinity between the surface to 800 meters (Figure 13). In the TOTO, the HYCOM was almost as likely to overestimate as it was to underestimate salinity. Underestimation occurred more often between 35 and 400 meters, while overestimation occurred more often for all other depths (Figure 14).

Table 6: The HYCOM under- and overestimation percentages of temperature in the TOTO and GoM

	TOTO	GoM
HYCOM Under Estimates	69.97%	72.81%
HYCOM Over Estimates	30.03%	27.19%

Table 7: The HYCOM under and overestimation percentages of salinity in the TOTO and GoM

	TOTO	GoM
HYCOM Under Estimates	54.39%	74.77%
HYCOM Over Estimates	45.61%	25.23%

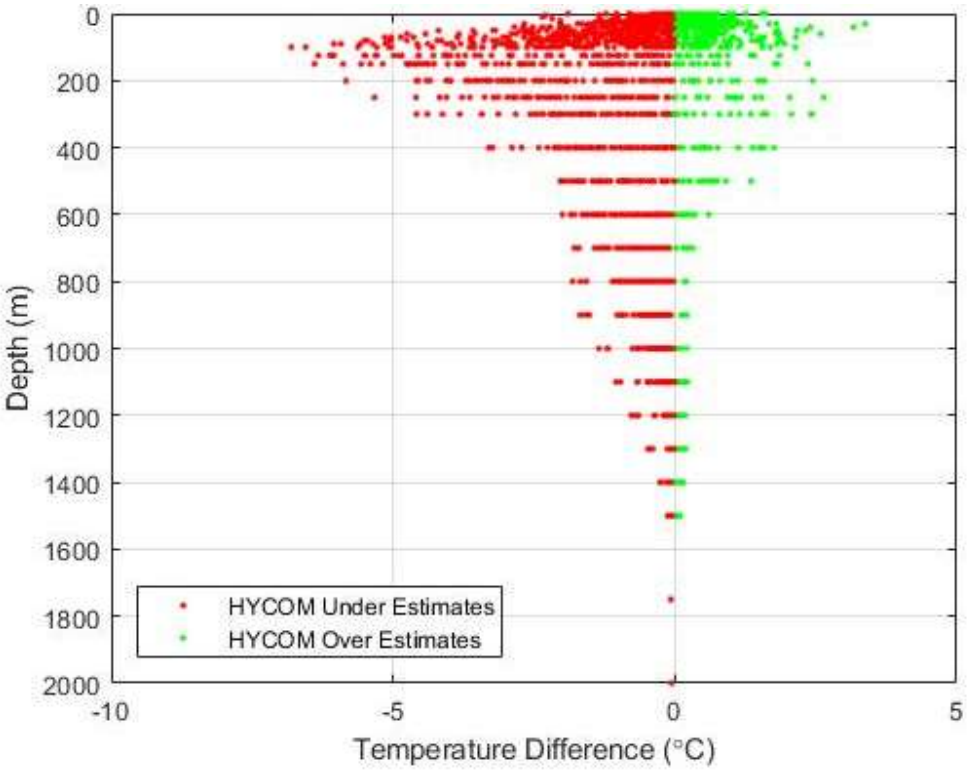

Figure 11: Temperature errors between the HYCOM estimate and observational data at each standard depth level in the GoM

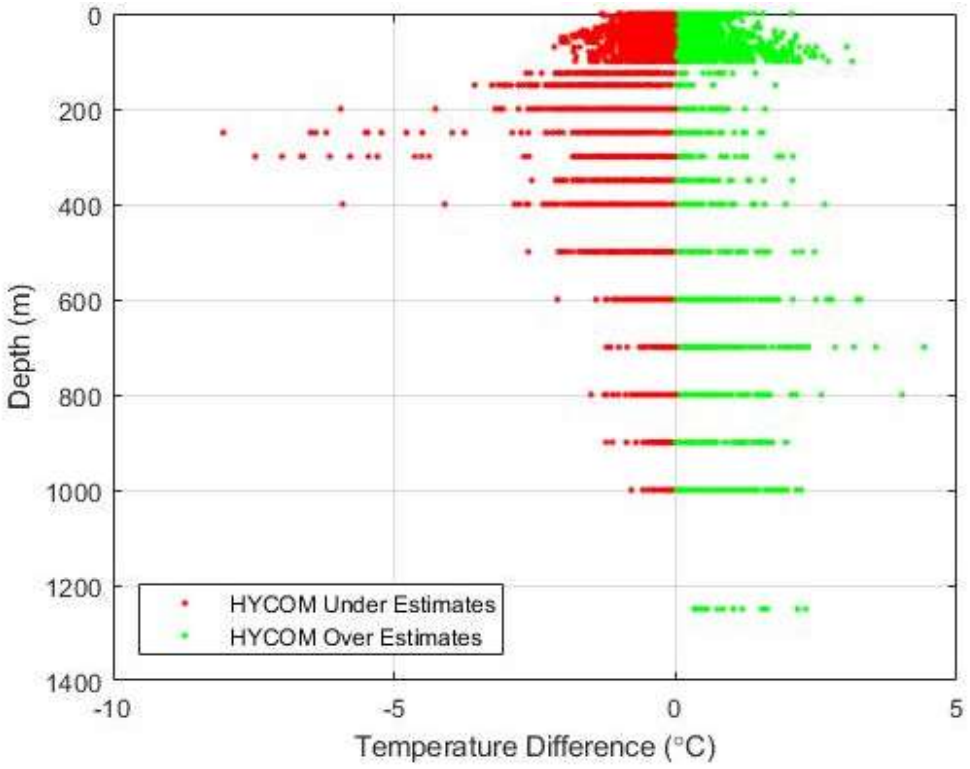

Figure 12: Temperature errors between the HYCOM estimate and observational data at each standard depth level in the TOTO

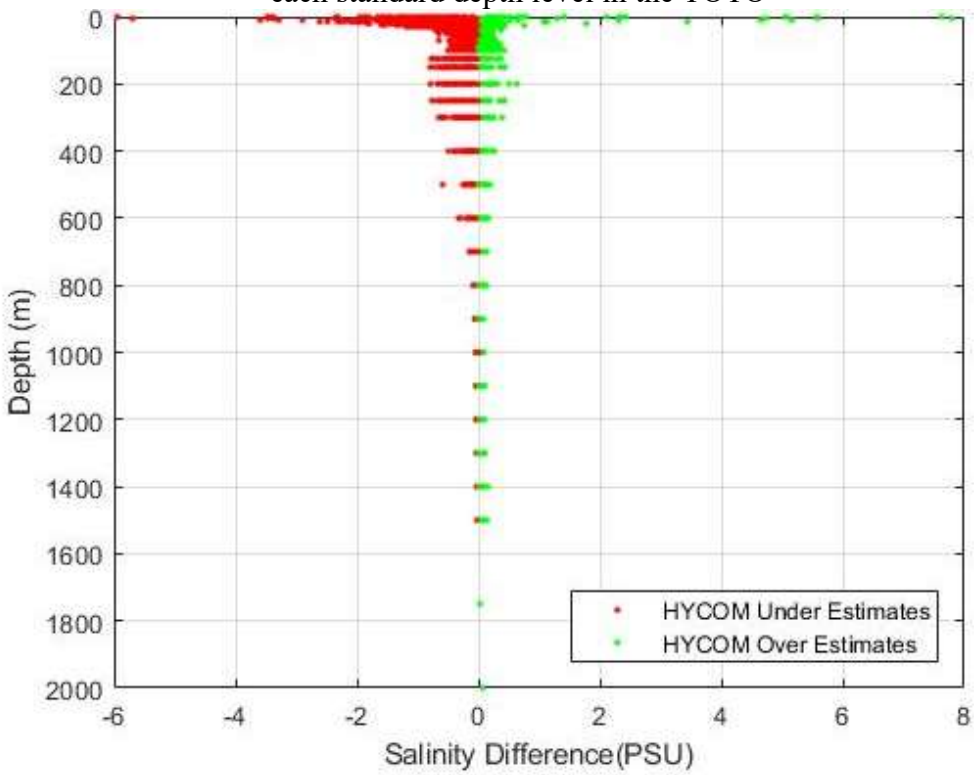

Figure 13: Salinity errors between the HYCOM estimate and observational data at each standard depth level in the GoM

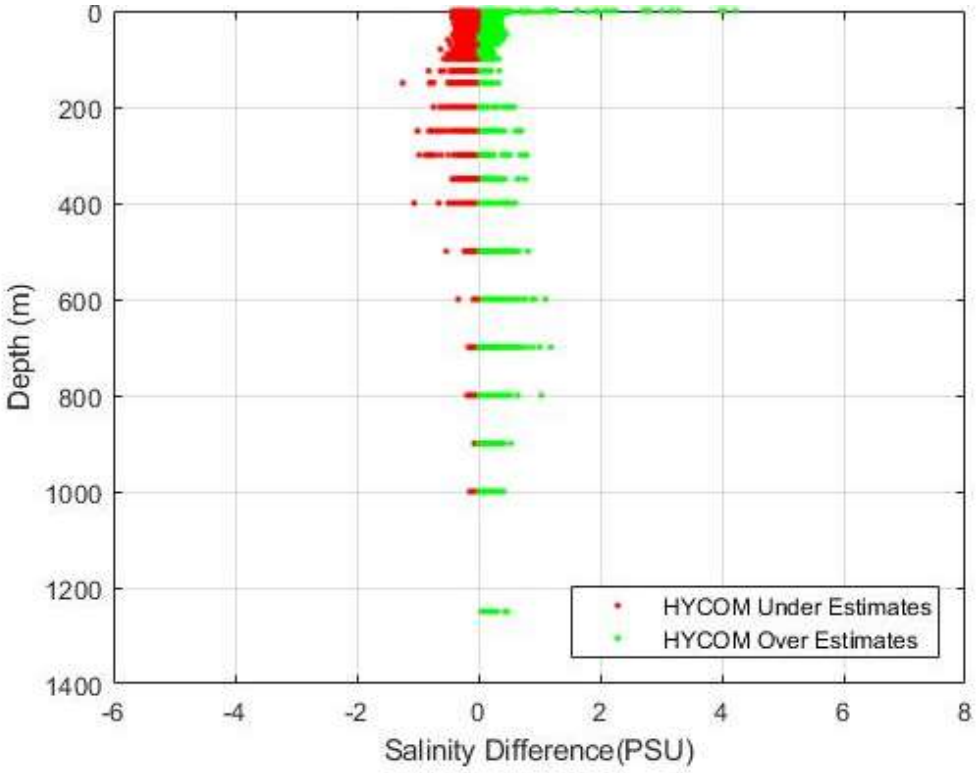

Figure 14: Salinity errors between the HYCOM estimate and observational data at each standard depth level in the TOTO

4.5 Depth Analysis of RMS Error

Plotting RMS error against depth was the most indicative of a trend in the HYCOM's performance over the study period. The GoM 1/25° and the global 1/12° HYCOM models use different standard depth levels in the water column and therefore direct comparisons could not be made at all depths, but an overall trend was quantified. Based on the mean error, the HYCOM underestimated ocean temperature at most depths. In the TOTO, the HYCOM underestimated the temperature for all depths 500 meters and shallower, while in the GoM, HYCOM underestimated the temperature at all depths except 0, 1300, and 1400 meters. For salinity mean error in the TOTO, HYCOM underestimated the conditions between 30 and 400 meters, while overestimating for all other depths. In the GoM, salinity was under estimated for all depths 800 meters and shallower.

For temperature, the RMS error in the TOTO was less than that in the GoM for all comparable depths shallower than 500 meters, while the TOTO's RMS error was greater than in the GoM for all depths 500 meters and below (Figure 15). The salinity RMS error in the TOTO was less than the GoM for all depths less than 300 meters, after which the GoM RMS error was less than the error in the TOTO (Figure 16). The temperature and salinity error in the GoM converged towards zero with increasing depth, while the error in the TOTO remained around 1°C and 0.2 PSU, respectively, with increasing depth.

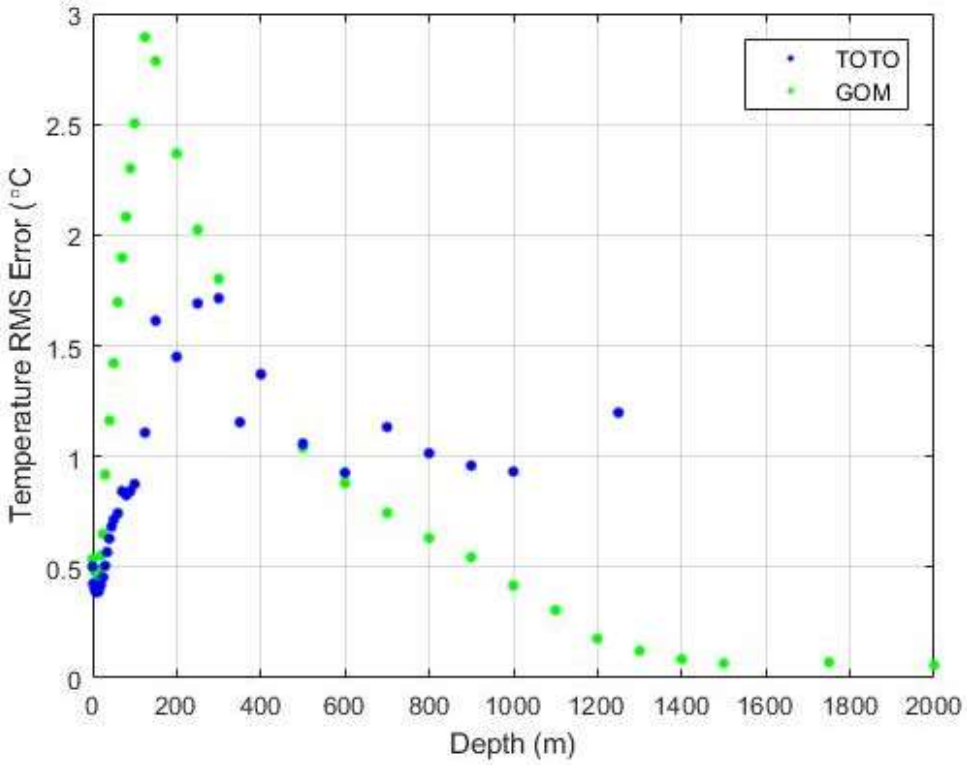

Figure 15: Temperature RMS Error vs Depth

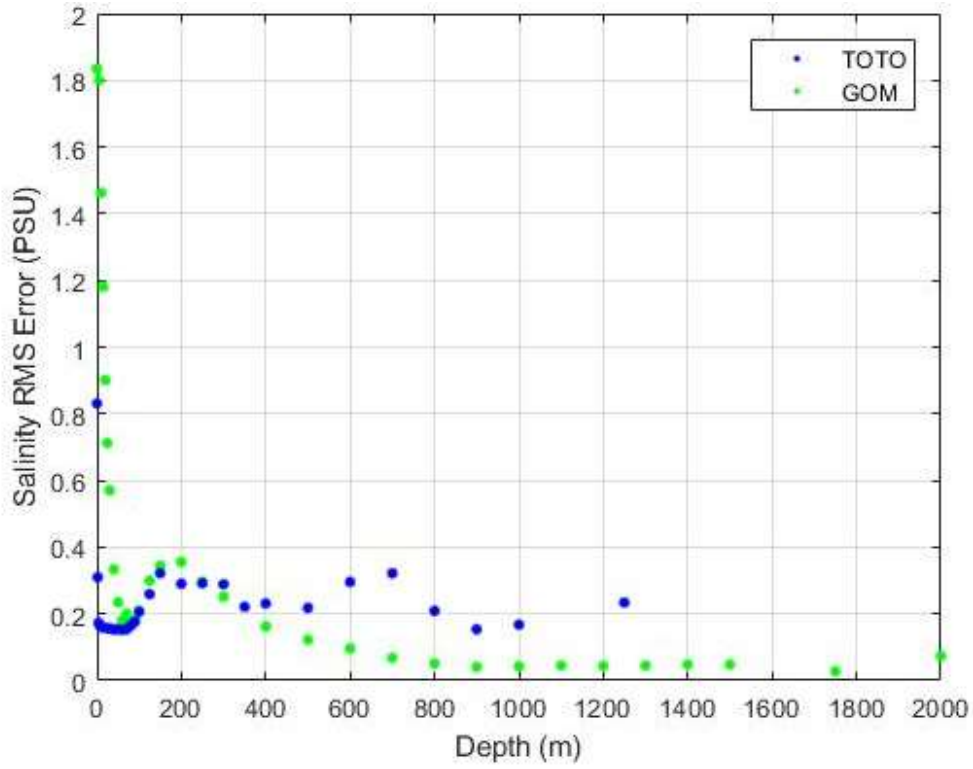

Figure 16: Salinity RMS Error vs Depth

4.6 Monthly Analysis of RMS Error

When comparing the months of the year, the temperature RMS error in May and August in the GoM were higher than the same months in the TOTO (as well as all other months) (Figure 17). The temperature RMS error in the GoM was greater than 1.2 °C for both May (1.2194°C) and August (1.6898°C), while the highest error in the TOTO was during the month of May (1.1520 °C). The lowest temperature RMS errors in the TOTO were in October and December. There was no discernable association between the TOTO's RMS error and the month of year. Although the error was lower in May than in August in the GoM, there was not enough year-round data to make a statement regarding the relationship between temperature error and time of year. The mean error for temperature during each month indicates that the HYCOM underestimated the ocean conditions year-round in both regions.

For salinity, the RMS error in the GoM was higher in both May and August than during the same months in the TOTO (as well as all other months) (Figure 18). In the GoM the salinity RMS error was greater than 0.5 PSU for both May (0.5442 PSU) and August (0.7552 PSU), while in the TOTO June and September had the highest RMS error (0.3232 PSU and 0.3244 PSU, respectively). There was a slight difference between the salinity error and the time of year, whereas the RMS error was higher during summer months (May through September) than the rest of the year, with the exception of December, which was also higher. Additional year-round data would be required to further evaluate this assessment. Although the salinity RMS error was lower in May than in August in the GoM, there was not enough year-round data to make a statement regarding the relationship between the HYCOM's performance and time of year.

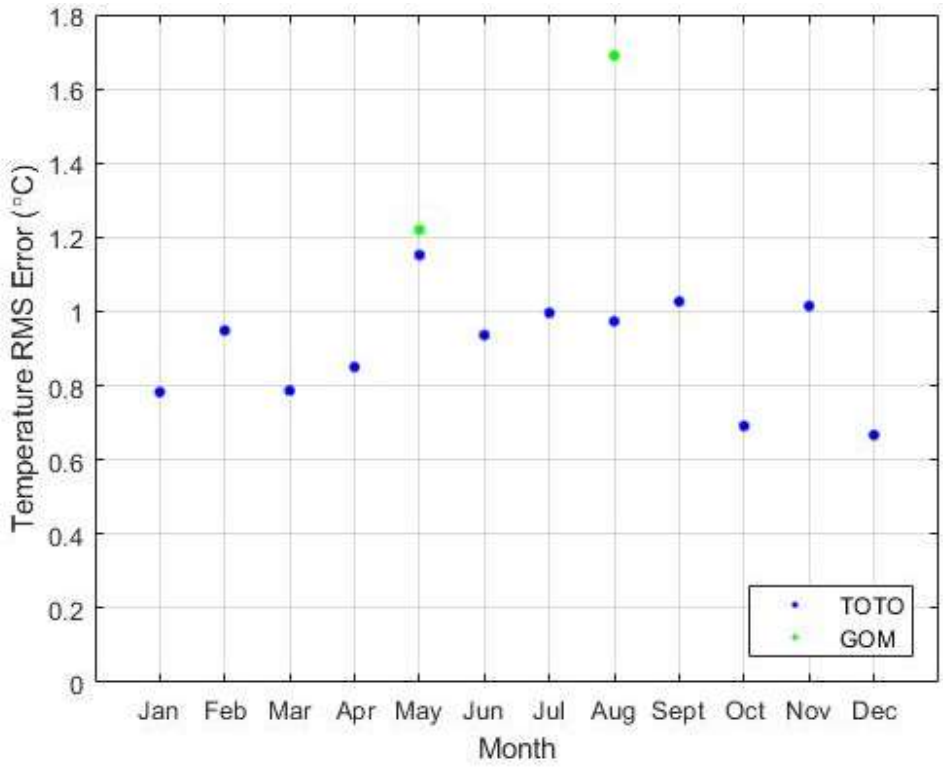

Figure 17: Temperature RMS Error vs Month

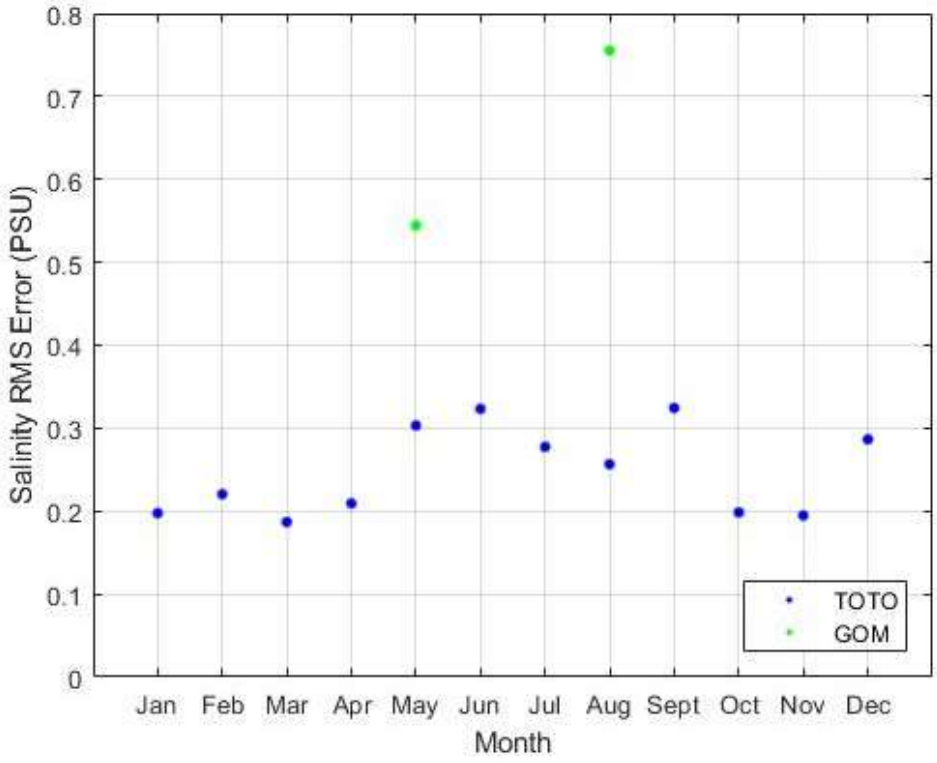

Figure 18: Salinity RMS Error vs Month

4.7 Yearly Analysis of RMS Error

Although both the temperature and salinity RMS error (Figure 19 and Figure 20 respectively), decreased over the three years of GoM observational data, the time series analyzed here was not long enough to isolate a definitive relationship between the HYCOM's performance and year. The observational data in the TOTO spans 13 years, though during the years 2009-2013 and 2017 a limited number of CTD casts were taken - seven or less casts were taken during these years and only two casts were taken in 2013. The temperature RMS error was the greatest in the TOTO in 2007 (1.0759 °C), while the smallest RMS error was in 2012 (0.5896 °C), with no discernable relationship between the RMS error and years. The salinity RMS error in the TOTO ranged between 0.1068 °C in 2013 and 0.4455 °C in 2011, also without an apparent relationship to the year.

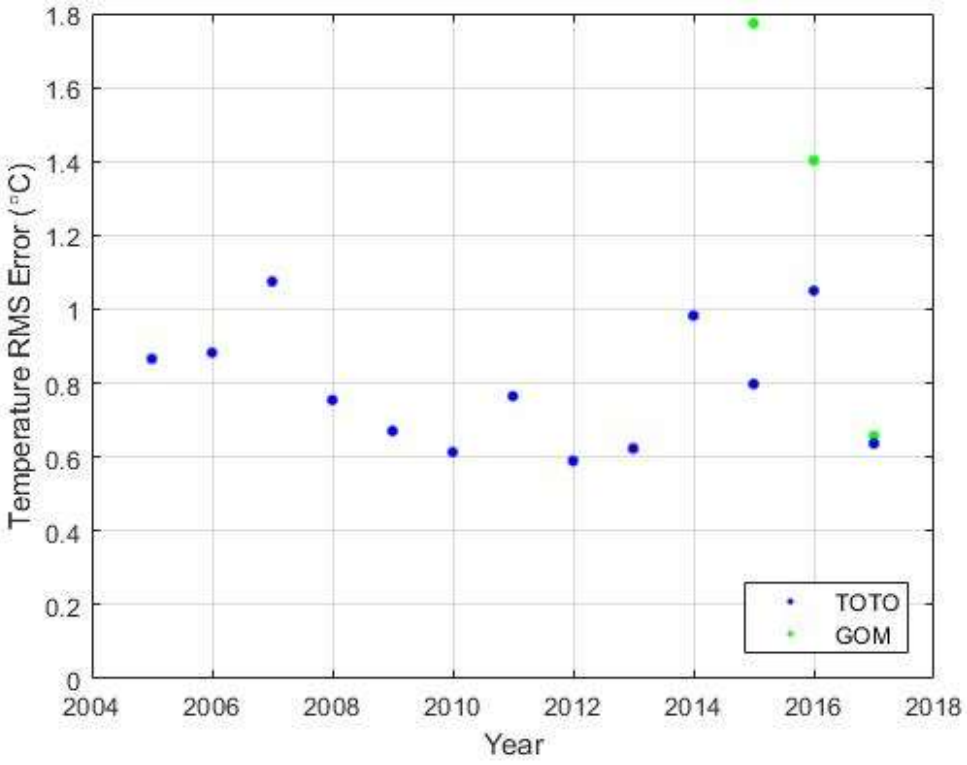

Figure 19: Temperature RMS Error vs Year

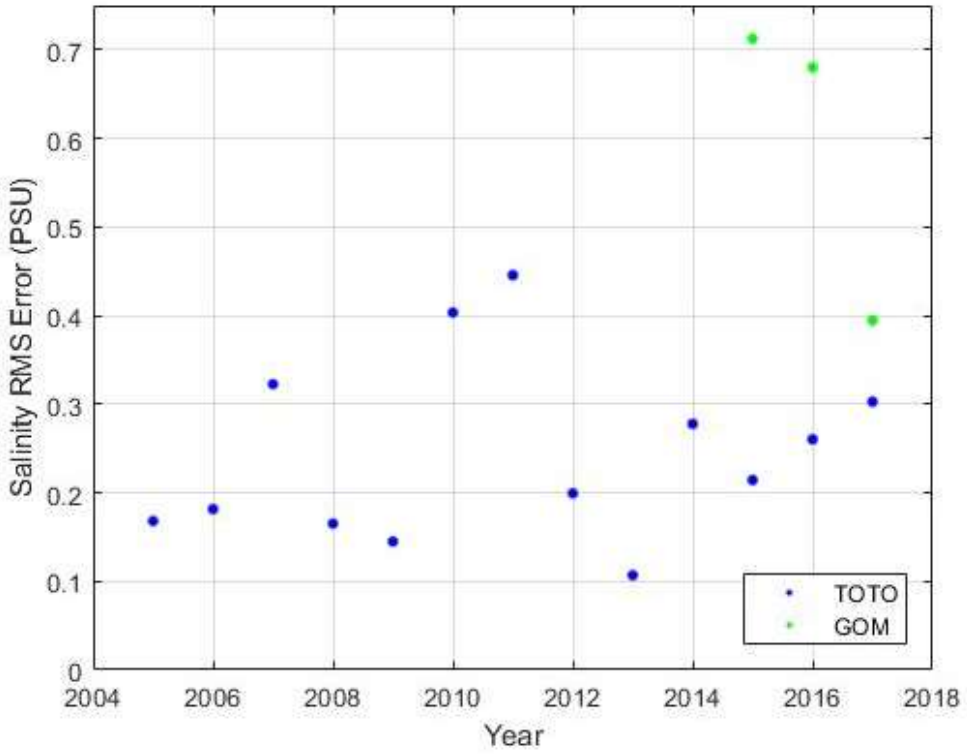

Figure 20: Salinity RMS Error vs Year

4.8 GoM Cruise Analysis of RMS Error

Although the research cruises in the GoM were only conducted during two months of the year for three years, the high volume of observational CTD casts taken during the five cruises made it possible to analyze the cruises individually. The temperature RMS error ranged from 0.6577 °C during cruise DP05 (May 2017) to the greatest RMS error of 1.9343°C during DP02 (August 2015) (Figure 21). With the exception of DP01 (May 2015), the temperature RMS error decreased over the course of the remaining four cruises (DP02 to DP05). The salinity RMS error ranged from 0.3945°C, occurring in DP05 (May 2017), to 0.8900°C during DP04 (August 2016) (Figure 22). The salinity RMS error decreased with each cruise, with the exception of DP04.

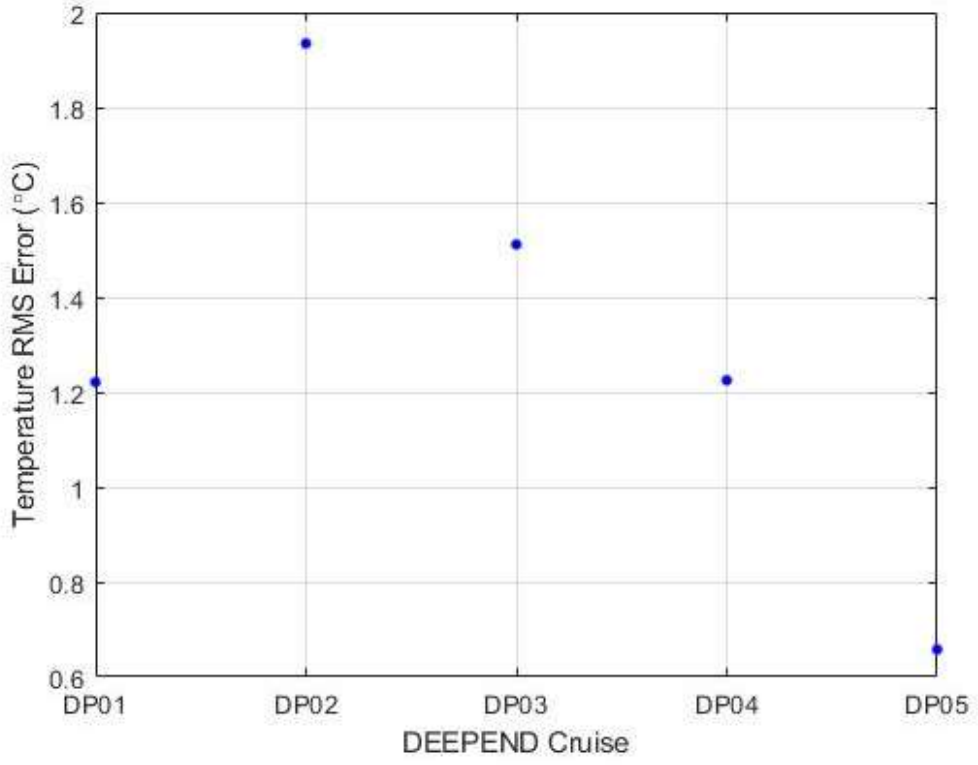

Figure 21: Temperature RMS Error vs GoM Cruise

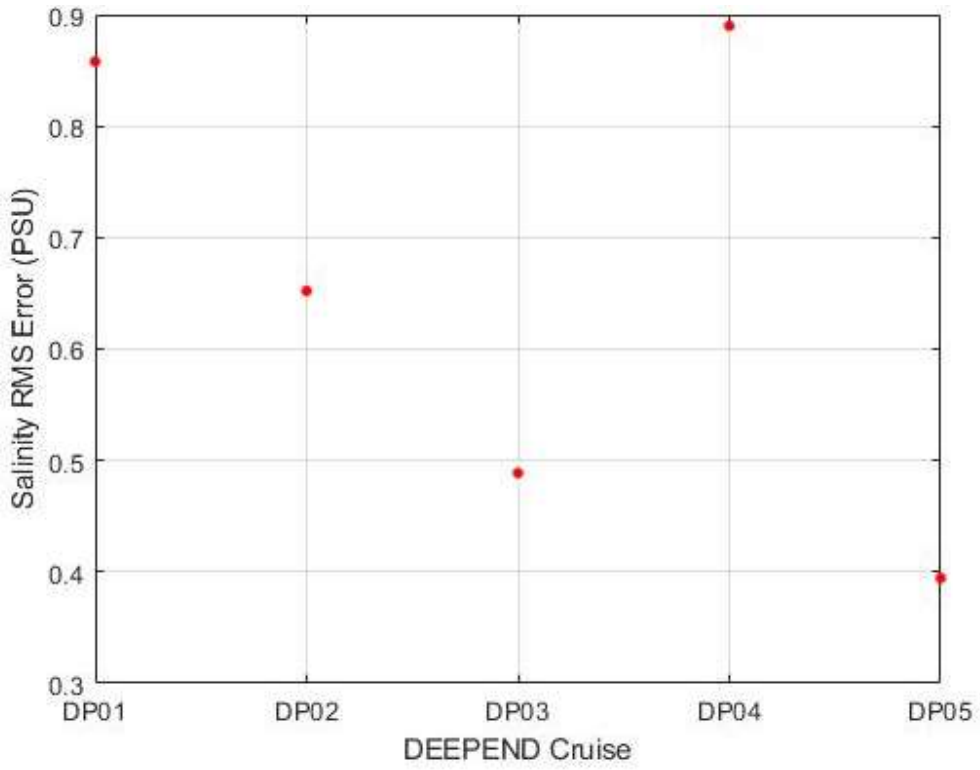

Figure 22: Salinity RMS Error vs GoM Cruise

4.9 Experiment Analysis of RMS Error

The observational data in the TOTO spans the course of 13 years and the GLBu0.08 configuration contains multiple experiments (both analysis and reanalysis) over this period which were used in this study. 171 CTD casts were collected in the TOTO from 2005 to 2012 and the reanalysis experiment 19.1 was used to analyze these casts. Four analysis experiments (90.9, 91, 91.1, and 91.2) were used for the remaining 57 casts collected between 2012 and 2017. The reanalysis and analysis overlapped approximately eight months in 2012, the HYCOM estimations during this period were analyzed as part of each experiment 19.1 and 90.9 with their corresponding CTD casts (4 casts) (Additional analysis in Section 4.11). For both temperature and salinity, the RMS error using the GOMI0.04 1/25° HYCOM configuration in the GoM (experiment 32.5) was higher than the RMS error in all analysis and reanalysis experiments used for the TOTO (Figure 23 and Figure 24, respectively). Within the GLBu0.08 1/12° configuration, there did not appear to be an

improvement between the analysis and reanalysis, nor within the analysis experiments. For both temperature and salinity, the RMS error was the least for experiment 90.9 and the greatest for experiment 91.2. It should be noted that there were far fewer casts during experiments 90.9 (6 casts) and 91 (5 casts), while experiments 19.1 covered the most (171 casts), while experiments 91.1 and 91.2 covered 29 and 17 CTD casts, respectively.

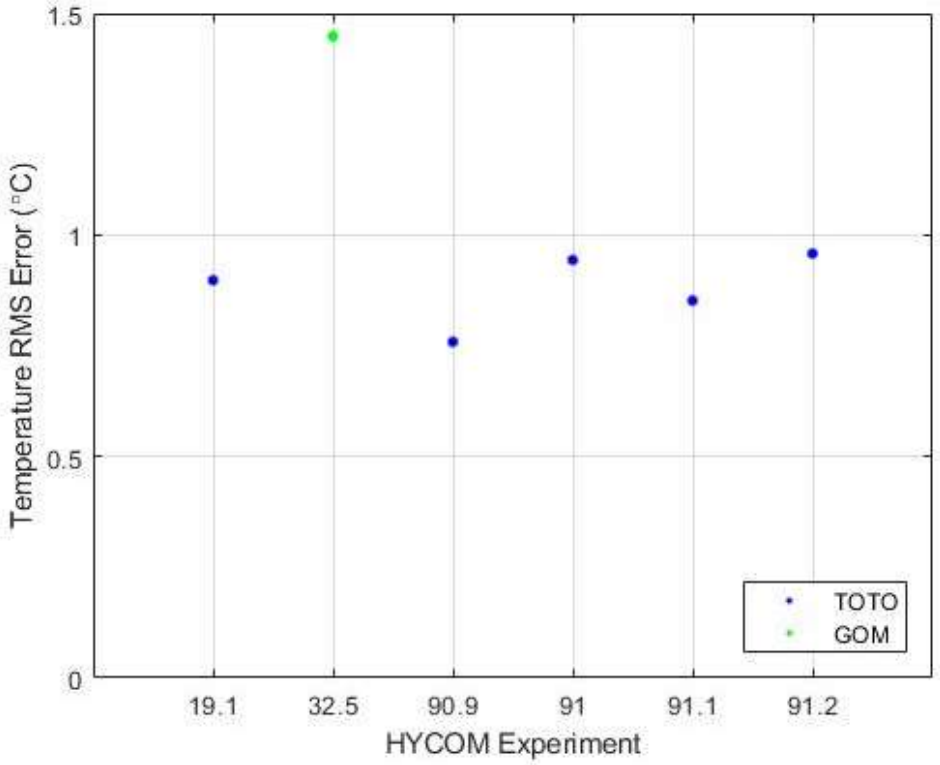

Figure 23: Temperature RMS Error vs Experiment

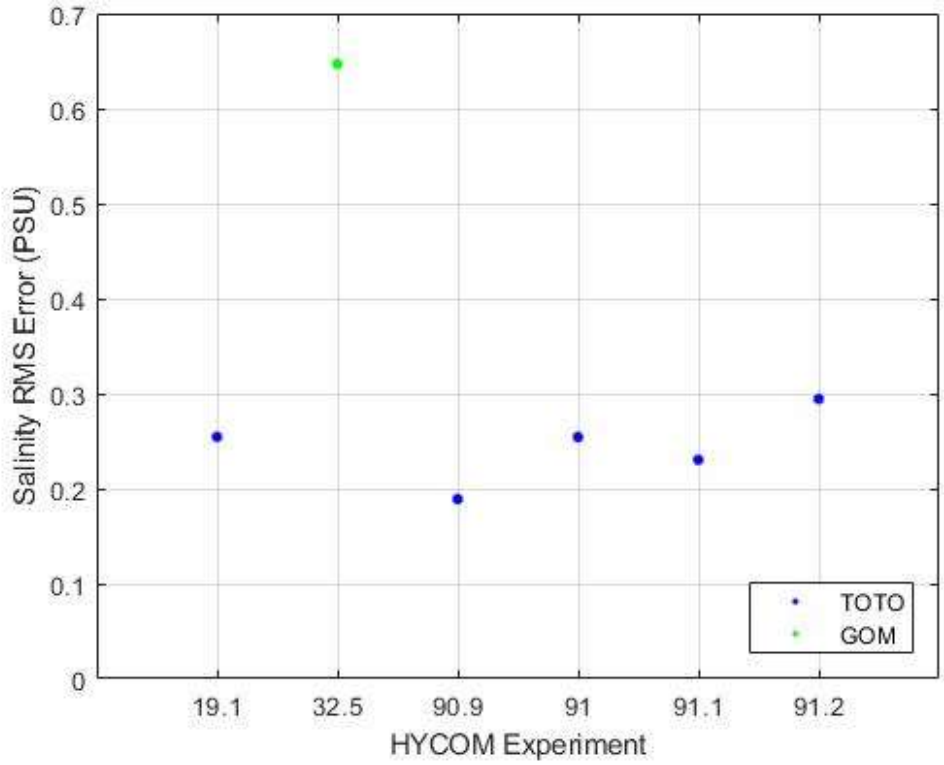

Figure 24: Salinity RMS Error vs Experiment

4.10 Quality Control of HYCOM data

In the GoM, the required HYCOM grid was unavailable for 0.04% of the data, the equivalent of one HYCOM data point. In the TOTO, the required HYCOM grid was unavailable for 6.47% and 6.51% of the temperature and salinity data, respectively (454 total data points). Overall statistics were evaluated to determine the impact of the HYCOM uncertainty on RMS error. In the GoM, the removal of the uncertain point resulted in a minimal change of RMS error on the order of 0.0003 °C for temperature and .0001 PSU for salinity Table 8). In the TOTO, the overall temperature RMS error decreased by 0.0343 °C, while the overall salinity RMS error increased by 0.0016 PSU (Table 9).

Table 8: Overall Statistics for the GoM with and without Quality Control of the HYCOM data

	Temperature			Salinity	
	Without Quality Control	With Quality Control		Without Quality Control	With Quality Control
Mean Error	-0.6690	-0.6690	**Mean Error**	-0.2099	-0.2100
Standard Deviation	1.2848	1.2851	**Standard Deviation**	0.6120	0.6121
RMSE	1.4483	1.4486	**RMSE**	0.6469	0.6470
Maximum	3.3746	3.3746	**Maximum**	7.7979	7.7979
Minimum	-6.8053	-6.8053	**Minimum**	-5.9452	-5.9452

Table 9: Overall Statistics for the TOTO with and without Quality Control of the HYCOM data

	Temperature			Salinity	
	Without Quality Control	With Quality Control		Without Quality Control	With Quality Control
Mean Error	-0.2898	-0.2798	**Mean Error**	-0.0157	-0.0152
Standard Deviation	0.8819	0.8491	**Standard Deviation**	0.2514	0.2531
RMSE	0.9282	0.8939	**RMSE**	0.2519	0.2535
Maximum	4.4187	4.4187	**Maximum**	4.2197	4.2197
Minimum	-8.7652	-8.0386	**Minimum**	-1.2424	-1.2424

The results in the TOTO were further evaluated to describe the influence of the missing HYCOM data on the RMS error. Evaluating the different depth levels in the TOTO, the RMS error changed the most at the deepest depth of 1250 meters, increasing for both salinity and temperature with the removal of the uncertain data points. For temperature (Appendix 46), the RMS error increases with the removal of the uncertain data points for all depths between 0 and 50 meters and at 1000 and 1250 meters and decreases between 60 and 900 meters. For salinity (Appendix 47), the RMS error increases with the removal of the uncertain data points at depths of 2 to 45 meters, 60 to 70 meters, 300 to 400 meters, 1000 and 1250 meters, while decreasing at 0 meters, 80 to 90 meters, 125 to 250 meters, 500 to 900 meters and remained unchanged at 50 and 100 meters. While evaluating the

different months analyzed for the TOTO data, the RMS error for temperature decreased with the removal of the data for all months with the exception of February (Appendix 49). For salinity, the RMS error increased in eight out of twelve months, only decreasing in March, April, October and November (Appendix 50). The RMS error for temperature decreased in nine of the years analyzed, increasing in 2007, 2008, and 2012, while remaining unchanged in 2009 (Appendix 52). Salinity RMS error also remained unchanged in 2009, while increasing in six of the years studied (2005, 2007, 2010, 2011, 2012, and 2017) and decreasing in six years (2006, 2008, 2013, 2104, 2015, and 2016)(Appendix 53). For the different HYCOM experiments, the RMS error for temperature decreased with the removal of uncertain data points for experiments 19.1, 91, 91.1 and 91.2, with a slight increase in error for experiment 90.9 (Appendix 55). For salinity, the RMS error decreased in experiments 91 and 91.1, increased by 0.0035 PSU for experiment 19.1, with a slight increase for experiments 90.9 and 91.2 (Appendix 56).

4.11 Reanalysis and Analysis RMS Error Comparison

The observational data in the TOTO spanned four experiments during the analysis (90.9, 91, 91.1, and 91.2) and one experiment during the reanalysis (19.1). The analysis and reanalysis overlap for approximately eight months, during which time six CTD casts were collected. Of the six CTD casts, two did not contain enough HYCOM data in the analysis to make a comparison. Of the remaining four CTD casts, a definitive conclusion cannot be made as to which experiment performed better during the overlap with the limited quantity of data. For temperature, experiment 19.1 performed better in the upper ocean for three of the four CTD casts, from the surface to at least 100 meters (Appendix 57). Experiment 19.1 also performed better in the upper ocean for two of the four casts for salinity (to at least 50 meters), while 90.9 performed better in the upper ocean in the other two casts (to at least 60 meters) (Appendix 58).

4.12 HYCOM Correction

Due to the complexity of the mean error as a function of the standard depth levels (Mean error data available in Table 10), Generalized Additive Models (GAM) were used

to find the optimal fit of the mean error data as a function of depth in each region. Using R Studio, a separate GAM was computed to find the optimal fit for each variable and predict its range within each region. The GAM for the temperature mean error in the GoM produced the best fit to the data, explaining 97% of the deviation with an R-squared of 0.959 (Appendix 59). The GAM for the GoM salinity mean error explained 79.4% of the deviation with an R-squared of 0.722 (Appendix 60). In the TOTO, the GAM for temperature mean error explained 89.9% of the deviation with an R-squared of 0.865 (Appendix 61). The GAM for salinity mean error in the TOTO explained 87.2% of the deviation with and R-squared of 0.842 (Appendix 62).

Table 10: Mean error data for each depth level in the GoM and the TOTO

GoM Depth Level	GoM Temperature Mean Error	GoM Salinity Mean Error	TOTO Depth Level	TOTO Temperature Mean Error	TOTO Salinity Mean Error
0	0.0916	-0.4655	**0**	0.0025	0.2719
5	-0.0899	-0.5941	**2**	-0.0875	0.0911
10	-0.0765	-0.7557	**4**	-0.1024	0.0327
15	-0.0785	-0.8031	**6**	-0.0896	0.0270
20	-0.0811	-0.6945	**8**	-0.1168	0.0219
25	-0.1053	-0.5731	**10**	-0.1282	0.0167
30	-0.1550	-0.4584	**12**	-0.1446	0.0131
40	-0.4401	-0.2513	**15**	-0.1604	0.0101
50	-0.7681	-0.1617	**20**	-0.1791	0.0083
60	-1.0190	-0.1055	**25**	-0.2138	0.0025
70	-1.1414	-0.1019	**30**	-0.2523	0.0003
80	-1.2261	-0.0772	**35**	-0.2720	-0.0041
90	-1.3596	-0.0794	**40**	-0.2890	-0.0082
100	-1.5425	-0.0891	**45**	-0.2904	-0.0138
125	-1.9958	-0.1888	**50**	-0.2719	-0.0246
150	-1.9262	-0.2320	**60**	-0.1907	-0.0423
200	-1.6078	-0.2260	**70**	-0.0531	-0.0552
250	-1.3428	-0.1910	**80**	0.0032	-0.0761
300	-1.0643	-0.1443	**90**	-0.0408	-0.1060
400	-0.7893	-0.0735	**100**	-0.1374	-0.1407
500	-0.6741	-0.0439	**125**	-0.8987	-0.2073
600	-0.6552	-0.0288	**150**	-1.3809	-0.2566
700	-0.5945	-0.0141	**200**	-1.0683	-0.1808
800	-0.5116	-0.0016	**250**	-1.0050	-0.1550
900	-0.4304	0.0030	**300**	-0.9756	-0.1250
1000	-0.3145	0.0087	**350**	-0.7801	-0.0706
1100	-0.1815	0.0106	**400**	-0.8493	-0.0461
1200	-0.0414	0.0111	**500**	-0.5244	0.0778
1300	0.0119	0.0144	**600**	0.1150	0.1934
1400	0.0006	0.0206	**700**	0.5172	0.2069
1500	-0.0303	0.0257	**800**	0.3940	0.0946
1750	-0.0703	0.0274	**900**	0.1808	0.0766
2000	-0.0564	0.0735	**1000**	0.5679	0.0962
			1250	0.9966	0.1882

5.0 Discussion and Conclusion

The primary focus of this study was to validate the HYCOM in the GoM and TOTO, achieved by comparing the HYCOM estimations to observational CTD cast data at standard depth levels. A comprehensive comparison of the vertical profile between the model and observational data characterized both oceanic areas of interest and provides insight to the application of HYCOM data in future applications in the respective basins. The results indicate that overall, the GLUb0.08 1/12° HYCOM configuration is a better fit in the TOTO than the GOMI0.04 1/25° HYCOM configuration is in the GoM for both temperature and salinity over the study period. When considering depth, the GLUb0.08 configuration fit in the TOTO for temperature was better in water depths shallower than 500 meters, while the GOMI0.04 configuration fit better for depths 500 meters and deeper. For salinity, the GLUb0.08 configuration was a better predictor in water depths shallower than 300 meters, while the GOMI0.04 configuration fit better at depths 300 meters and deeper. The long term and seasonal trends in GLUb0.08 configuration's fit to the TOTO did not show any trends of improving or worsening over the 13 years the study span or over the change of seasons.

Seasonal variation in the TOTO CTD data was observed in the upper 150 meters. This variation is likely because waters of the TOTO are subject to seasonal variation in precipitation and the influx of high salinity waters from surrounding shallow banks. Therefore, salinity remains high in the winter dry season, while surface salinity is lower in the wet summer months. The surface temperature range in this study also fluctuated with the seasons, as did the depth of the thermocline. Interestingly, the highest mean error was found at the depth of the prominent thermocline (150 meters).

Prior research characterized hydrographic station data for one location in the TOTO in 1956 (See Figure 25 in Shonting (1970)). The study found that the TOTO is made up of North Atlantic Central Water (NAWC) and North Atlantic Deep Water (NADW). NAWC was found at depths greater than 400 meters, defined by water temperatures between +4°C and +17°C and salinity between 35 PSU and 36.3 PSU, while NADW is between 1500 and 2000 meters and the sea floor and defined by water temperature between

+2°C and +4°C and salinity between 34.9 PSU and 35.0 PSU. The TOTO's observational data from the present study (Figure 26), falls into the same characterizations as the data collected in 1956, albeit with slightly warmer bottom water. For waters deeper than 1500 meters, the minimum and maximum water temperatures were 3.41°C and 4.52°C respectively, while the salinity maximum was 34.94 PSU and the minimum was 35.01 PSU.

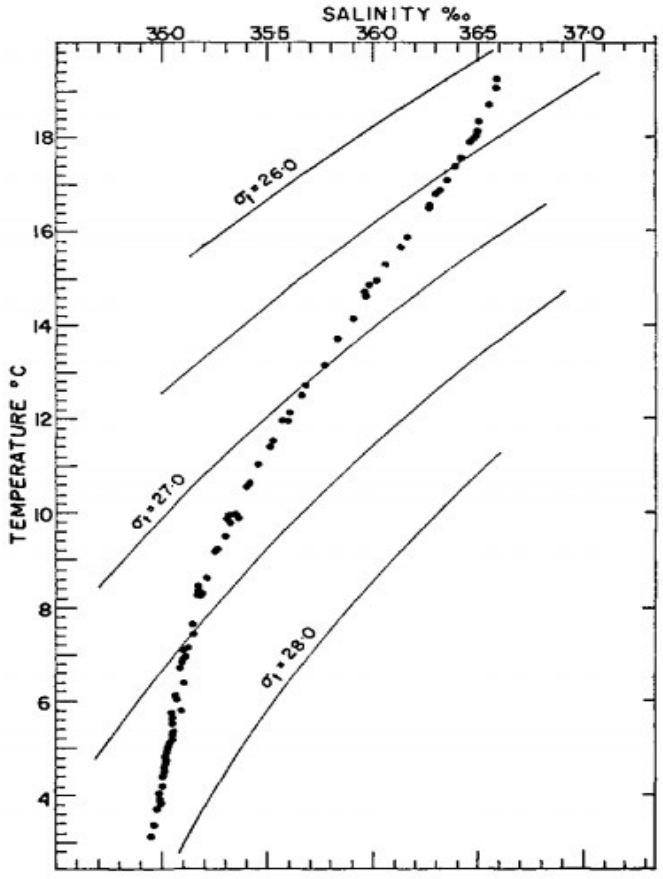

Figure 25: Temperature-Salinity relationship in the TOTO from 1956 data collection (Shonting, D. H., 1970)

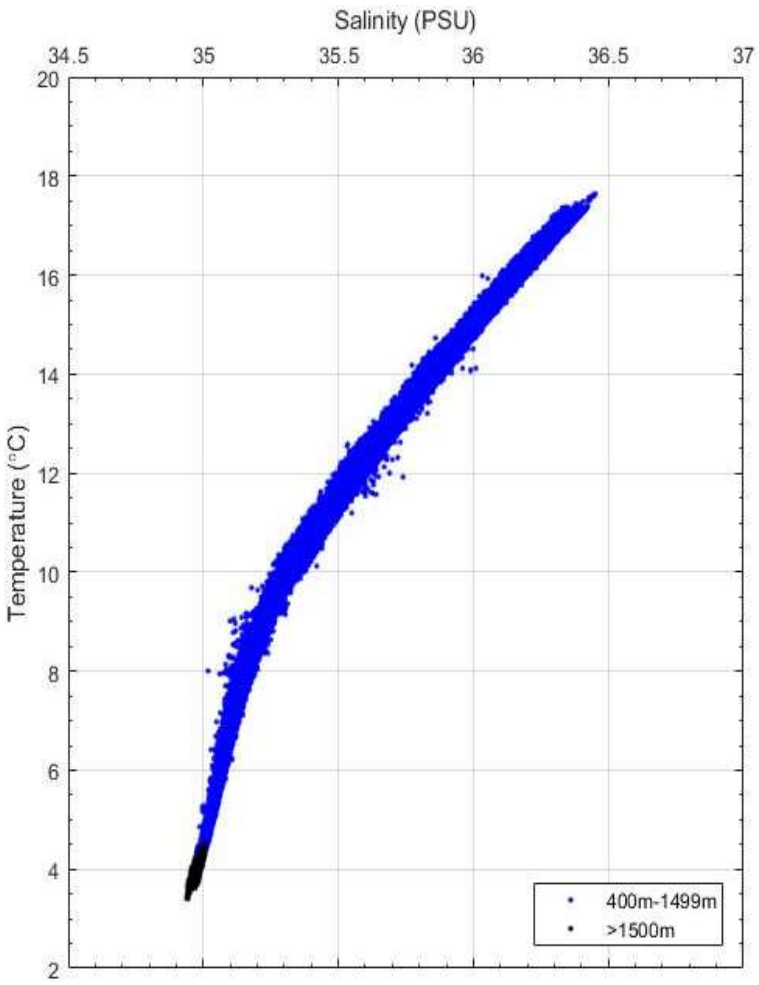

Figure 26: Temperature -Salinity Relationship in the TOTO between 2005 and 2017. Data collected between 400 and 1500 meters are displayed in blue, while data deeper than 1500 meters are in black.

The GoM is a more dynamic region than the TOTO with influences from the different water types (LC, GCW, and MIX) and fresh water input from river water. As such the thermocline and salinity profiles in the GoM were not static over the course of a month as they were in the TOTO for the study period. The profiles in August 2015 and August 2016 were similar, offering more variability over the duration of the cruise. The data in May 2015 and May 2017 showed less variation through the water column, while the cruise in May 2016 was more variable and consistent with the data collected in August. In the GoM the largest mean error for temperature was between a depth of 125 and 150 meters. The largest error for salinity was concentrated at the surface with a second rise in

mean error around 150 meters. The variability observed between cruises can likely be explained by the location of the LC and its associated eddies.

The GoM was characterized by DEEPEND personnel for water features present during cruises DP01 through DP04 (May 2015 and August 2016) (Figure 27). They found that during DP01 (May 2015) CTD samples were taken in GCW, during DP02 (August 2015) samples were taken in GCW, MIX, and LCOW, during DP03 (May 2016) samples were collected in GCW and MIX, and during DP04 (August 2016) samples were collected in GCW, MIX, and LCOW. Although the features indicate that DP03 was collected in similar waters as DP01, the temperature and salinity profiles of DP03 assembled for this study resemble casts taken through the conditions present in both DP02 and DP04. Three samples from DP03 bordered the LCOW, resulting in MIX conditions, these three samples correlate with the present study which found a temperature profile with two deep thermoclines (60-80 meter and 130-140 meter) and warmer surface temperatures compared to those of the remaining DP03 samples. These MIX conditions can likely explain deviation of the DP03 temperature and salinity profiles from those collected during DP01 and DP05.

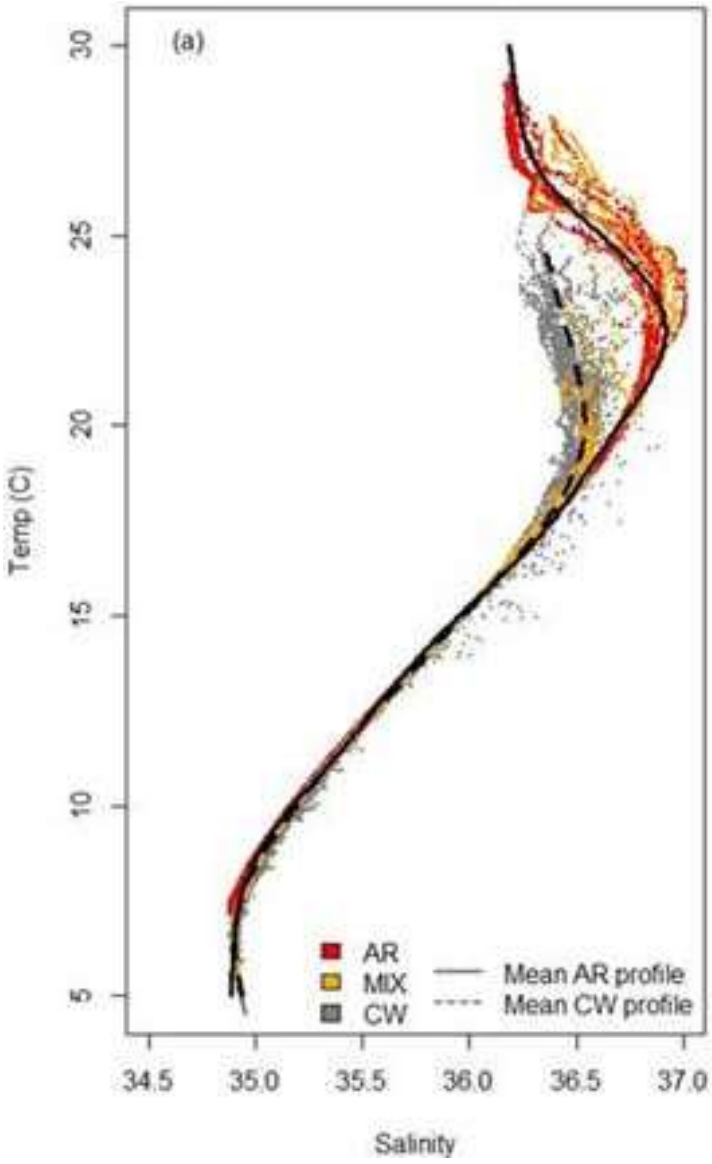

Figure 27: Temperature-Salinity relationship in the GOM of DP01-DP04 (Johnston et al., in review)

This study's validation of the HYCOM in the GoM and TOTO was a first step in evaluating the performance of the model in the interior ocean for the regions of interest in this study. It should be noted however that this study has limitations. For example, the data in the TOTO spanned 13 years, but the number of casts available by year or month were limited, and in the GoM observational data were of high resolution during May and August, but lacked consistent data collection over time to analyze seasonal and long-term

dependability. Therefore, future studies that aim to validate the model should collect CTD or XCTD casts at more frequent and regular intervals in order to increase the confidence in the HYCOM's performance. XBT casts are also taken in the TOTO in support of U.S. Navy testing and could be used for validation, though they only measure temperatures. Still, evaluating the XBTs against the HYCOM could fill in additional gaps in the historical time scale for the water temperature.

More than half (59%) of the CTD casts in the TOTO extend deeper than the HYCOM's estimation - most of the HYCOM data only extended half to two-thirds of the 1,800 meter total depth of the TOTO. As AUTEC's testing utilizes the entire water column, removing the depth constraint used by the HYCOM would provide a complete estimation that could be used to evaluate the deep interior of the TOTO. Additionally, the reanalysis uses a bathymetry contour close to the coastline, which is likely why the complete HYCOM grid was available during the reanalysis but not for the analysis (experiment 90.9) during the same time period. As further reanalysis model runs become available, it would be valuable to compare these data to the analysis data to validate closer to the coastline and ideally to deeper TOTO depths. Further evaluation of the reanalysis would also show more reliable long-term trends in the HYCOM's performance.

This study used the HYCOM GOMI0.04 configuration in the GoM and the GLUb0.08 configuration in the TOTO, yet the spatial extent of each HYCOM configuration includes both the GoM and the TOTO. An evaluation of the 1/12° GLUb0.08 configuration in the GoM would allow for a direct performance assessment between the two model configurations (GLUb0.08 and GOMI0.04) with the same set of DEEPEND observational data. Additionally, a direct assessment could be made in the TOTO between the two model configurations using the AUTEC observational CTD data. The GLUb0.08 configuration has a finer depth resolution in the upper ocean, making a comparison between the two configurations invaluable for GoM applications near the surface. The horizontal resolution of the GOMI0.04 configuration is finer than the GLUb0.08 configuration, although the TOTO is proximal to the boundary of the GOMI0.04 model configuration. Further evaluation of the GOMI0.04 configuration in the TOTO would identify if model boundary limitations impact the HYCOM's performance or show if

AUTEC could benefit from the increased spatial resolution. Additionally, the GLUb0.08 reanalysis is available in both daily snapshots taken at zero UTC and 3-hour snapshots. This study evaluated the reanalysis' daily snapshot in the TOTO. The 3-hour snapshots account for local diurnal effects that may be aliased during the daily snapshot. A comparison of the two temporal resolutions available in the reanalysis would be invaluable for determining the influence of the local effect on fine time scale.

A thorough understanding of HYCOM validity in the GoM and the TOTO can be used to help characterize the impact of ocean dynamics on deep pelagic fauna and enhance acoustical accuracy for naval exercises, respectively. For DEEPEND, mesoscale features in the GoM may dramatically impact the native biology, therefore a validated HYCOM can provide DEEPEND with reliable insight into this dynamic ocean region. Furthermore, by understanding the discrepancies between the HYCOM and observational ocean conditions, DEEPEND can apply the correction factor outlined here to adjust HYCOM outputs to better match true ocean conditions in the GoM. The mission at NUWC det. AUTEC is to provide precise under water tracking. This is possible by determining the sound velocity profile of the water column, but doing so requires an accurate knowledge of changing ocean conditions. As the climate warms, the sound velocity profile and ocean dynamics of the TOTO may shift more rapidly, and by using the HYCOM model's forecast feature, AUTEC may be able to predict these rapid shifts. Without the use of an ocean model such as HYCOM, sound velocity discrepancies are currently isolated too late, only after experiencing poor underwater track. By using HYCOM's five day forecast in conjunction with the correction noted here, early indications of annual and decadal variability within the basin may be detected and allow AUTEC to update their sound velocity profiles in advance, avoiding delays and inaccuracies in testing.

Acknowledgements

I would like to thank my advisor Dr. Matthew Johnston for his guidance and patience. His expertise of the HYCOM and the research conducted by the DEEPEND Consortium were invaluable throughout this study. I would also like to thank my committee members Adam Akif who allowed me to pursue this study with the use of AUTEC data, it would not be the project I envisioned without it, and Dr. Bernard Riegl for his time and perspective during this process. Special thanks to Robin Bolin, Zan Milligan and David English for their insight into the observational data in each region. I thank Zahra Shivji who took time out of her busy schedule to assist with processing data. I deeply appreciate the love, encouragement and support my family has given me throughout this long process, you mean the world to me. I am thankful for my coworkers and friends at NUWC det. AUTEC and NSWC Carderock det. Fort Lauderdale for their endless support and encouragement while I pursue my Master's Degree and advanced my career. I thank the faculty, students and staff at Nova Southeastern University's Halmos College of Natural Sciences and Oceanography for their endless knowledge, support and encouragement. And lastly, Cusco for always being happy to see me at the end of the longest of days and raising my spirits no matter the obstacle I encountered during this process.

References

Bleck, R., Dean, S., O'Keefe, M., & Sawdey, A. (1995). A comparison of data-parallel and message-passing versions of the Miami Isopycnic Coordinate Ocean Model (MICOM). *Parallel computing*, *21*(10), 1695-1720.

Boyer, T. P., & Levitus, S. (1994). *Quality control and processing of historical oceanographic temperature, salinity, and oxygen data* (Vol. 81). US Department of Commerce, National Oceanic and Atmospheric Administration, National Environmental Satellite, Data, and Information Service.

Bryan, K. (1969). A numerical method for the study of the circulation of the world ocean. *Journal of computational physics*, *4*(3), 347-376.

Castellanos, P., Campos, E. J. D., Giddy, I., & Santis, W. (2016). Inter-comparison studies between high-resolution HYCOM simulation and observational data: The South Atlantic and the Agulhas leakage system. *Journal of Marine Systems*, *159*, 76-88.

Cecil, J.B., (1992). Underwater Hydrophone Location Survey. 24th Annual Precise Time and Time Interval (PTTI) Applications and Planning Meeting. McLean, Virginia. 1992. United States, NASA. Goddard Space Flight Center.

Chassignet, E. P., Smith, L. T., Halliwell, G. R., & Bleck, R. (2003). North Atlantic simulations with the Hybrid Coordinate Ocean Model (HYCOM): Impact of the vertical coordinate choice, reference pressure, and thermobaricity. *Journal of Physical Oceanography*, *33*(12), 2504-2526.

Chassignet, E. P., Hurlburt, H. E., Smedstad, O. M., Halliwell, G. R., Hogan, P. J., Wallcraft, A. J., & Bleck, R. (2006). Ocean prediction with the hybrid coordinate ocean model (HYCOM). *Ocean weather forecasting*, 413-426.

Chassignet, E. P., Hurlburt, H. E., Smedstad, O. M., Halliwell, G. R., Hogan, P. J., Wallcraft, A. J., ... & Bleck, R. (2007). The HYCOM (hybrid coordinate ocean model) data assimilative system. *Journal of Marine Systems*, *65*(1), 60-83.

Chassignet, E. P., Hurlburt, H. E., Metzger, E. J., Smedstad, O. M., Cummings, J. A., Halliwell, G. R., ... & Tolman, H. L. (2009). US GODAE: global ocean prediction with the HYbrid Coordinate Ocean Model (HYCOM). *Oceanography*, *22*(2), 64-75.

Chassignet, E. P. & Wallcraft A. J. (2016). HYCOM (Hybrid Coordinate Ocean Model) and CESM [PowerPoint slides]. Retrieved from http://www.cesm.ucar.edu/events/workshops/ws.2016/presentations/cross/chassignet.pdf

Crease, J., DAUPHINEE, T., Grose, P. L., Lewis, E. L., Fofonoff, N. P., Plakhin, E. A., ... & Zenk, W. (1988). The acquisition, calibration and analysis of CTD data. *UNESCO Tech. Pap. Mar. Sci*, *54*, 94.

Dee, D. P. (1995). A pragmatic approach to model validation. *Quantitative Skill Assessment for Coastal Ocean Models*, 1-13.

DEEPEND. (2017 a). DEEPEND (DEEP-Pelagic Nekton Dynamics) Consortium Project Summary. Retrieved from http://www.deependconsortium.org/index.php/about

DEEPEND. (2017 b). Mesoscale Physical Oceanography. Retrieved from http://www.deependconsortium.org/index.php/research/environmental-variability/mesoscale-physical-oceanography

Gulf of Mexico Research Initiative. (2013). GoMRI Mission. Retrieved from http://gulfresearchinitiative.org/about-gomri/gri-mission/

HYCOM. (2017 a). HYCOM + NCODA Global 1/12° Analysis. Retrieved from https://hycom.org/dataserver/gofs-3pt0/analysis

HYCOM. (2017 b). HYCOM Overview. Retrieved from https://hycom.org

Johnson, D. R., Boyer, T. P., Garcia, H. E., Locarnini, R. A., Baranova, O. K., & Zweng, M. M. (2013). World Ocean Database 2013 User's Manual.

Johnston, M. W., Milligan, R. J., Easson, C. G., deRada S., English, D. C., Penta, B., & Sutton, T. T. (in review). Characterizing Pelagic Habitats in the Gulf of Mexico Using Model, Empirical, and Remotely-Sensed Data.

Kara, A. B., & Hurlburt, H. E. (2006). Daily inter-annual simulations of SST and MLD using atmospherically forced OGCMs: Model evaluation in comparison to buoy time series. *Journal of Marine Systems*, *62*(1), 95-119.

Kantha, L. H., & Clayson, C. A. (2000). *Numerical models of oceans and oceanic processes* (Vol. 66). Academic press.

Kelly, K. A., Thompson, L., Cheng, W., & Metzger, E. J. (2007). Evaluation of HYCOM in the Kuroshio Extension region using new metrics. *Journal of Geophysical Research: Oceans*, *112*(C1).

Levitus, S. (1982). Climatological Atlas of the World Ocean, NOAA/ERL GFDL Professional Paper 13, Princeton, NJ, 173 pp. *NTIS PB83-184093*.

Levitus, S., & Boyer, T. P. (1994). *World ocean atlas 1994. Volume 4. Temperature* (No. PB--95-270112/XAB; NESDIS--4). National Environmental Satellite, Data, and Information Service, Washington, DC (United States).

Levitus, S., & Oort, A. H. (1977). Global analysis of oceanographic data. *Bulletin of the American Meteorological Society*, *58*(12), 1270-1284.

Liu, Y., Weisberg, R. H., Hu, C., & Zheng, L. (2011). Tracking the Deepwater Horizon oil spill: A modeling perspective. *Eos, Transactions American Geophysical Union*, *92*(6), 45-46.

Luo, J. J., Masson, S., Behera, S. K., & Yamagata, T. (2008). Extended ENSO predictions using a fully coupled ocean–atmosphere model. *Journal of Climate*, *21*(1), 84-93.

Madec, G., Delecluse, P., Imbard, M., & Levy, C. (1997). Ocean general circulation model reference manual. *Note du Pôle de modélisation*.

Mamayev, O. I., Dooley, H., Millard, R. C., Taira, K., & Morcos, S. (1991). Processing of oceanographic station data. *Joint panel on Oceanographic Tables and Standards (JPOTS) UNESCO 138pp*.

Metzger, E. J., Helber, R. W., Hogan, P. J., Posey, P. G., Thoppil, P. G., Townsend, T. L., ... & Phelps, M. W. (2017). *Global Ocean Forecast System 3.1 Validation Test*. NAVAL RESEARCH LAB STENNIS DETACHMENT STENNIS SPACE CENTER MS STENNIS SPACE CENTER United States.

Millard, R. C., & Yang, K. (1993). *CTD calibration and processing methods used at Woods Hole Oceanographic Institution*. Woods Hole Oceanographic Institution.

Milligan, R. J. (2017). Generalized Additive Models (GAMs) [PowerPoint presentation]. Retrieved from NSU. Biostatistics.

Rattray Jr, M. (1962, January). Interpolation errors and oceanographic sampling. In *Deep Sea Research and Oceanographic Abstracts* (Vol. 9, No. 1-2, pp. 25-37). Elsevier.

Reiniger, R. F., & Ross, C. K. (1968, April). A method of interpolation with application to oceanographic data. In *Deep Sea Research and Oceanographic Abstracts* (Vol. 15, No. 2, pp. 185-193). Elsevier.

Ridley, E. L. (1962). *A Preliminary Study of the Oceanography of the Tongue of the Ocean, Bahamas* (No. NOO-IM-O-39-62). NAVAL OCEANOGRAPHIC OFFICE WASHINGTON DC MARINE SCIENCES DEPT.

Robinson, L. M., Elith, J., Hobday, A. J., Pearson, R. G., Kendall, B. E., Possingham, H. P., & Richardson, A. J. (2011). Pushing the limits in marine species distribution modelling: lessons from the land present challenges and opportunities. *Global Ecology and Biogeography*, *20*(6), 789-802.

Sandvik, A. D., Skagseth, Ø., & Skogen, M. D. (2016). Model validation: Issues regarding comparisons of point measurements and high-resolution modeling results. *Ocean Modelling*, *106*, 68-73.

Semtner, A. J. (1986). History and methodology of modelling the circulation of the world ocean. In *Advanced Physical Oceanographic Numerical Modelling* (pp. 23-32). Springer, Dordrecht.

Shchepetkin, A. F., & McWilliams, J. C. (2005). The regional oceanic modeling system (ROMS): a split-explicit, free-surface, topography-following-coordinate oceanic model. *Ocean Modelling*, *9*(4), 347-404.

She, J., Berg, P., Høyer, J. L., Larsen, J., & Nielsen, J. W. (2006). On operational three dimensional hydrodynamic model validation. In *Proceedings of EuroGOOS 4th Conference* (pp. 519-526).

Shonting, D. H. (1970). On the Distribution of Temperature, Salinity, and Oxygen in the Tongue of the Ocean, Bahamas. *Bulletin of Marine Science*, *20*(1), 35-56.

Sutton, Tracey. CTD data salinity, temperature, depth for Cruise DP01 R/V Point Sur in-situ deep seawater and associated fauna, May 1-8, 2015, Viosca Knoll GoM. 2015. Distributed by: Gulf of Mexico Research Initiative Information and Data Cooperative (GRIIDC), Harte Research Institute, Texas A&M University – Corpus Christi. doi: 10.7266/N73R0QSX

Sutton, Tracey. CTD data salinity, temperature, depth for Cruise DP02 R/V Point Sur in-situ deep seawater and associated fauna, August 8-22, 2015, Viosca Knoll GoM. 2016. Distributed by: Gulf of Mexico Research Initiative Information and Data Cooperative (GRIIDC), Harte Research Institute, Texas A&M University – Corpus Christi. doi: 10.7266/N7PV6HS1

Sutton, Tracey. Conductivity, temperature and depth (CTD) data for DEEPEND stations, cruise DP03, May 2016. 2018 a. Distributed by: Gulf of Mexico Research Initiative Information and Data Cooperative (GRIIDC), Harte Research Institute, Texas A&M University – Corpus Christi. doi: 10.7266/N7R49P43

Sutton, Tracey. Conductivity, temperature and depth (CTD) data for DEEPEND stations, cruise DP04, August 2016. 2017. Distributed by: Gulf of Mexico Research Initiative Information and Data Cooperative (GRIIDC), Harte Research Institute, Texas A&M University – Corpus Christi. doi: 10.7266/N7MC8XDC

Sutton, Tracey. Conductivity, temperature and depth (CTD) data for DEEPEND stations, cruise DP05, May 2017. 2018 b. Distributed by: Gulf of Mexico Research Initiative Information and Data Cooperative (GRIIDC), Harte Research Institute, Texas A&M University – Corpus Christi. doi: 10.7266/N7GM85P1

Wallcraft, A. J., Hurlburt, H. E., Townsend, T. L., & Chassignet, E. P. (2005). 1/25 degree Atlantic Ocean simulation using HYCOM. In *Users Group Conference, 2005* (pp. 222-225). IEEE.

Wallcraft, A. J. (2014, October 14). Global analysis vs Global reanalysis, which is more accurate in temperature profile? [Online discussion group]. Retrieved from https://groups.google.com/a/hycom.org/forum/#!msg/forum/-tj-6nLL1_Y/TMBKHQbvzosJ

Wallcraft, A. J. (2015, March 7). Global Analysis and Global Reanalysis [Online discussion group]. Retrieved from https://groups.google.com/a/hycom.org/forum/#!topic/forum/yguvJxnxDPE/discussion

Wood, S. N. (2006). *Generalized additive models: an introduction with R*. Chapman and Hall/CRC.

Urick, R. J. (1983). *Principals of Underwater Sound*.

U.S. Naval Research Laboratory. (2017). Global Ocean Forecast System (GOFS) 3.1. Retrieved from https://www7320.nrlssc.navy.mil/dynamic/gofs/gofs.php

U.S. Navy. (1967). Environmental Atlas of the Tongue of the Ocean Bahamas. U.S. Naval Oceanographic Office, Spec. Publ. SP-94.

Appendices

Appendix 1: Standard Depth Levels used in the GOMI0.04 and the GLBu0.08 HYCOM Configurations

Standard Level	GoMI0.04 Standard Depths	GLBu0.08 Standard Depths	Standard Level	GoMI0.04 Standard Depths	GLBu0.08 Standard Depths
1	0	0	21	500	125
2	5	2	22	600	150
3	10	4	23	700	200
4	15	6	24	800	250
5	20	8	25	900	300
6	25	10	26	1000	350
7	30	12	27	1100	400
8	40	15	28	1200	500
9	50	20	29	1300	600
10	60	25	30	1400	700
11	70	30	31	1500	800
12	80	35	32	1750	900
13	90	40	33	2000	1000
14	100	45	34	2500	1250
15	125	50	35	3000	1500
16	150	60	36	3500	2000
17	200	70	37	4000	2500
18	250	80	38	4500	3000
19	300	90	39	5000	4000
20	400	100	40	5500	5000

Appendix 2: Ocean basin boundaries as defined in World Ocean Database 2013. The GoM and the TOTO both fall within the boundaries of the North Atlantic. (Johnson et al., 2013)

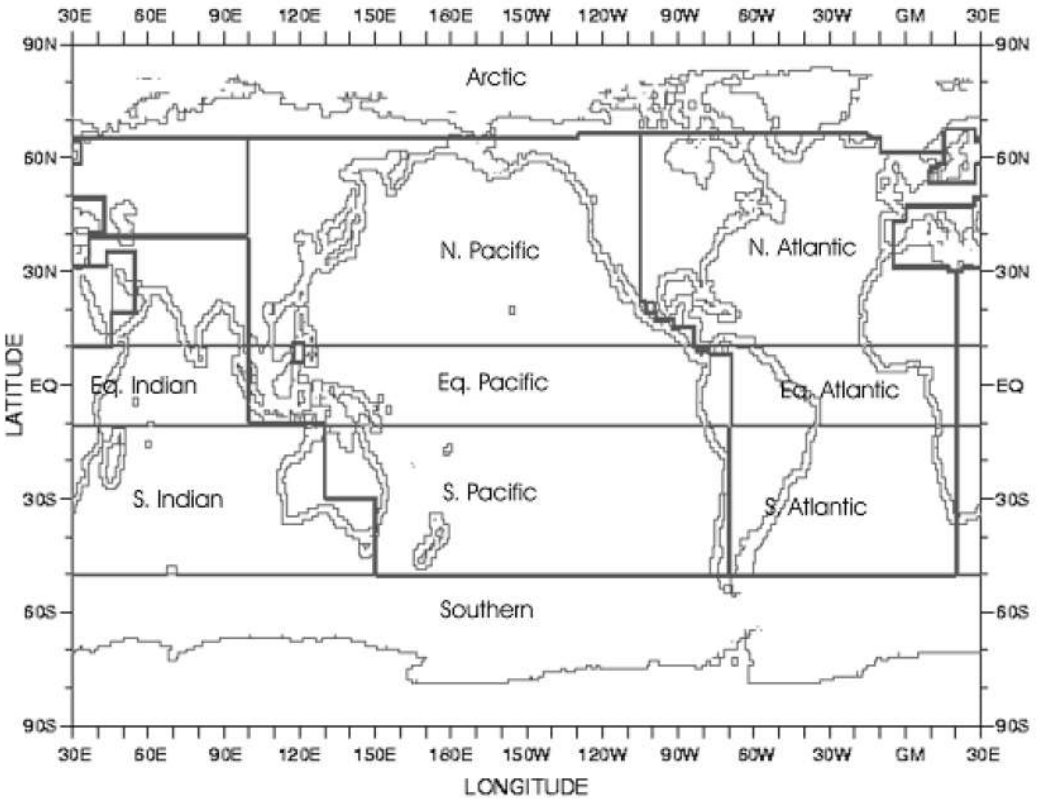

Appendix 3: Observational Temperature Data vs Depth in the GoM during May 2015

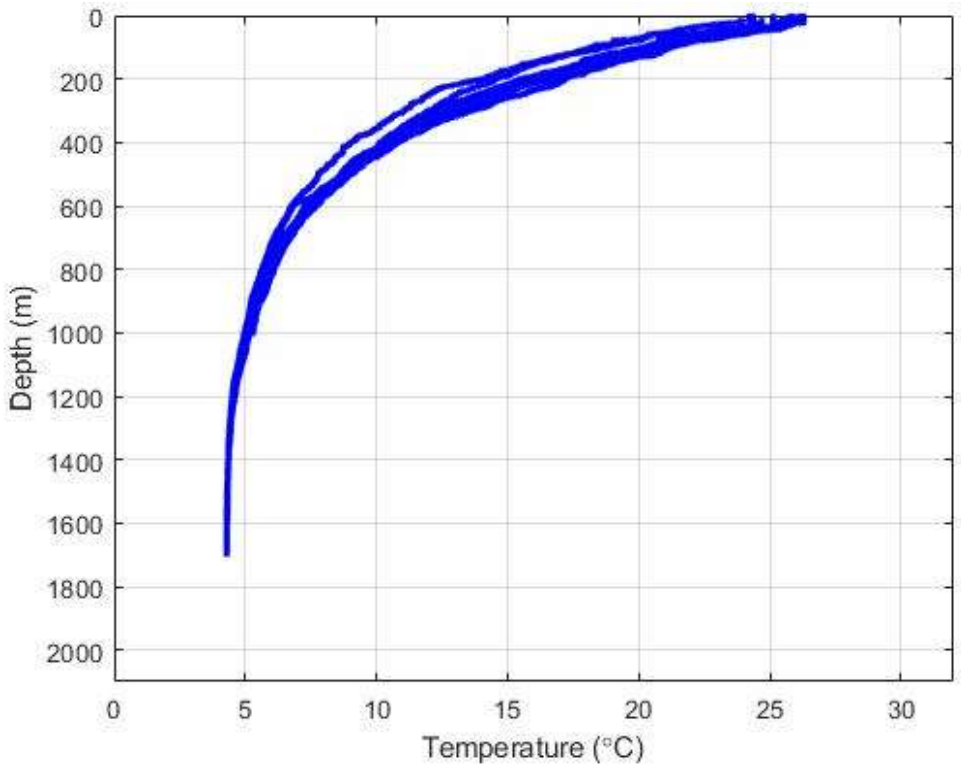

Appendix 4: Observational Salinity Data vs Depth in the GoM during May 2015

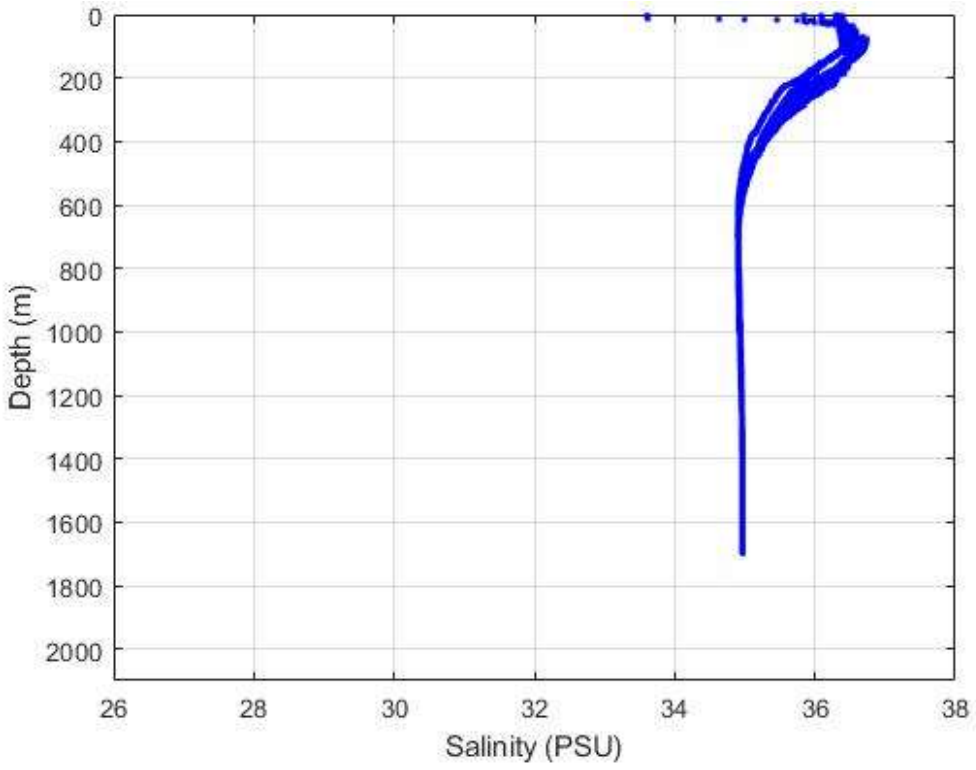

Appendix 5: Observational Temperature Data vs Depth in the GoM during August 2015

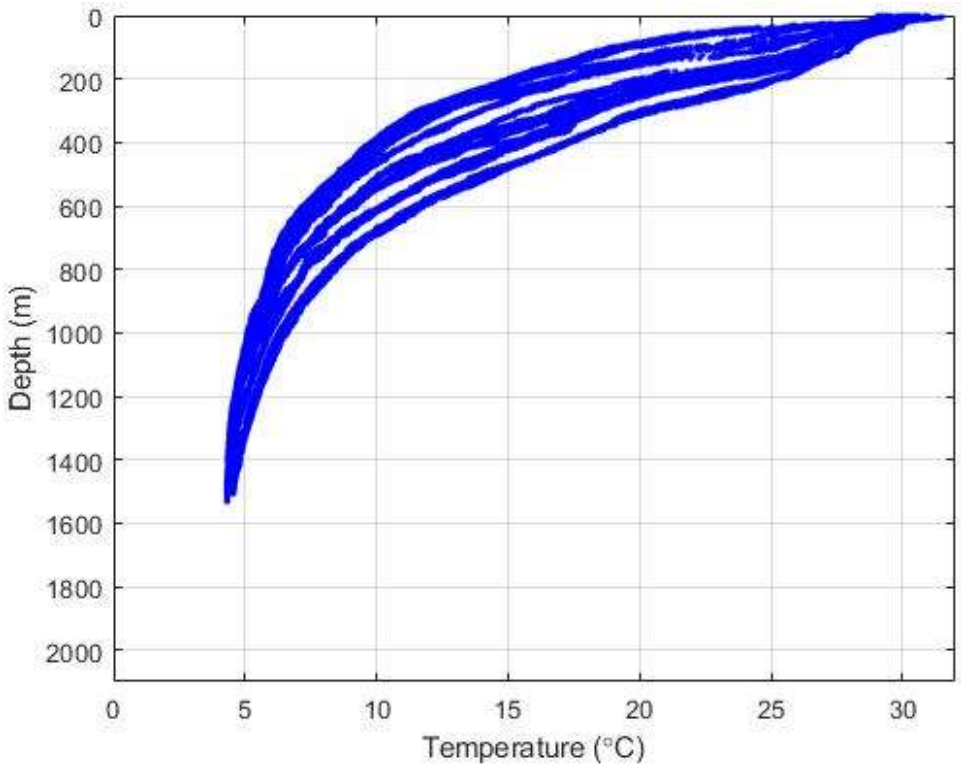

Appendix 6: Observational Salinity Data vs Depth in the GoM during August 2015

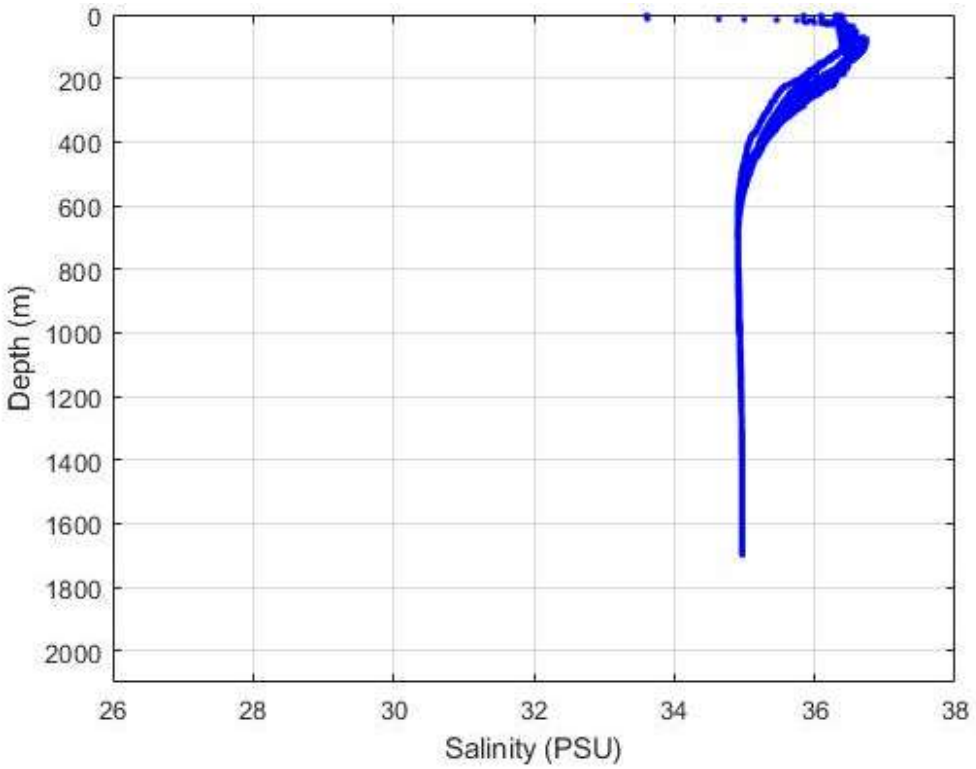

Appendix 7: Observational Temperature Data vs Depth in the GoM during May 2016

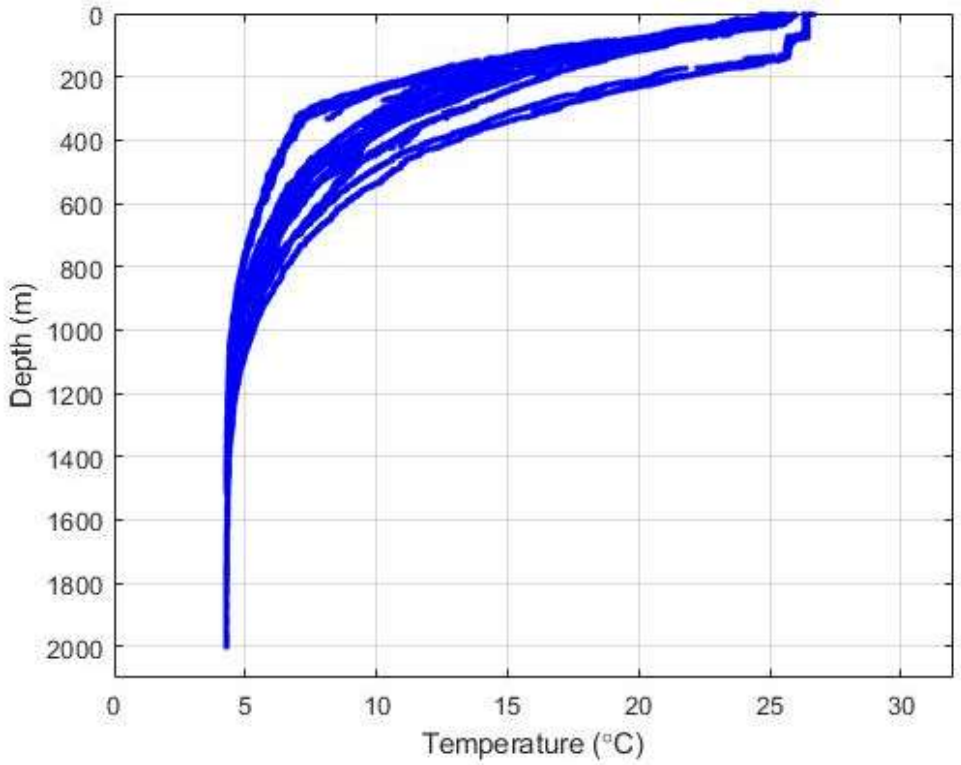

Appendix 8: Observational Salinity Data vs Depth in the GoM during May 2016

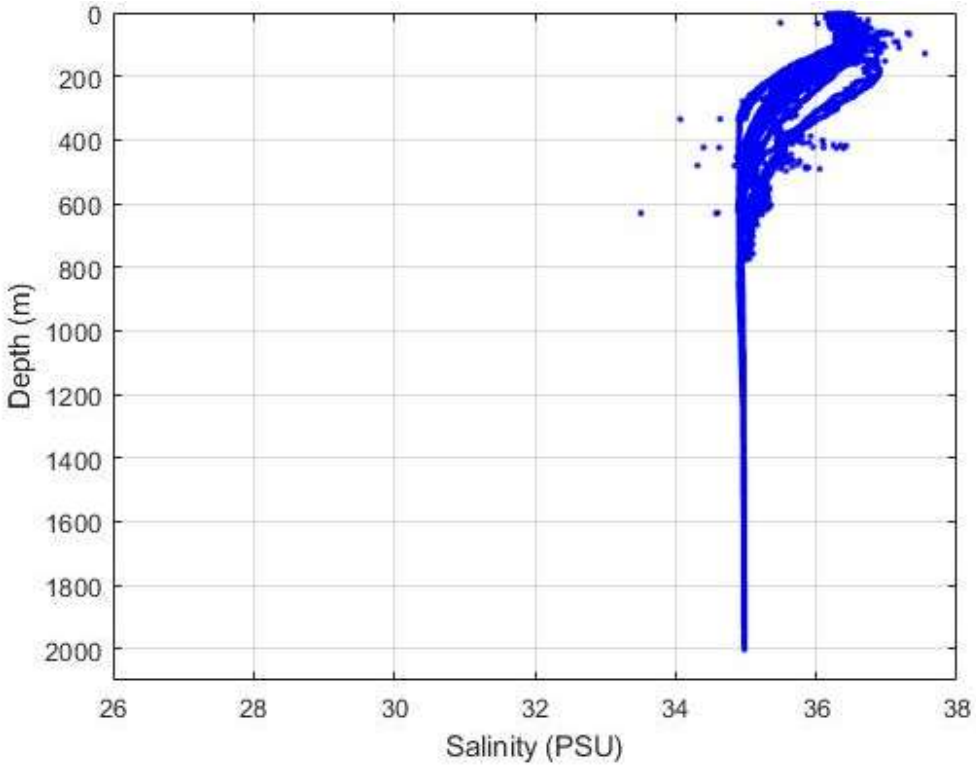

Appendix 9: Observational Temperature Data vs Depth in the GoM during August 2016

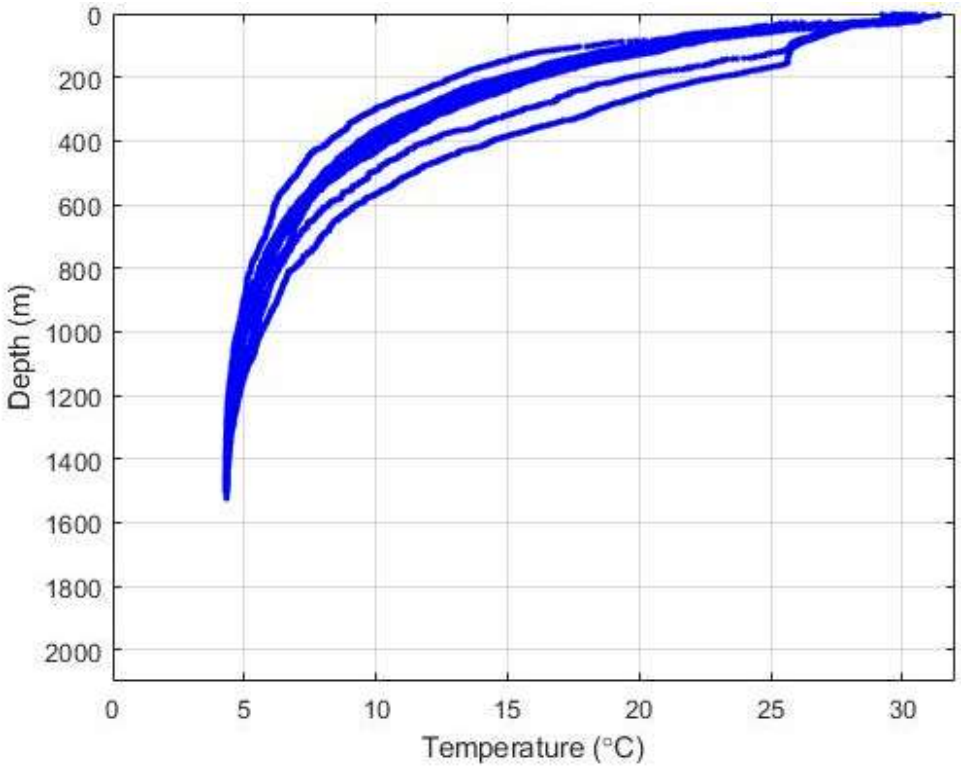

Appendix 10: Observational Salinity Data vs Depth in the GoM during August 2016

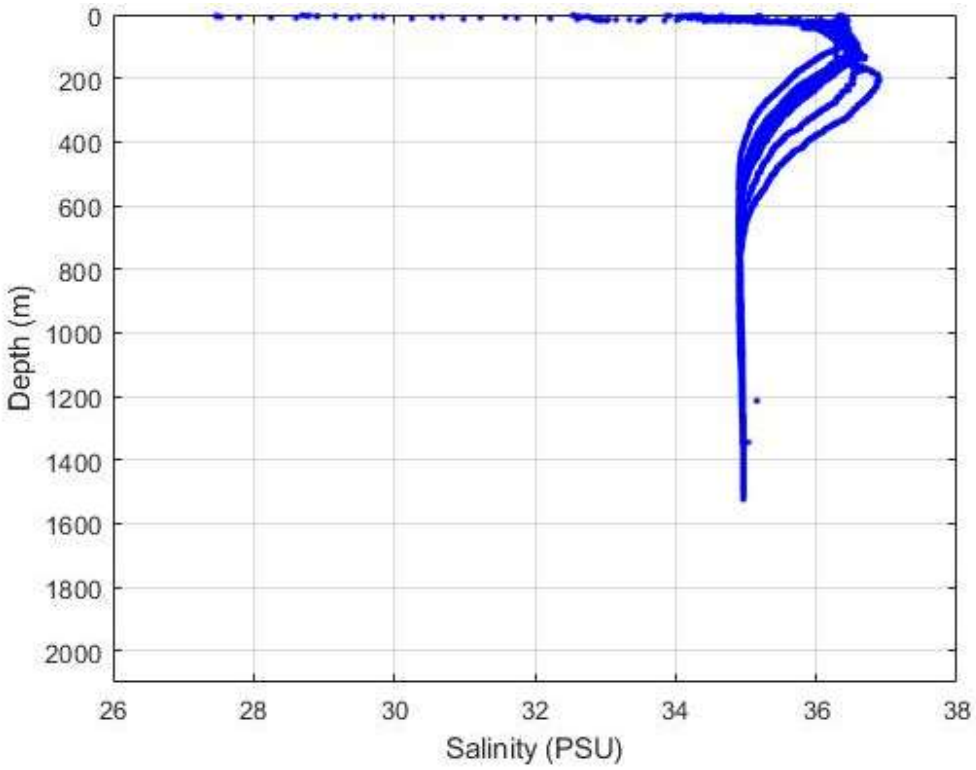

Appendix 11: Observational Temperature Data vs Depth in the GoM during May 2017

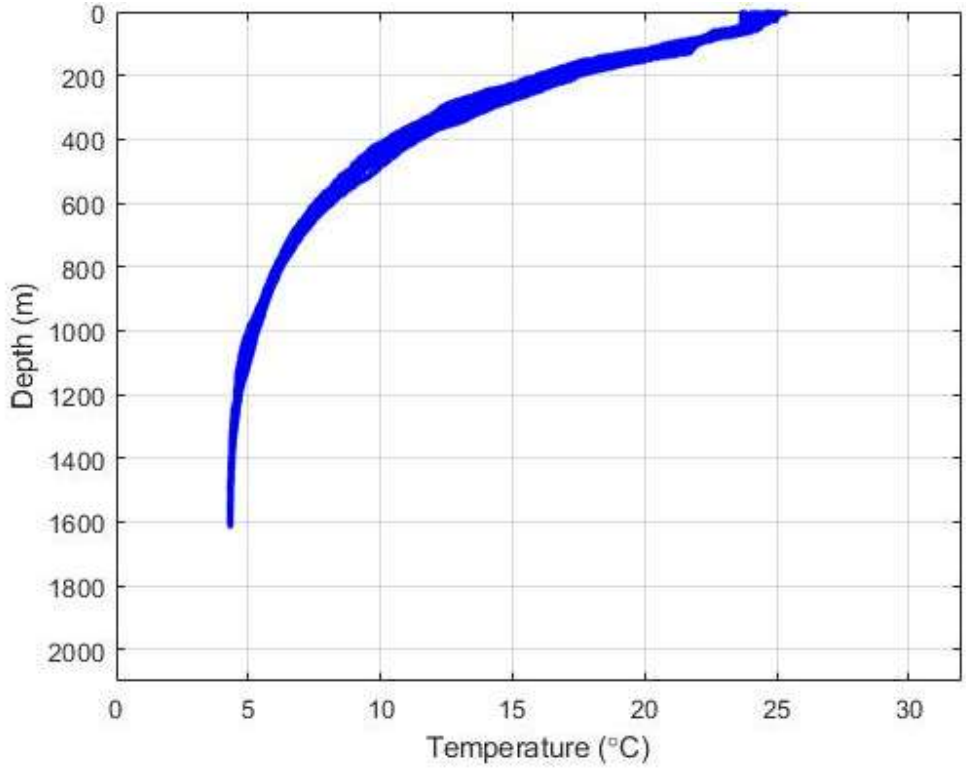

Appendix 12: Observational Salinity Data vs Depth in the GoM during May 2017

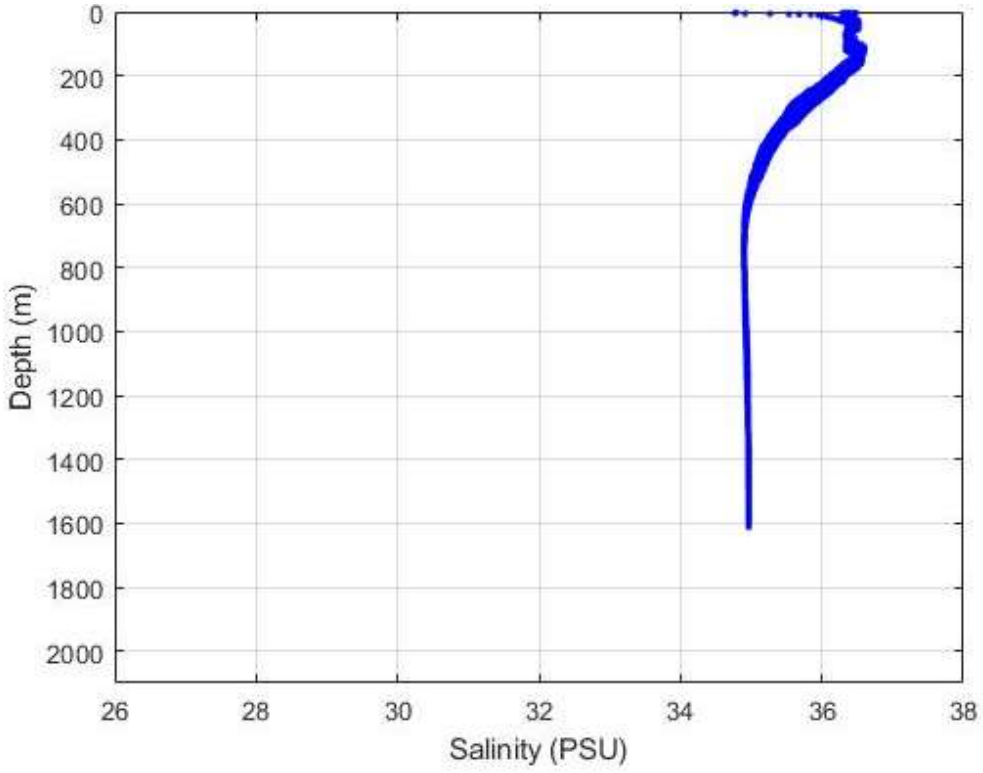

Appendix 13 Observational Temperature Data vs Depth in the TOTO during January

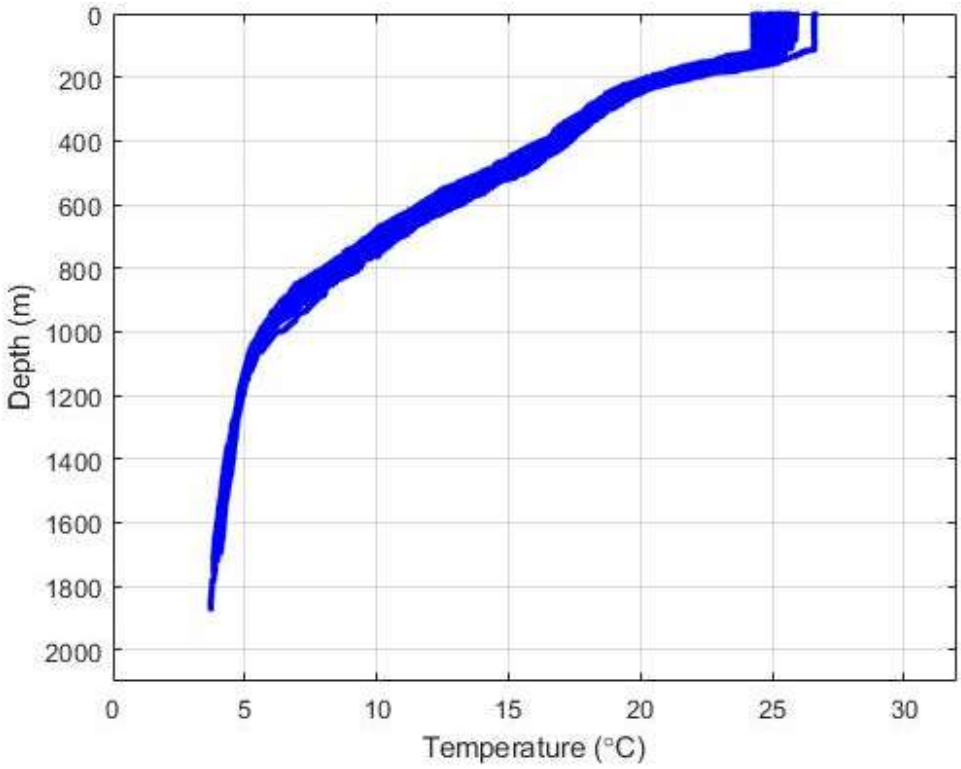

Appendix 14: Observational Temperature Data vs Depth in the TOTO during February

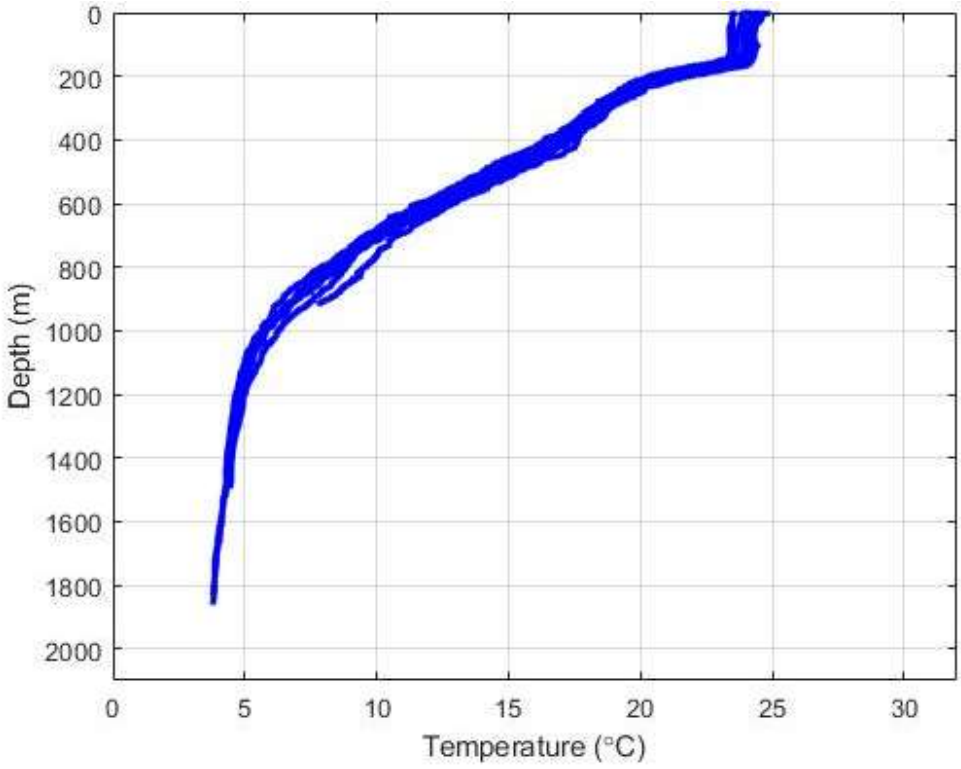

Appendix 15: Observational Temperature Data vs Depth in the TOTO during March

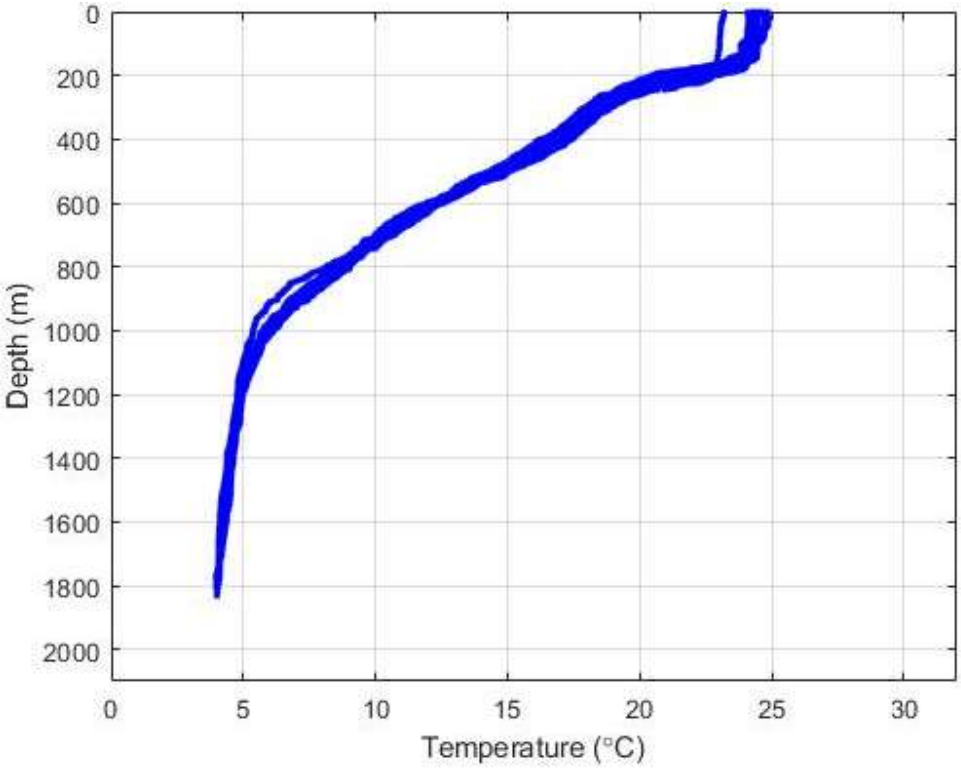

Appendix 16: Observational Temperature Data vs Depth in the TOTO during April

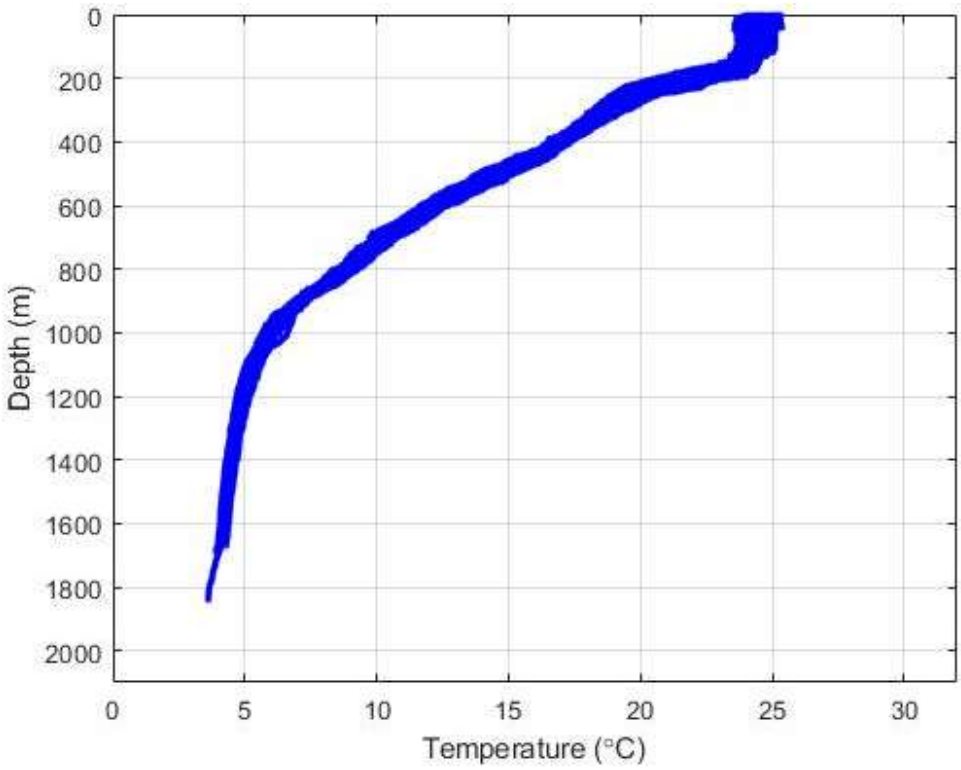

Appendix 17: Observational Temperature Data vs Depth in the TOTO during May

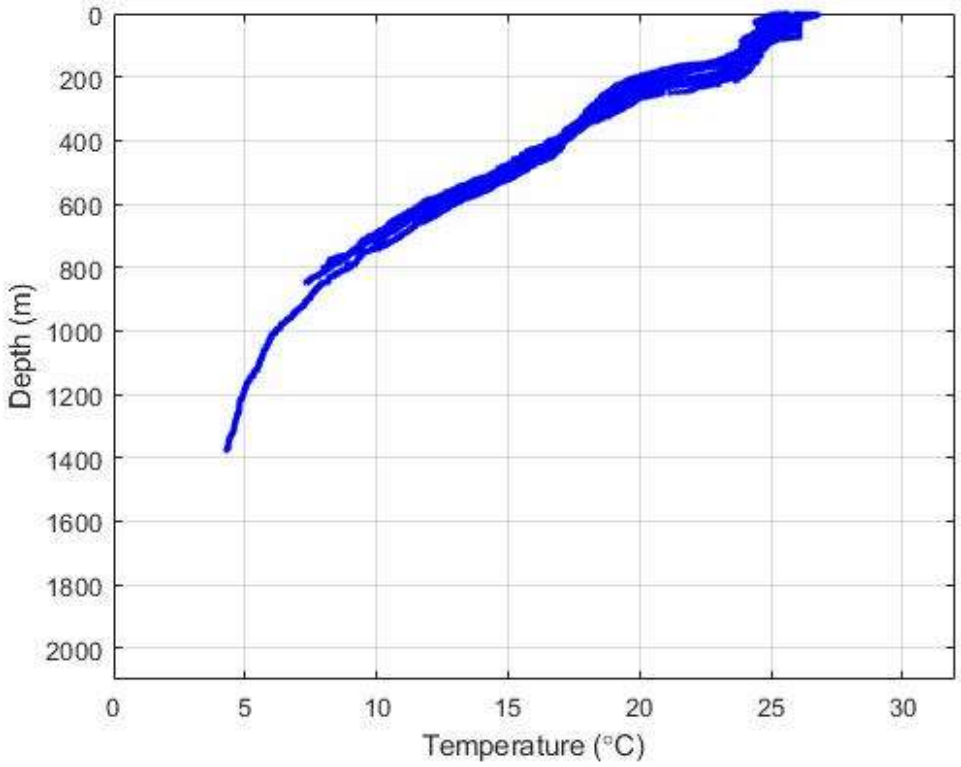

Appendix 18: Observational Temperature Data vs Depth in the TOTO during June

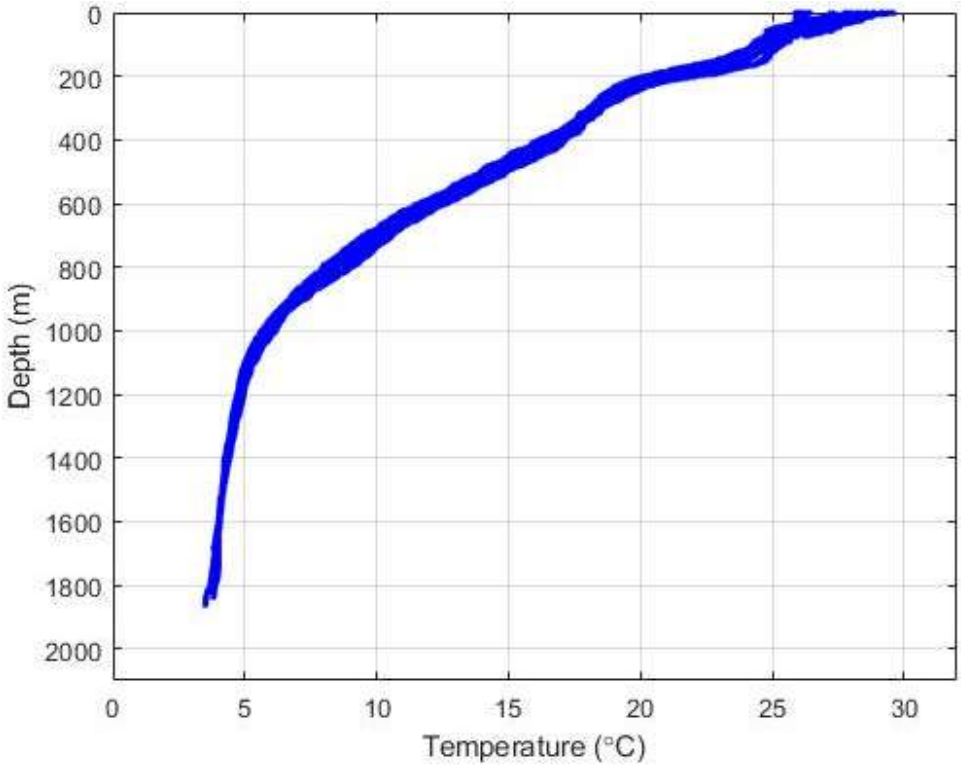

Appendix 19: Observational Temperature Data vs Depth in the TOTO during July

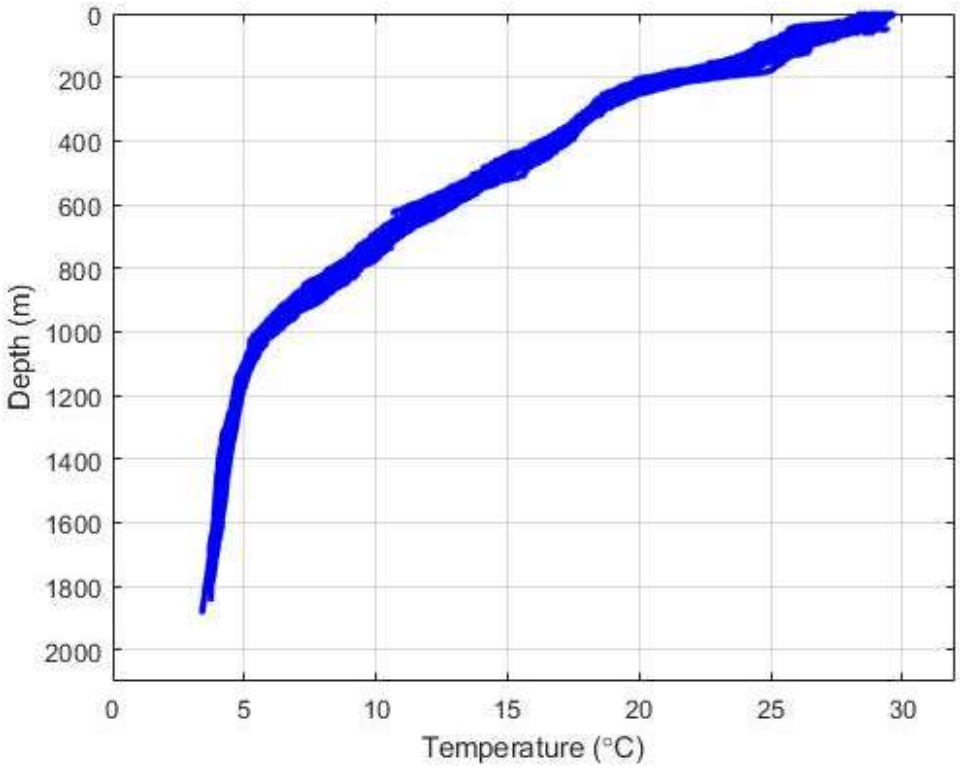

Appendix 20: Observational Temperature Data vs Depth in the TOTO during August

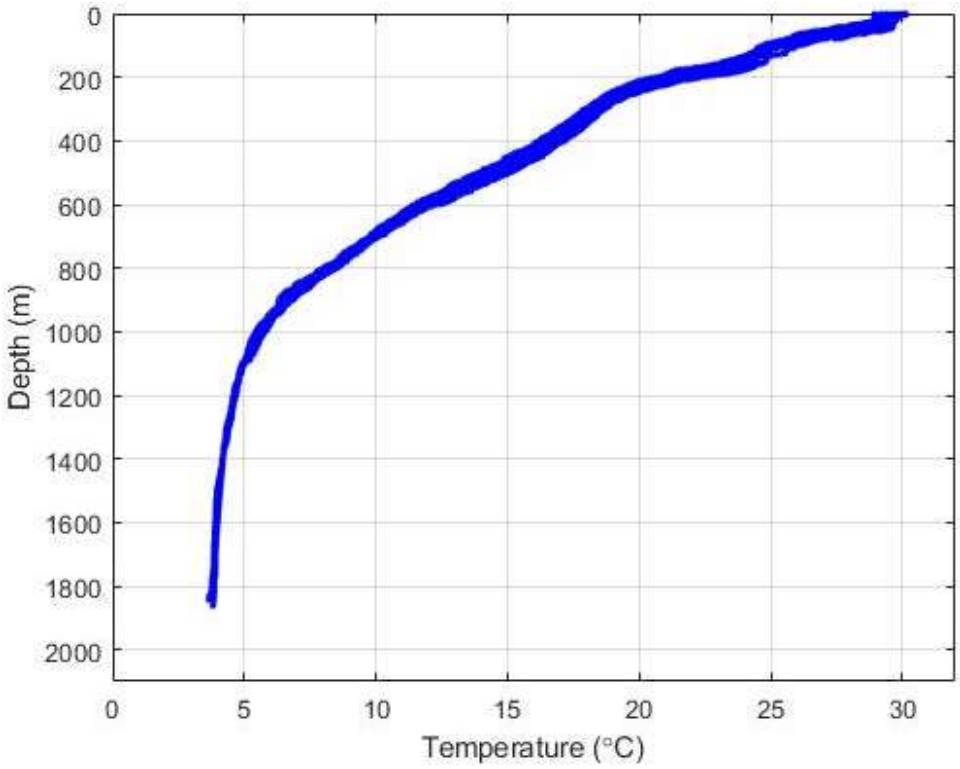

Appendix 21: Observational Temperature Data vs Depth in the TOTO during September

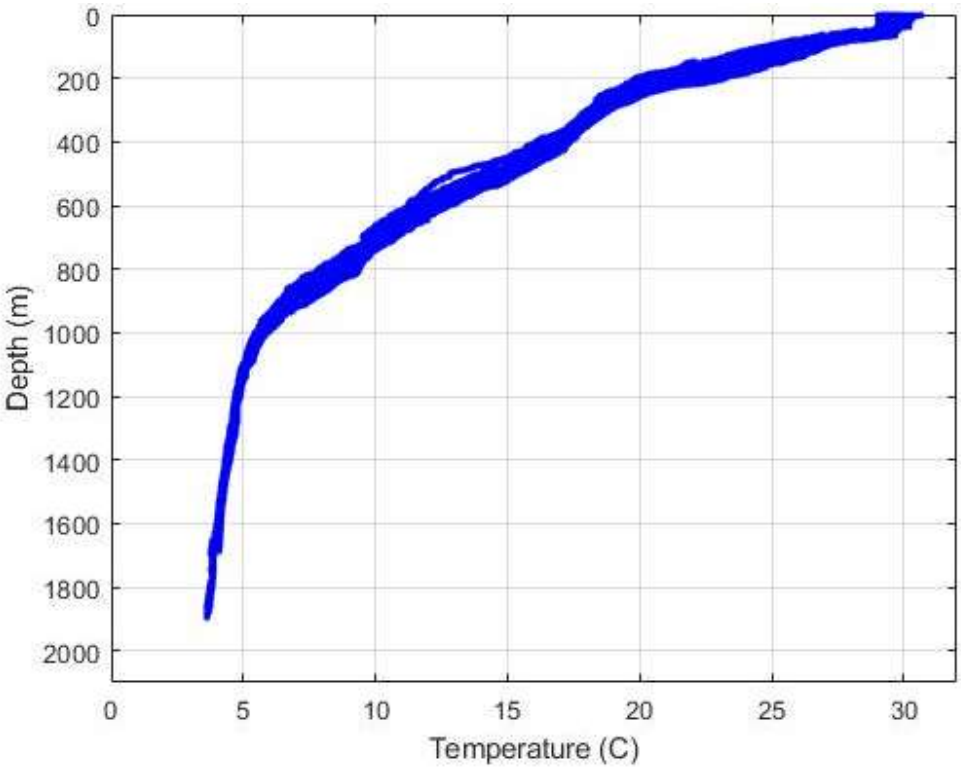

Appendix 22: Observational Temperature Data vs Depth in the TOTO during October

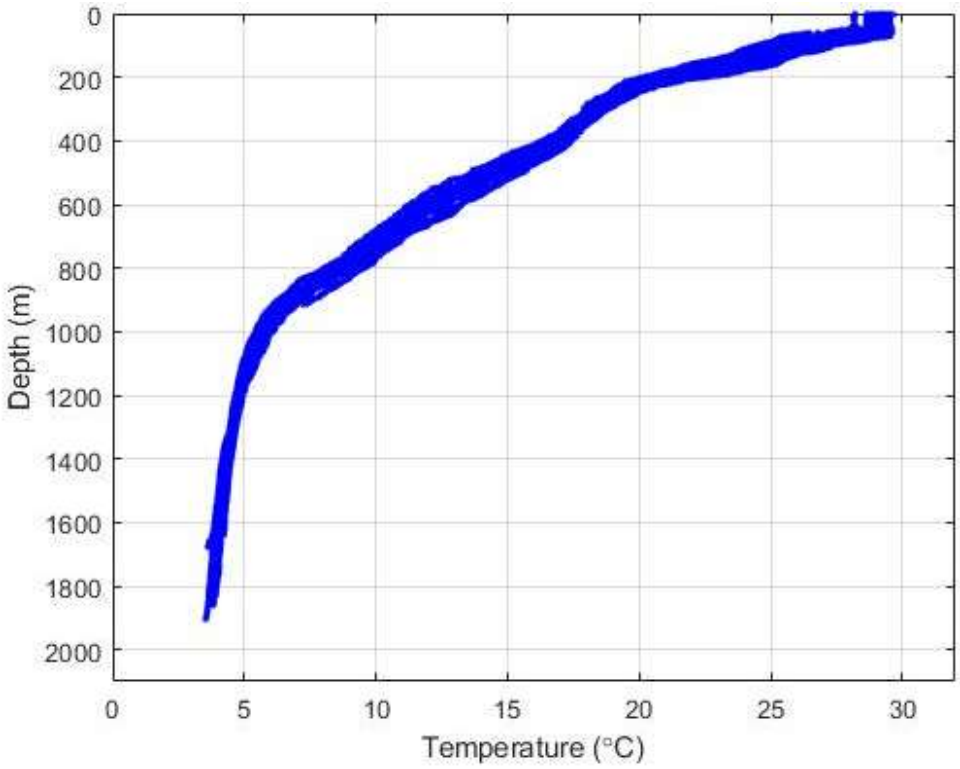

Appendix 23: Observational Temperature Data vs Depth in the TOTO during November

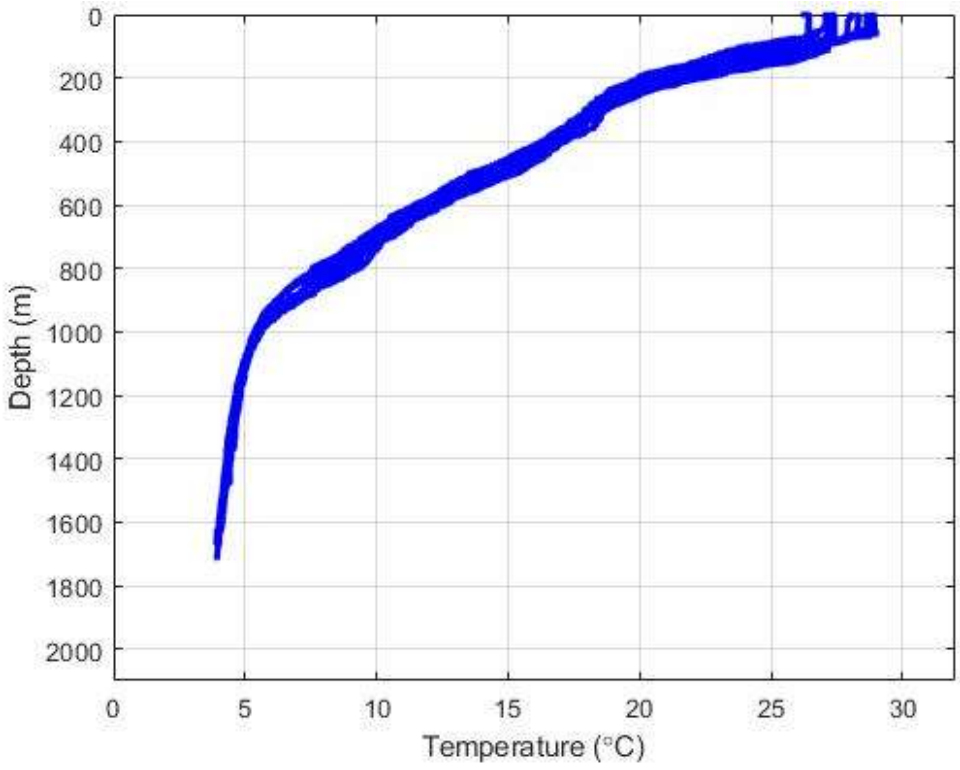

Appendix 24: Observational Temperature Data vs Depth in the TOTO during December

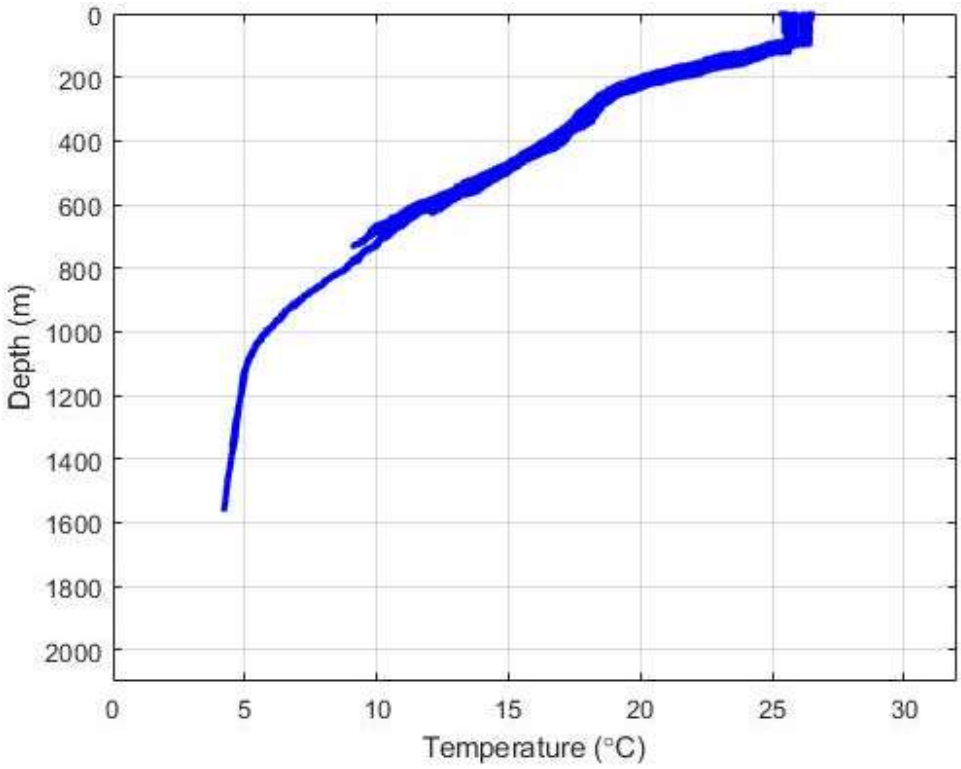

Appendix 25: Observational Salinity Data vs Depth in the TOTO during January

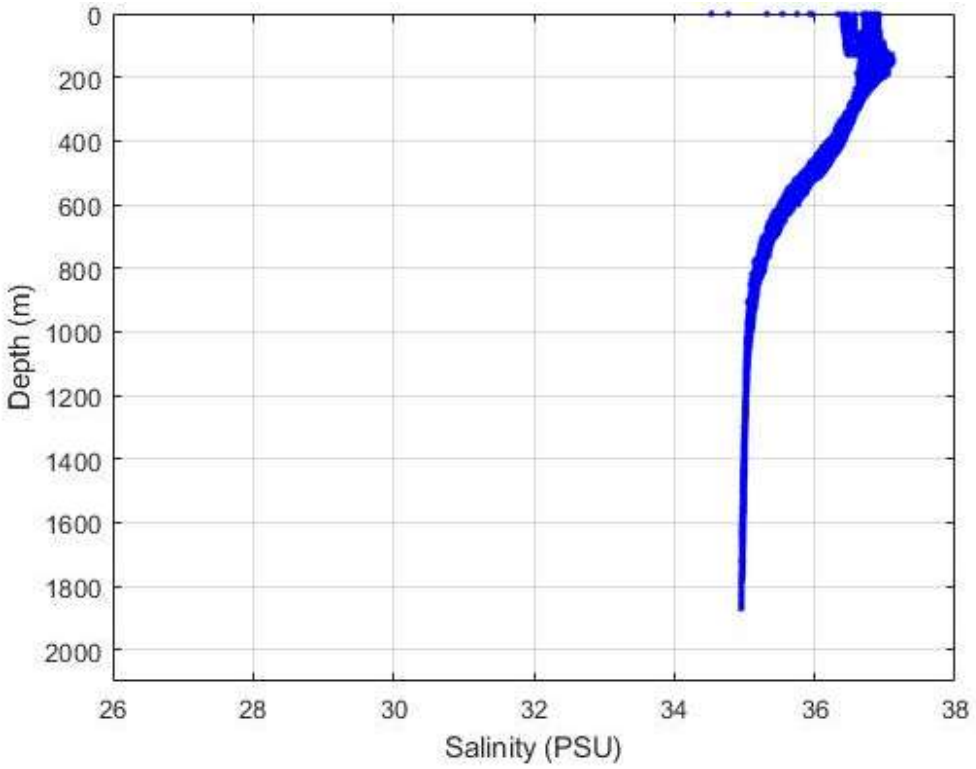

Appendix 26: Observational Salinity Data vs Depth in the TOTO during February

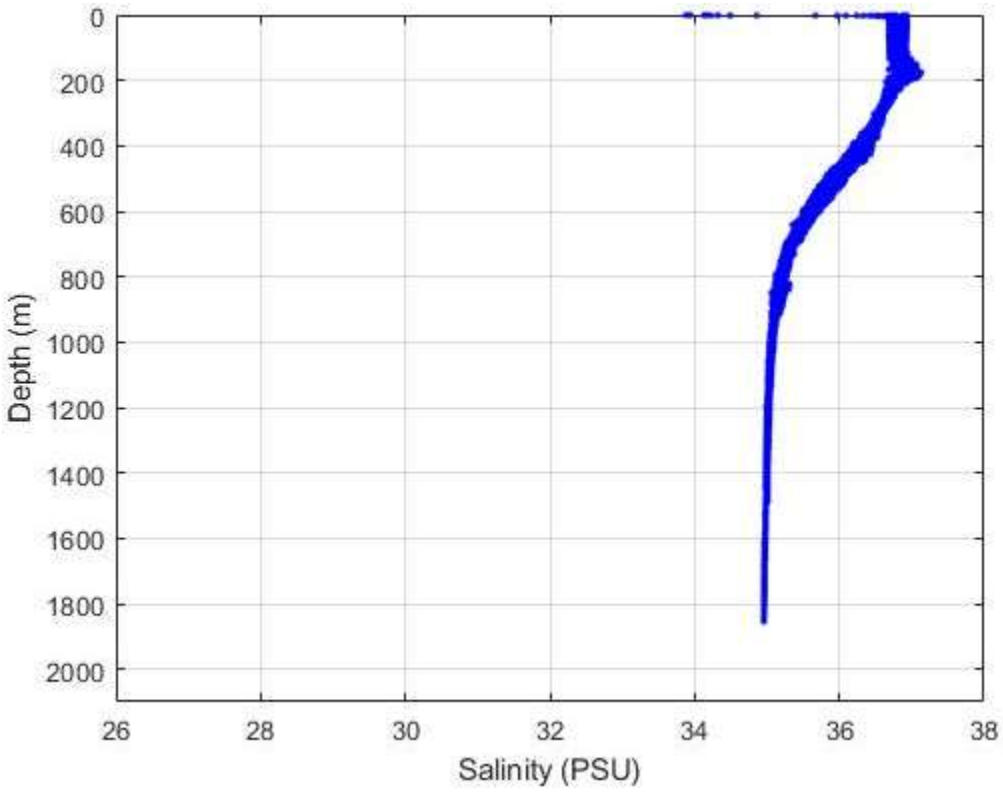

Appendix 27: Observational Salinity Data vs Depth in the TOTO during March

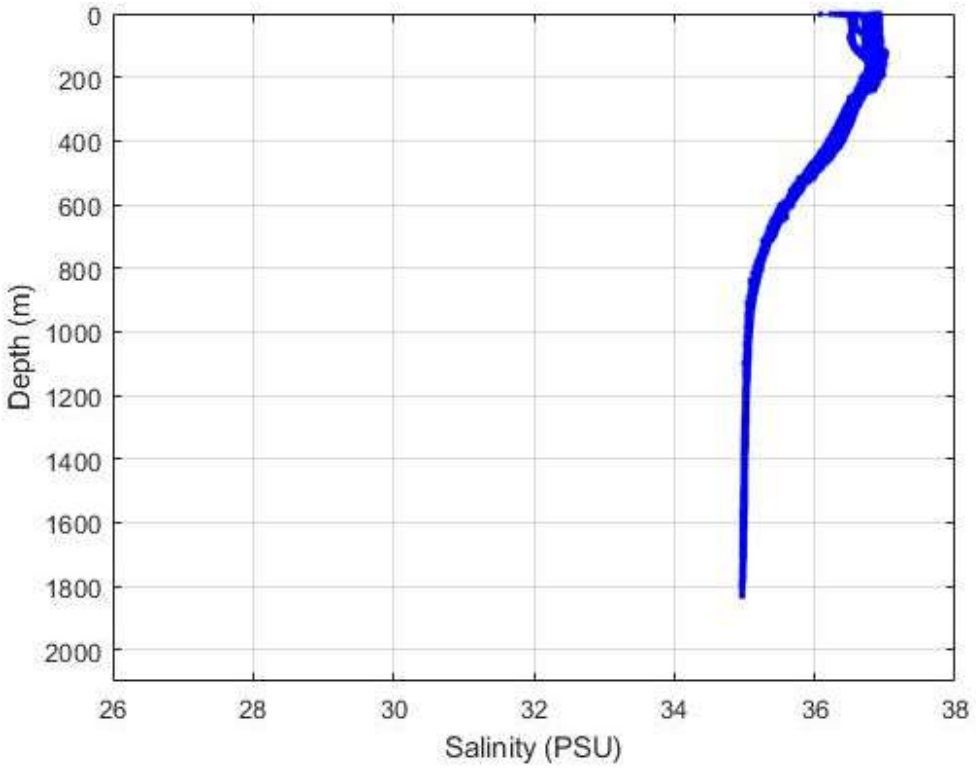

Appendix 28: Observational Salinity Data vs Depth in the TOTO during April

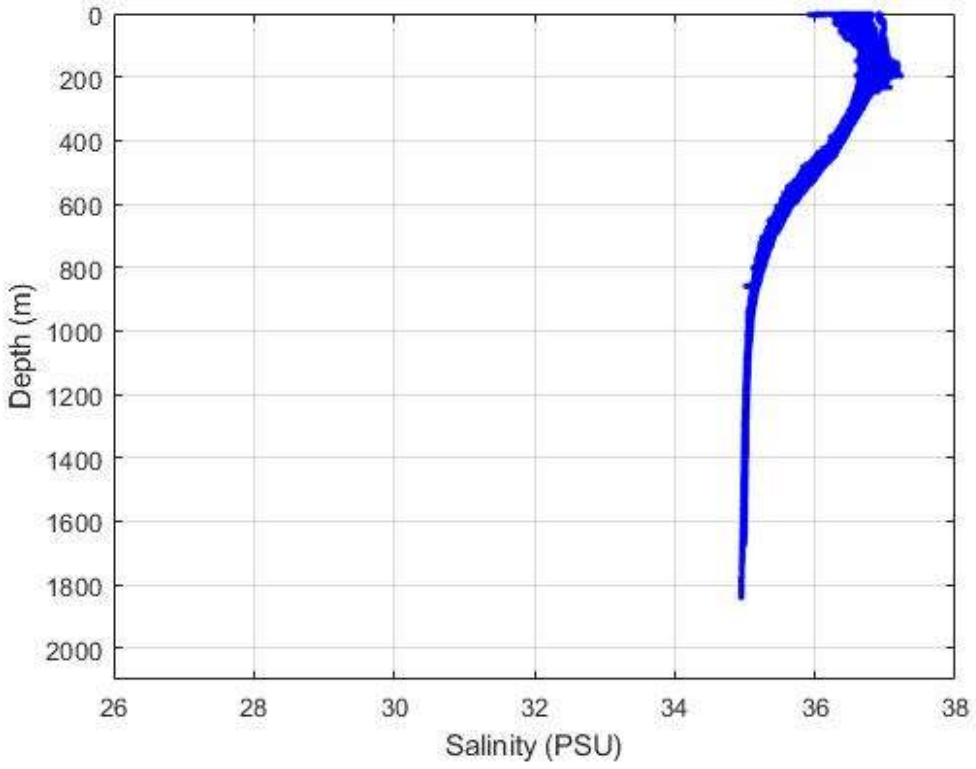

Appendix 29: Observational Salinity Data vs Depth in the TOTO during May

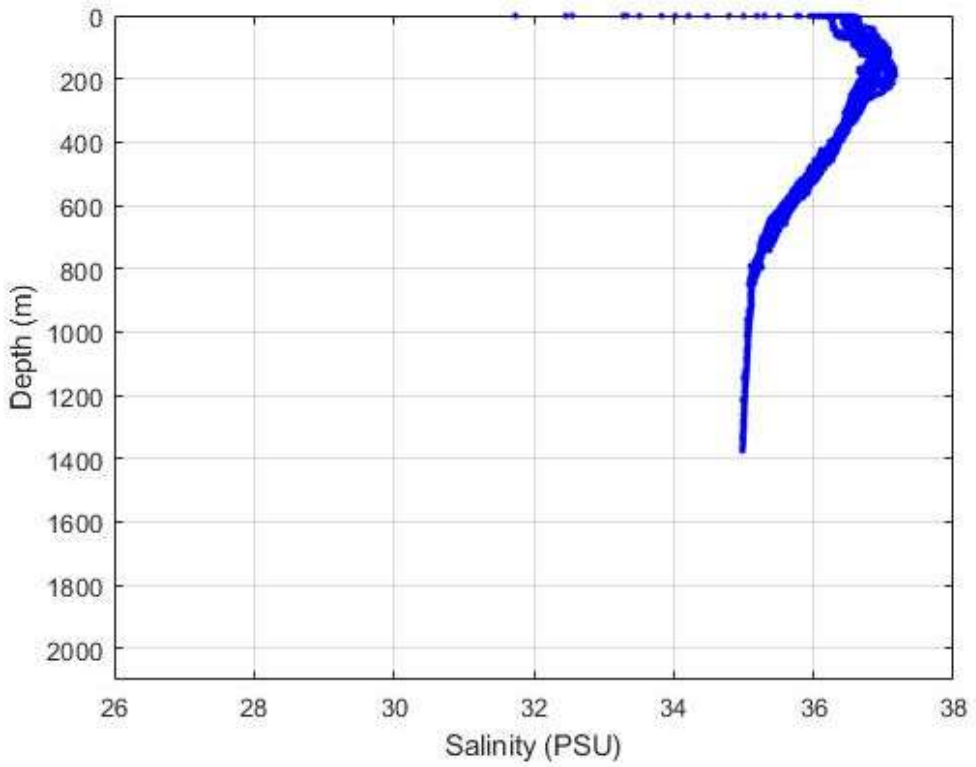

Appendix 30: Observational Salinity Data vs Depth in the TOTO during June

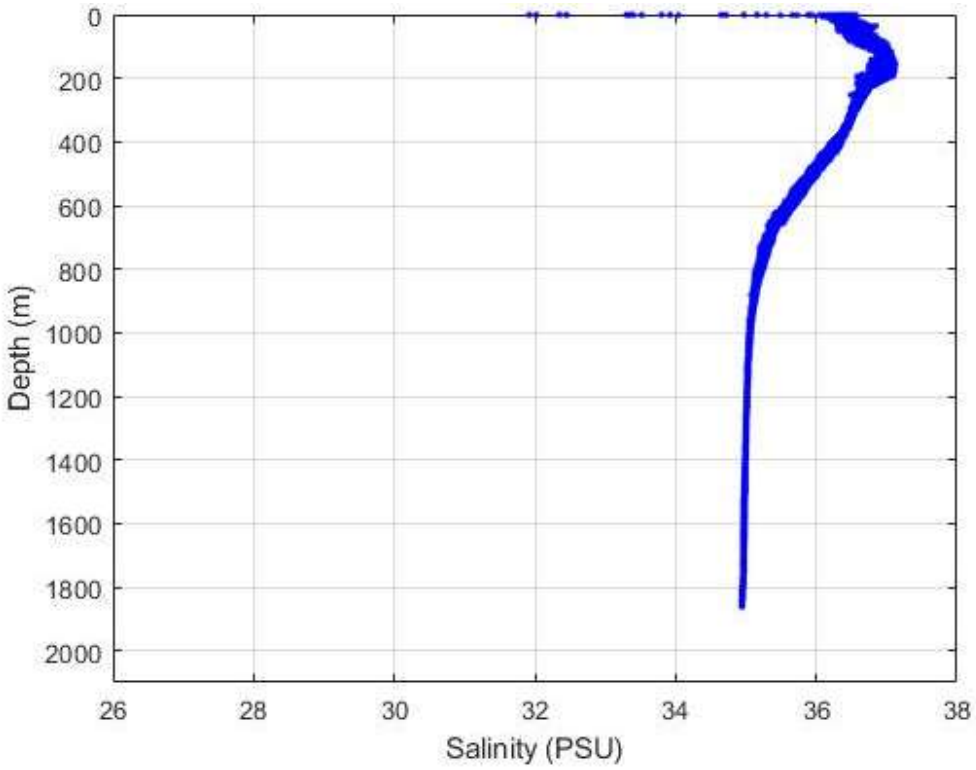

Appendix 31: Observational Salinity Data vs Depth in the TOTO during July

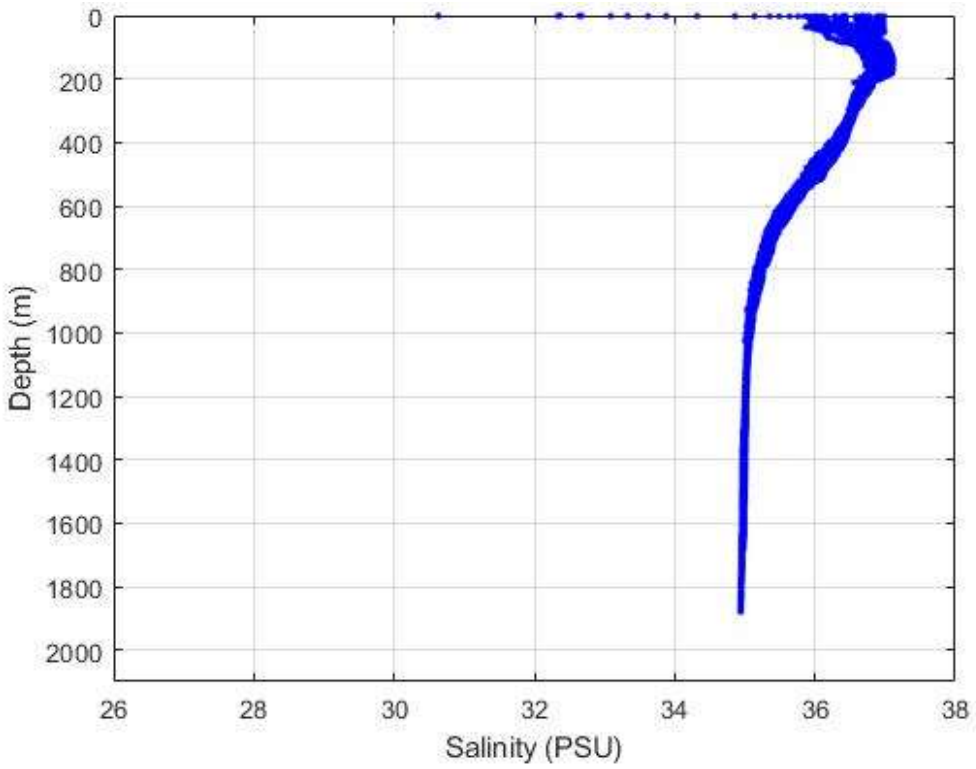

Appendix 32: Observational Salinity Data vs Depth in the TOTO during August

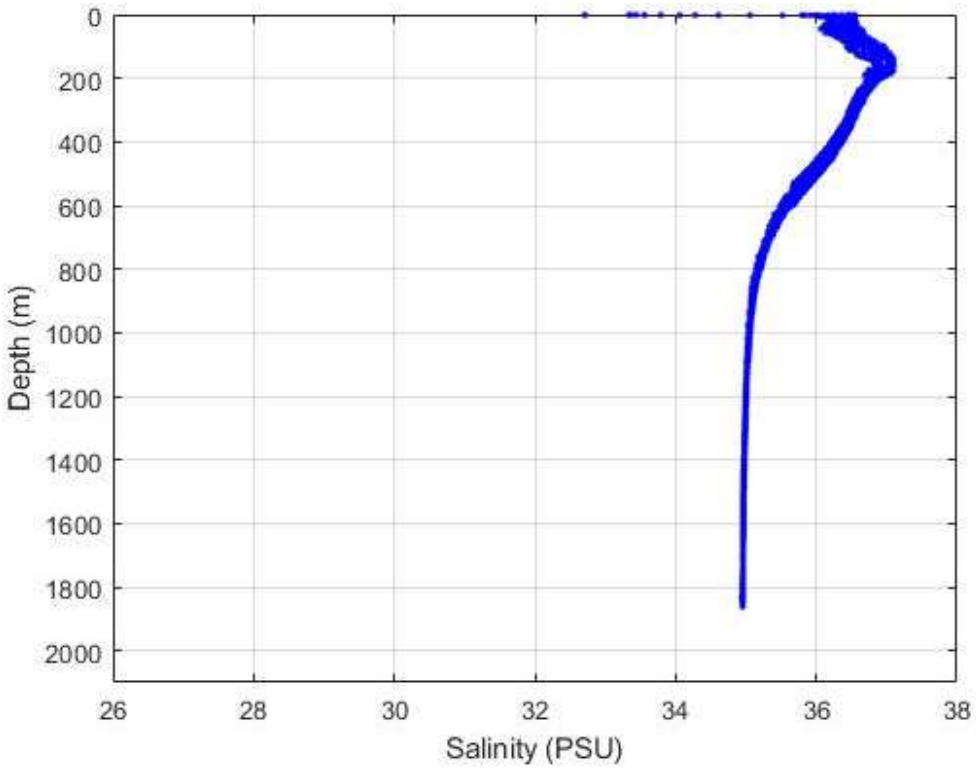

Appendix 33: Observational Salinity Data vs Depth in the TOTO during September

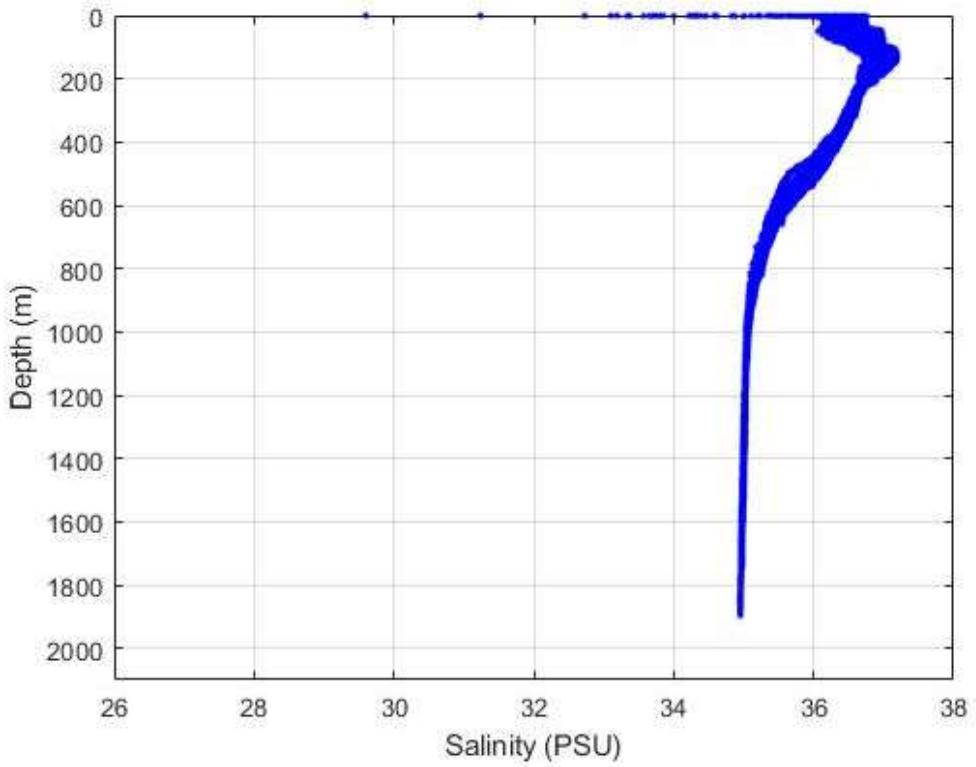

Appendix 34: Observational Salinity Data vs Depth in the TOTO during October

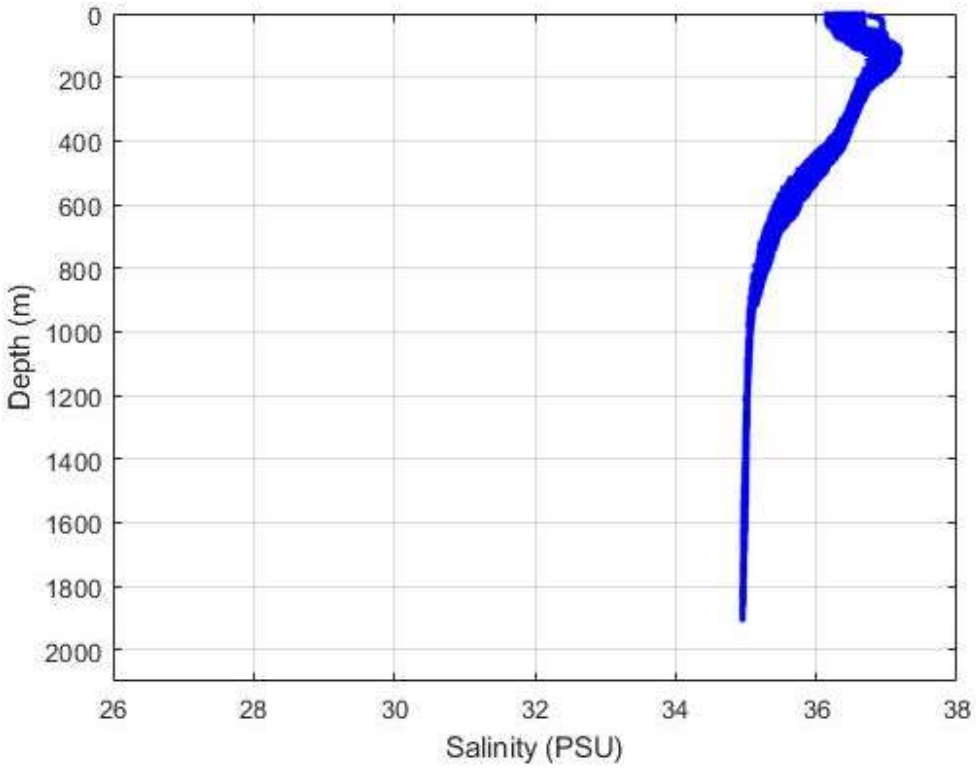

Appendix 35: Observational Salinity Data vs Depth in the TOTO during November

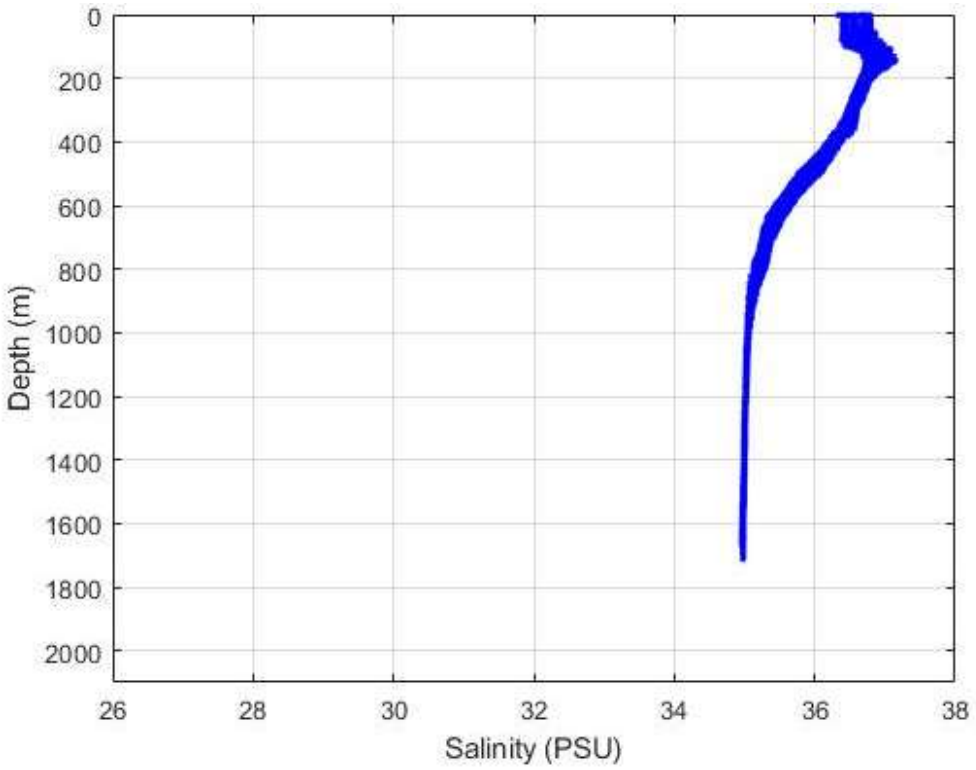

Appendix 36: Observational Salinity Data vs Depth in the TOTO during December

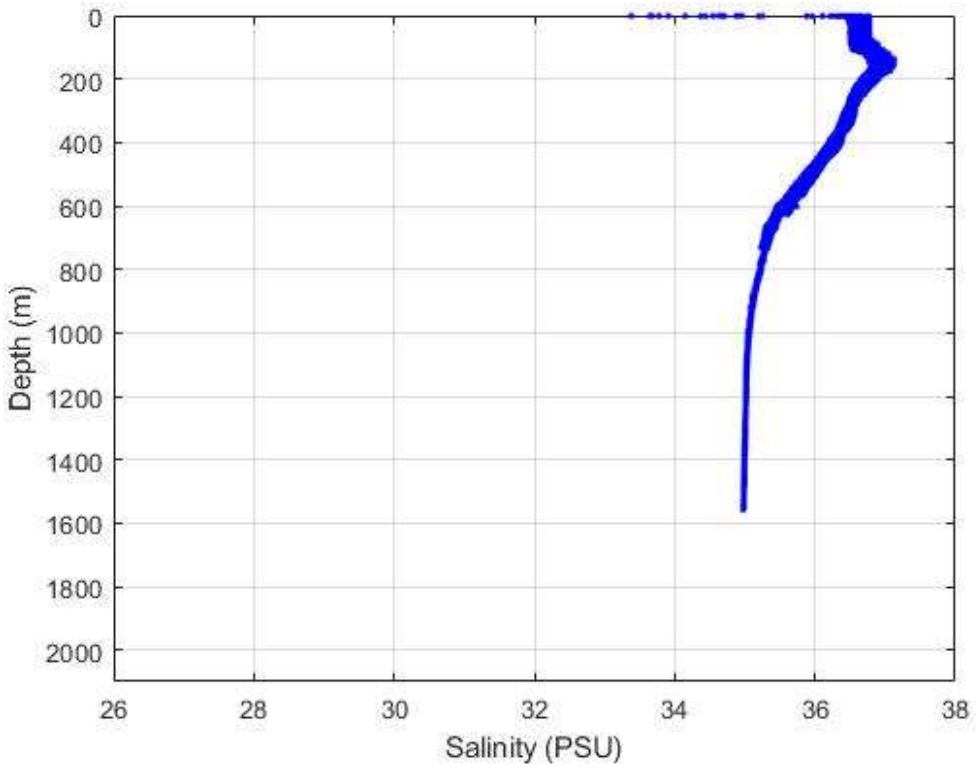

Appendix 37: Statistics Summary of Error as a Function of Depth in the GOM

Depth	Temperature					Salinity				
	Mean	**Standard Deviation**	**RMS Error**	**Maximum**	**Minimum**	**Mean**	**Standard Deviation**	**RMS Error**	**Maximum**	**Minimum**
0	0.0916	0.5326	0.5371	1.6034	-1.8970	-0.4655	1.7857	1.8344	7.6308	-5.9452
5	-0.0899	0.4783	0.4838	0.6954	-2.2996	-0.5941	1.7101	1.8002	7.7979	-5.6926
10	-0.0765	0.4643	0.4678	0.9868	-2.3519	-0.7557	1.2599	1.4626	5.1659	-3.5927
15	-0.0785	0.4821	0.4856	1.0282	-2.1761	-0.8031	0.8713	1.1811	3.4413	-2.6082
20	-0.0811	0.5496	0.5523	1.0905	-2.0297	-0.6945	0.5770	0.9007	1.7769	-1.8316
25	-0.1053	0.6449	0.6496	1.3363	-2.0377	-0.5731	0.4257	0.7124	0.7539	-1.5830
30	-0.1550	0.9104	0.9181	3.3746	-2.6689	-0.4584	0.3415	0.5704	0.4107	-1.1893
40	-0.4401	1.0827	1.1627	3.1718	-2.8467	-0.2513	0.2207	0.3336	0.3663	-0.7063
50	-0.7681	1.2032	1.4213	2.3124	-4.1921	-0.1617	0.1710	0.2346	0.2322	-0.6543
60	-1.0190	1.3639	1.6959	2.5860	-4.7490	-0.1055	0.1472	0.1804	0.2589	-0.4162
70	-1.1414	1.5246	1.8971	2.1461	-5.1484	-0.1019	0.1738	0.2006	0.2872	-0.6473
80	-1.2261	1.6930	2.0821	1.8869	-5.5071	-0.0772	0.1550	0.1723	0.3540	-0.4560
90	-1.3596	1.8663	2.3000	1.9501	-6.0494	-0.0794	0.1644	0.1817	0.3608	-0.4219
100	-1.5425	1.9853	2.5045	2.1367	-6.8053	-0.0891	0.1913	0.2100	0.4278	-0.4998
125	-1.9958	2.1059	2.8921	1.8554	-6.3265	-0.1888	0.2341	0.2996	0.3753	-0.7752
150	-1.9262	2.0243	2.7853	2.3624	-6.3907	-0.2320	0.2564	0.3446	0.4373	-0.7959
200	-1.6078	1.7490	2.3679	2.4420	-5.8336	-0.2260	0.2758	0.3553	0.6353	-0.7849
250	-1.3428	1.5226	2.0232	2.6419	-5.3276	-0.1910	0.2278	0.2962	0.4335	-0.7647
300	-1.0643	1.4626	1.8017	2.4332	-4.5837	-0.1443	0.2073	0.2515	0.3916	-0.6511
400	-0.7893	1.1276	1.3706	1.7589	-3.3011	-0.0735	0.1454	0.1621	0.2619	-0.4891
500	-0.6741	0.7959	1.0392	1.3515	-2.0292	-0.0439	0.1146	0.1221	0.1907	-0.5855
600	-0.6552	0.5901	0.8793	0.5983	-1.9954	-0.0288	0.0923	0.0961	0.1584	-0.3206
700	-0.5945	0.4524	0.7452	0.3152	-1.7848	-0.0141	0.0666	0.0677	0.1376	-0.1453

Appendix 37 – Continued

800	-0.5116	0.3729	0.6316	0.2005	-1.8135	-0.0016	0.0511	0.0508	0.1339	-0.0826
900	-0.4304	0.3369	0.5452	0.2090	-1.6858	0.0030	0.0406	0.0405	0.0836	-0.0590
1000	-0.3145	0.2753	0.4167	0.2039	-1.3442	0.0087	0.0422	0.0428	0.0880	-0.0468
1100	-0.1815	0.2474	0.3055	0.2223	-1.0421	0.0106	0.0442	0.0452	0.1030	-0.0423
1200	-0.0414	0.1735	0.1772	0.1876	-0.7738	0.0111	0.0427	0.0439	0.0986	-0.0373
1300	0.0119	0.1220	0.1217	0.1917	-0.4745	0.0144	0.0426	0.0447	0.1103	-0.0335
1400	0.0006	0.0851	0.0845	0.1503	-0.2641	0.0206	0.0436	0.0479	0.1560	-0.0278
1500	-0.0303	0.0585	0.0655	0.0948	-0.1266	0.0257	0.0408	0.0480	0.1399	-0.0210
1750	-0.0703	0.0000	0.0703	-0.0703	-0.0703	0.0274	0.0000	0.0274	0.0274	0.0274
2000	-0.0564	0.0000	0.0564	-0.0564	-0.0564	0.0735	0.0000	0.0735	0.0735	0.0735

Appendix 38: Statistics Summary of Error as a Function of Depth in the TOTO

Depth	Temperature					Salinity				
	Mean	**Standard Deviation**	**RMS Error**	**Maximum**	**Minimum**	**Mean**	**Standard Deviation**	**RMS Error**	**Maximum**	**Minimum**
0	0.0025	0.5143	0.5132	2.0622	-1.3126	0.2719	0.7796	0.8239	4.2197	-0.4283
2	-0.0875	0.4310	0.4388	1.7084	-1.2897	0.0911	0.2974	0.3104	1.9873	-0.4282
4	-0.1024	0.4107	0.4224	1.6888	-1.2643	0.0327	0.1727	0.1754	0.4717	-0.4128
6	-0.0896	0.4033	0.4122	1.6558	-1.1594	0.0270	0.1700	0.1718	0.4617	-0.4190
8	-0.1168	0.3865	0.4029	1.5998	-1.1203	0.0219	0.1656	0.1667	0.4346	-0.4201
10	-0.1282	0.3783	0.3987	1.5429	-1.1108	0.0167	0.1632	0.1637	0.4256	-0.4292
12	-0.1446	0.3715	0.3979	1.4839	-1.1089	0.0131	0.1624	0.1626	0.4166	-0.4318
15	-0.1604	0.3717	0.4041	1.4711	-1.1078	0.0101	0.1620	0.1620	0.3978	-0.4262
20	-0.1791	0.3907	0.4290	1.4767	-1.1701	0.0083	0.1604	0.1603	0.3794	-0.4042
25	-0.2138	0.4115	0.4630	1.4890	-1.2824	0.0025	0.1592	0.1589	0.3736	-0.4056
30	-0.2523	0.4463	0.5118	1.5044	-1.4267	0.0003	0.1585	0.1581	0.3798	-0.3792
35	-0.2720	0.5027	0.5706	1.7589	-1.6455	-0.0041	0.1575	0.1572	0.4352	-0.3727
40	-0.2890	0.5596	0.6287	1.9082	-1.7081	-0.0082	0.1558	0.1556	0.4022	-0.3664
45	-0.2904	0.6165	0.6803	2.1404	-1.8327	-0.0138	0.1536	0.1539	0.4410	-0.3785
50	-0.2719	0.6576	0.7102	2.1349	-2.0274	-0.0246	0.1532	0.1548	0.4525	-0.4153
60	-0.1907	0.7154	0.7389	2.0828	-2.0300	-0.0423	0.1462	0.1519	0.3997	-0.5031
70	-0.0531	0.8386	0.8384	3.0479	-3.5947	-0.0552	0.1440	0.1539	0.3270	-0.4631
80	0.0032	0.8224	0.8206	2.4392	-1.8126	-0.0761	0.1455	0.1639	0.2339	-0.6230
90	-0.0408	0.8395	0.8386	2.6172	-1.7681	-0.1060	0.1408	0.1760	0.2617	-0.5066
100	-0.1374	0.8630	0.8720	3.1349	-1.7836	-0.1407	0.1512	0.2063	0.3354	-0.5698
125	-0.8987	0.6451	1.1054	1.4203	-2.6516	-0.2073	0.1558	0.2591	0.3425	-0.8147
150	-1.3809	0.8429	1.6169	1.7757	-3.5694	-0.2566	0.1933	0.3210	0.3309	-1.2424
200	-1.0683	0.9937	1.4575	1.5910	-5.9512	-0.1808	0.2269	0.2897	0.5838	-0.7390

Appendix 38 – Continued

250	-1.0050	1.3466	1.6776	1.5483	-8.0386	-0.1550	0.2460	0.2902	0.7106	-0.9962
300	-0.9756	1.3959	1.7002	2.0864	-7.4696	-0.1250	0.2588	0.2869	0.7924	-0.9741
350	-0.7801	0.8435	1.1474	2.0737	-2.9050	-0.0706	0.2088	0.2199	0.7744	-0.5055
400	-0.8493	1.0689	1.3631	2.6490	-5.9176	-0.0461	0.2252	0.2293	0.6262	-1.0553
500	-0.5244	0.9167	1.0539	2.4689	-2.6176	0.0778	0.2023	0.2162	0.8201	-0.5292
600	0.1150	0.9128	0.9174	3.2934	-2.1002	0.1934	0.2198	0.2923	1.1017	-0.3325
700	0.5172	0.9935	1.1168	4.4187	-1.4639	0.2069	0.2417	0.3174	1.1889	-0.1594
800	0.3940	0.9219	0.9994	4.0295	-1.8956	0.0946	0.1834	0.2058	1.0373	-0.1864
900	0.1808	0.9319	0.9458	1.9764	-2.5735	0.0766	0.1317	0.1520	0.5301	-0.0966
1000	0.5679	0.7229	0.9168	2.2299	-0.7852	0.0962	0.1340	0.1645	0.4164	-0.1408
1250	0.9966	0.6439	1.1812	2.3112	0.2480	0.1882	0.1361	0.2311	0.4743	0.0217

Appendix 39: Statistics Summary of Error as a Function of Month in the GoM

Month	**Number of Casts**	Temperature					Salinity				
		Mean	**Standard Deviation**	**RMS Error**	**Maximum**	**Minimum**	**Mean**	**Standard Deviation**	**RMS Error**	**Maximum**	**Minimum**
May	**47**	-0.5454	1.0915	1.2198	2.5860	-6.0489	-0.2517	0.4829	0.5444	2.3210	-5.9452
August	**36**	-0.8224	1.4769	1.6898	3.3746	-6.8053	-0.1583	0.7388	0.7552	7.7979	-3.4705

Appendix 40: Statistics Summary of Error as a Function of Month in the TOTO

Month	Number of Casts	Temperature					Salinity				
		Mean	Standard Deviation	RMS Error	Maximum	Minimum	Mean	Standard Deviation	RMS Error	Maximum	Minimum
January	**30**	-0.4650	0.6299	0.7826	2.2012	-4.1038	-0.0317	0.1950	0.1975	2.0907	-0.4918
February	**14**	-0.5422	0.7792	0.9486	2.0054	-6.9949	-0.0905	0.2010	0.2203	2.7072	-0.8687
March	**12**	-0.3279	0.7159	0.7866	1.4603	-3.0720	-0.0954	0.1608	0.1868	0.5143	-1.0553
April	**22**	-0.2106	0.8251	0.8510	4.4187	-5.4603	-0.0039	0.2063	0.2062	1.1889	-0.8173
May	**13**	-0.4234	1.0730	1.1520	1.5044	-8.0386	-0.0163	0.3032	0.3032	3.9808	-0.9962
June	**17**	-0.1823	0.9192	0.9362	2.1404	-4.3833	-0.0363	0.3215	0.3232	4.2197	-0.7984
July	**24**	-0.2089	0.9580	0.9799	2.3514	-5.2988	0.0155	0.2777	0.2779	4.0432	-0.8147
August	**14**	-0.2215	0.9491	0.9735	2.6172	-3.2641	0.0080	0.2568	0.2566	3.0175	-0.4862
September	**29**	-0.1723	1.0126	1.0266	3.1349	-5.7866	0.0117	0.3244	0.3244	3.2931	-1.2424
October	**21**	-0.1558	0.6737	0.6910	3.2255	-2.8606	0.0380	0.1950	0.1986	1.1017	-0.5292
November	**16**	-0.3142	0.9658	1.0147	2.4912	-6.6479	-0.0216	0.1937	0.1948	0.8008	-0.8094
December	**12**	-0.4203	0.5185	0.6669	1.0286	-2.6289	-0.0367	0.2845	0.2865	3.1792	-0.4641

Appendix 41: Statistics Summary of Error as a Function of Year in the GOM

Year	Number of Casts	Temperature					Salinity				
		Mean	Standard Deviation	RMS Error	Maximum	Minimum	Mean	Standard Deviation	RMS Error	Maximum	Minimum
2015	**30**	-0.9354	1.5080	1.7739	2.5860	-6.8053	-0.2796	0.6555	0.7123	2.4250	-5.9452
2016	**36**	-0.6647	1.2357	1.4026	3.3746	-6.0899	-0.1897	0.6534	0.6801	7.7979	-1.9553
2017	**17**	-0.1814	0.6328	0.6577	2.1367	-3.0620	-0.1250	0.3745	0.3945	1.4194	-1.8164

Appendix 42: Statistics Summary of Error as a Function of Year in the TOTO

Year	Number of Casts	Temperature					Salinity				
		Mean	Standard Deviation	RMS Error	Maximum	Minimum	Mean	Standard Deviation	RMS Error	Maximum	Minimum
2005	**21**	-0.2342	0.8344	0.8659	3.0479	-6.6479	-0.0894	0.1424	0.1680	0.3492	-0.8094
2006	**67**	-0.3043	0.8284	0.8823	2.7128	-6.1420	-0.0488	0.1749	0.1815	0.4757	-0.7838
2007	**51**	-0.4349	0.9831	1.0747	3.5008	-8.0386	-0.0060	0.3224	0.3224	4.2197	-0.9962
2008	**13**	-0.4783	0.5837	0.7541	0.8897	-2.1478	-0.0275	0.1630	0.1651	0.3958	-1.0553
2009	**3**	-0.3764	0.5576	0.6702	0.4895	-4.1038	-0.1151	0.0885	0.1449	0.1983	-0.4918
2010	**5**	-0.3579	0.4996	0.6132	1.0286	-1.7699	-0.0286	0.4035	0.4032	3.1792	-0.4482
2011	**5**	0.0777	0.7629	0.7645	2.1569	-2.3130	0.1150	0.4317	0.4455	3.2931	-0.4692
2012	**6**	-0.0810	0.6861	0.6899	2.4823	-2.9169	0.0391	0.2039	0.2073	0.5748	-0.4462
2013	**2**	-0.3818	0.4961	0.6230	0.9433	-1.7256	-0.0369	0.1010	0.1068	0.2597	-0.2300
2014	**12**	0.0257	0.9836	0.9827	4.4187	-2.9614	0.0890	0.2634	0.2777	1.1889	-0.4318
2015	**19**	-0.0525	0.7964	0.7975	2.3514	-2.0274	0.1264	0.1733	0.2143	0.7924	-0.1927
2016	**13**	-0.5207	0.9129	1.0500	2.2214	-3.5694	-0.1124	0.2350	0.2603	0.6944	-0.8147
2017	**7**	-0.0992	0.6300	0.6364	2.1698	-2.1198	-0.1049	0.2844	0.3026	2.0907	-0.4056

Appendix 43: Statistics Summary of Error as a Function of Cruise in the GOM

Cruise	Number of Casts	Temperature					Salinity				
		Mean	Standard Deviation	RMS Error	Maximum	Minimum	Mean	Standard Deviation	RMS Error	Maximum	Minimum
DP01	**8**	-0.4771	1.1265	1.2212	2.5860	-3.2594	-0.3536	0.7832	0.8579	2.3210	-5.9452
DP02	**22**	-1.1002	1.5922	1.9343	1.8017	-6.8053	-0.2530	0.6015	0.6521	2.4250	-3.4705
DP03	**22**	-0.8459	1.2534	1.5113	2.4164	-6.0489	-0.3094	0.3784	0.4886	0.2372	-1.9553
DP04	**14**	-0.3977	1.1600	1.2251	3.3746	-6.0899	-0.0134	0.8910	0.8900	7.7979	-1.5225
DP05	**17**	-0.1814	0.6328	0.6577	2.1367	-3.0620	-0.1250	0.3745	0.3945	1.4194	-1.8164

Appendix 44: Statistics Summary of Error as a Function of Experiment in the TOTO

Experiment	Number of Casts	Temperature					Salinity				
		Mean	Standard Deviation	RMS Error	Maximum	Minimum	Mean	Standard Deviation	RMS Error	Maximum	Minimum
19.1	**171***	-0.3166	0.8401	0.8977	3.1349	-8.0386	-0.0273	0.2530	0.2544	4.2197	-1.2424
90.9	**6***	-0.2333	0.7234	0.7584	1.7607	-2.9169	-0.0047	0.1895	0.1890	0.4429	-0.4462
91	**5**	0.0630	0.9442	0.9433	4.4187	-1.5755	0.1201	0.2248	0.2543	1.1889	-0.3456
91.1	**29**	-0.0685	0.8493	0.8516	3.2255	-2.9614	0.0973	0.2088	0.2303	1.1017	-0.4318
91.2	**17**	-0.3798	0.8803	0.9580	2.2214	-3.5694	-0.1269	0.2660	0.2945	2.0907	-0.8147

*Four CTD casts overlapped between Experiments 19.1 and 90.9

Appendix 45: Statistics Summary of Error as a Function of Depth in the TOTO without HYCOM Quality Control Checks

Depth	Temperature					Salinity				
	Mean	**Standard Deviation**	**RMS Error**	**Maximum**	**Minimum**	**Mean**	**Standard Deviation**	**RMS Error**	**Maximum**	**Minimum**
0	0.0024	0.5105	0.5093	2.0622	-1.3126	0.2734	0.7842	0.8288	4.2197	-0.4283
2	-0.0895	0.4212	0.4297	1.0633	-1.2897	0.0896	0.2967	0.3092	1.9873	-0.4282
4	-0.1057	0.3968	0.4098	1.0871	-1.2643	0.0315	0.1701	0.1726	0.4717	-0.4128
6	-0.0928	0.3895	0.3995	1.1114	-1.1594	0.0257	0.1674	0.1690	0.4617	-0.4190
8	-0.1200	0.3727	0.3907	1.0272	-1.1203	0.0206	0.1628	0.1638	0.3901	-0.4201
10	-0.1311	0.3652	0.3872	0.9965	-1.1108	0.0155	0.1604	0.1608	0.3821	-0.4292
12	-0.1472	0.3593	0.3875	0.9856	-1.1089	0.0119	0.1596	0.1597	0.3739	-0.4318
15	-0.1631	0.3598	0.3943	1.1845	-1.1078	0.0090	0.1594	0.1593	0.3586	-0.4262
20	-0.1825	0.3789	0.4198	1.4689	-1.1701	0.0073	0.1579	0.1577	0.3647	-0.4042
25	-0.2184	0.3994	0.4544	1.4547	-1.2824	0.0015	0.1570	0.1567	0.3684	-0.4056
30	-0.2556	0.4365	0.5050	1.5044	-1.4267	-0.0013	0.1559	0.1556	0.3718	-0.3792
35	-0.2744	0.4975	0.5671	1.7589	-1.6455	-0.0060	0.1550	0.1548	0.3751	-0.3727
40	-0.2908	0.5573	0.6275	1.9082	-1.7081	-0.0098	0.1538	0.1538	0.3992	-0.3664
45	-0.2907	0.6172	0.6810	2.1404	-1.8327	-0.0155	0.1524	0.1529	0.4410	-0.3785
50	-0.2710	0.6600	0.7121	2.1349	-2.0274	-0.0264	0.1528	0.1548	0.4525	-0.4153
60	-0.1848	0.7219	0.7436	2.0828	-2.0300	-0.0440	0.1452	0.1514	0.3997	-0.5031
70	-0.0489	0.8406	0.8402	3.0479	-3.5947	-0.0568	0.1424	0.1530	0.3270	-0.4631
80	-0.0378	1.0100	1.0084	2.4392	-8.7652	-0.0819	0.1544	0.1745	0.2271	-0.8951
90	-0.0446	0.8441	0.8433	2.6172	-1.7681	-0.1071	0.1408	0.1766	0.2617	-0.5066
100	-0.1422	0.8685	0.8782	3.1349	-1.7836	-0.1410	0.1508	0.2063	0.3354	-0.5698
125	-0.9061	0.6516	1.1153	1.4203	-2.6516	-0.2082	0.1565	0.2602	0.3425	-0.8147
150	-1.3861	0.8467	1.6232	1.7757	-3.5694	-0.2576	0.1936	0.3220	0.3309	-1.2424
200	-1.0959	1.0025	1.4837	1.5910	-5.9512	-0.1891	0.2247	0.2933	0.5838	-0.7390

Appendix 45 - Continued

250	-1.0615	1.3451	1.7111	1.5483	-8.0386	-0.1642	0.2427	0.2926	0.7106	-0.9962
300	-1.0219	1.3828	1.7169	2.0864	-7.4696	-0.1325	0.2548	0.2866	0.7924	-0.9741
350	-0.8252	0.8396	1.1759	2.0737	-2.9050	-0.0768	0.2051	0.2185	0.7744	-0.5055
400	-0.8803	1.0525	1.3702	2.6490	-5.9176	-0.0493	0.2203	0.2252	0.6262	-1.0553
500	-0.5119	0.9546	1.0811	2.4689	-2.6176	0.0797	0.2037	0.2183	0.8201	-0.5292
600	0.1138	0.9333	0.9378	3.2934	-2.1002	0.1933	0.2201	0.2924	1.1017	-0.3325
700	0.5608	1.0085	1.1508	4.4187	-1.4639	0.2160	0.2462	0.3269	1.1889	-0.1594
800	0.4177	0.9294	1.0159	4.0295	-1.8956	0.0981	0.1867	0.2103	1.0373	-0.1864
900	0.2102	0.9379	0.9578	1.9764	-2.5735	0.0829	0.1354	0.1583	0.5301	-0.0966
1000	0.5277	0.7497	0.9145	2.2636	-0.7852	0.0904	0.1350	0.1621	0.4164	-0.1408
1250	0.7728	0.6377	0.9995	2.4553	-0.5353	0.1517	0.1267	0.1971	0.5282	-0.0069

Appendix 46: Temperature RMS Error vs Depth in the TOTO with and without Quality Control of HYCOM data

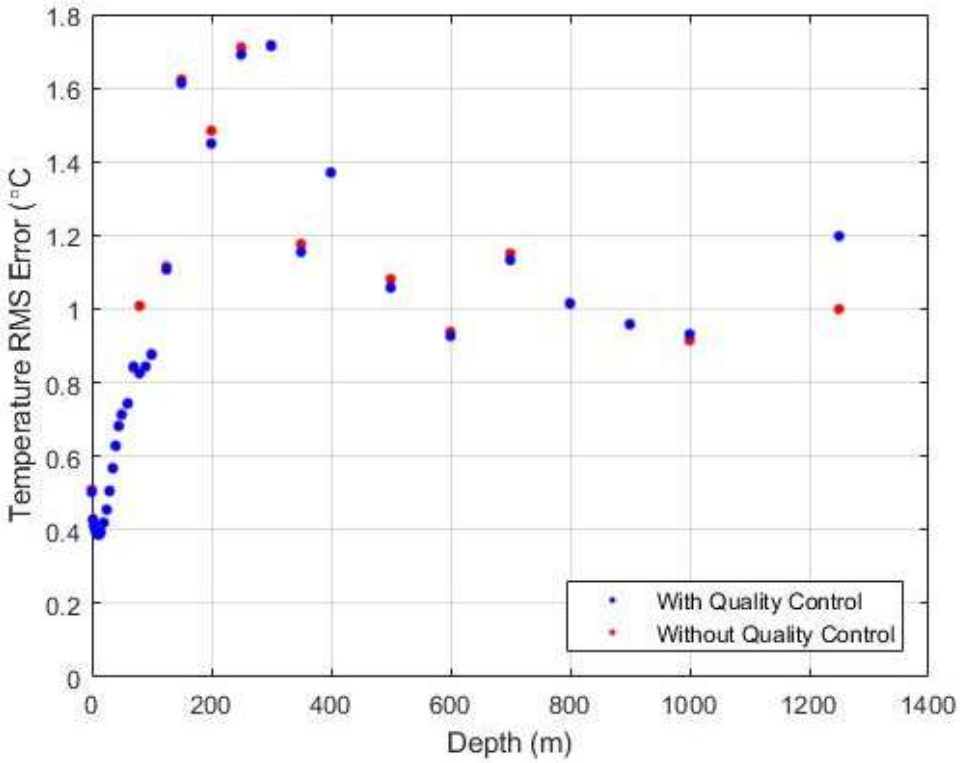

Appendix 47: Salinity RMS Error vs Depth in the TOTO with and without Quality Control of HYCOM data

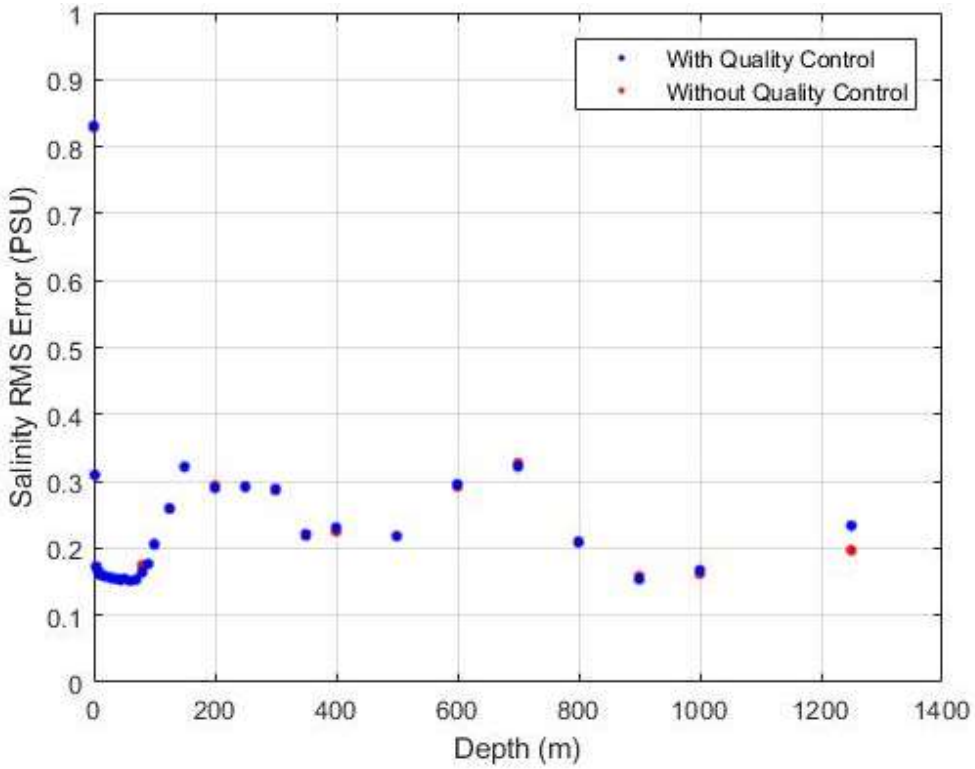

Appendix 48: Statistics Summary of Error as a Function of Month in the TOTO without HYCOM Quality Control Checks

Month	Number of Casts	Temperature					Salinity				
		Mean	Standard Deviation	RMS Error	Maximum	Minimum	Mean	Standard Deviation	RMS Error	Maximum	Minimum
January	**30**	-0.4666	0.6486	0.7987	2.2012	-4.1038	-0.0324	0.1945	0.1971	2.0907	-0.4918
February	**14**	-0.5333	0.7785	0.9429	2.0054	-6.9949	-0.0882	0.2006	0.2189	2.7072	-0.8687
March	**12**	-0.3633	0.7741	0.8542	1.4603	-3.2576	-0.0949	0.1628	0.1883	0.5143	-1.0553
April	**22**	-0.1963	0.8673	0.8886	4.4187	-5.4603	0.0027	0.2141	0.2140	1.1889	-0.8173
May	**13**	-0.4487	1.0862	1.1739	1.5044	-8.0386	-0.0243	0.2894	0.2901	3.9808	-0.9962
June	**17**	-0.2254	0.9923	1.0167	2.1404	-8.7652	-0.0425	0.3160	0.3185	4.2197	-0.8951
July	**24**	-0.2043	0.9755	0.9961	2.4553	-5.2988	0.0072	0.2754	0.2754	4.0432	-0.8147
August	**14**	-0.2344	0.9514	0.9788	2.6172	-3.2641	0.0061	0.2556	0.2554	3.0175	-0.4862
September	**29**	-0.1621	1.0145	1.0268	3.1349	-5.7866	0.0121	0.3211	0.3212	3.2931	-1.2424
October	**21**	-0.1439	0.6789	0.6935	3.2255	-2.8606	0.0399	0.1948	0.1988	1.1017	-0.5292
November	**16**	-0.2840	0.9851	1.0243	2.4912	-6.6479	-0.0154	0.1991	0.1995	0.8008	-0.8094
December	**12**	-0.4168	0.5363	0.6787	1.0286	-2.6289	-0.0352	0.2809	0.2828	3.1792	-0.4641

Appendix 49: Temperature RMS Error vs Month in the TOTO with and without Quality Control of HYCOM data

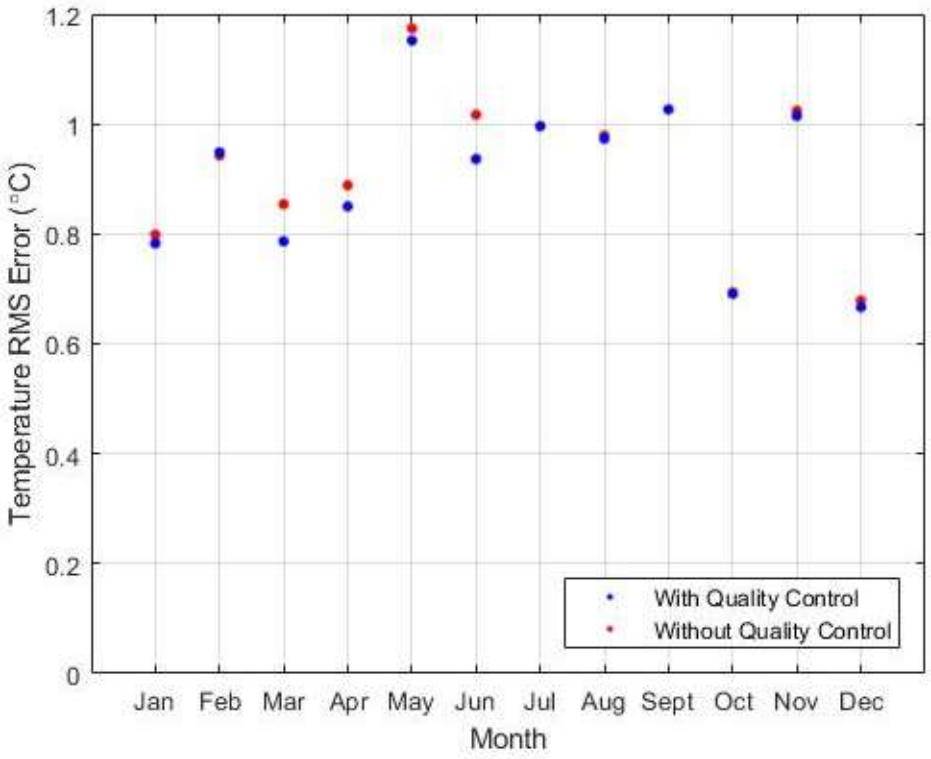

Appendix 50: Salinity RMS Error vs Month in the TOTO with and without Quality Control of HYCOM data

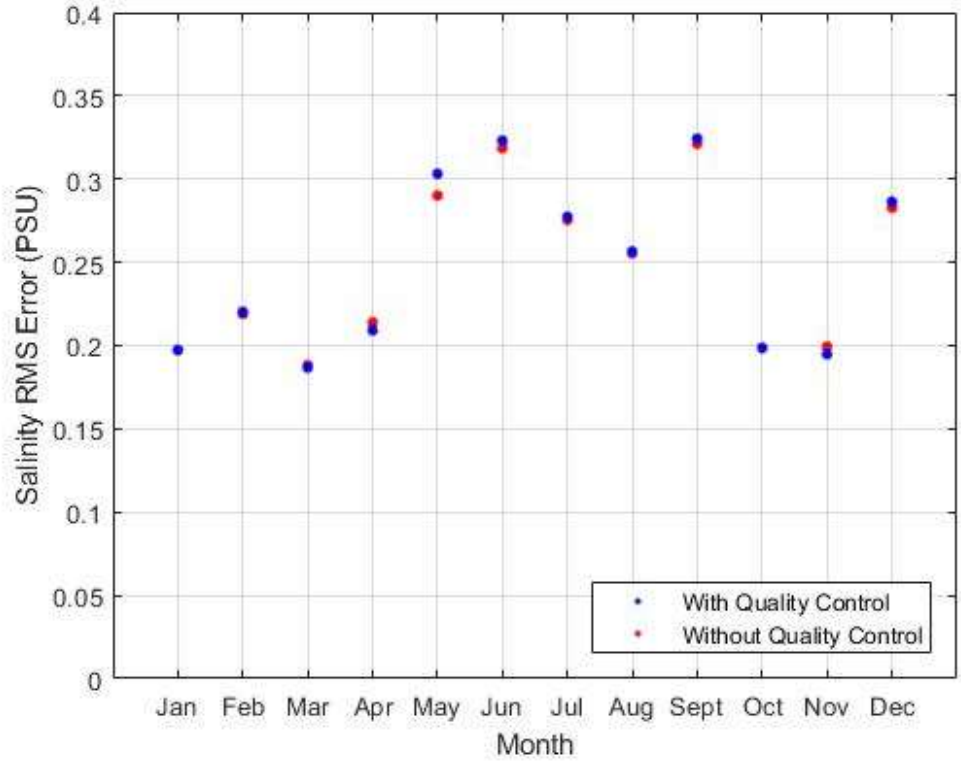

Appendix 51: Statistics Summary of Error as a Function of Year in the TOTO without HYCOM Quality Control Checks

Year	Number of Casts	Temperature					Salinity				
		Mean	Standard Deviation	RMS Error	Maximum	Minimum	Mean	Standard Deviation	RMS Error	Maximum	Minimum
2005	**21**	-0.2447	0.8368	0.8712	3.0479	-6.6479	-0.0880	0.1419	0.1668	0.3492	-0.8094
2006	**67**	-0.3325	0.8718	0.9328	2.7128	-8.7652	-0.0518	0.1767	0.1841	0.4757	-0.8951
2007	**51**	-0.4339	0.9806	1.0720	3.5008	-8.0386	-0.0074	0.3175	0.3175	4.2197	-1.2424
2008	**13**	-0.4688	0.5889	0.7521	0.8897	-2.1478	-0.0256	0.1634	0.1652	0.3958	-1.0553
2009	**3**	-0.3764	0.5576	0.6702	0.4895	-4.1038	-0.1151	0.0885	0.1449	0.1983	-0.4918
2010	**5**	-0.3666	0.6136	0.7132	1.0286	-3.2576	-0.0294	0.3904	0.3904	3.1792	-0.4482
2011	**5**	0.0860	0.7621	0.7647	2.1569	-2.3130	0.1151	0.4291	0.4430	3.2931	-0.4692
2012	**6**	-0.0130	0.5917	0.5904	2.4823	-1.7388	0.0582	0.1891	0.1974	0.5748	-0.3444
2013	**2**	-0.3634	0.5147	0.6269	0.9433	-1.7256	-0.0334	0.1043	0.1088	0.2597	-0.2300
2014	**12**	0.0933	1.0334	1.0364	4.4187	-2.9614	0.1028	0.2707	0.2893	1.1889	-0.4318
2015	**19**	-0.0419	0.8039	0.8043	2.4553	-2.0274	0.1275	0.1735	0.2152	0.7924	-0.1927
2016	**13**	-0.4731	0.9524	1.0625	2.2214	-3.5694	-0.1028	0.2399	0.2608	0.6944	-0.8147
2017	**7**	-0.0793	0.6427	0.6462	2.1698	-2.1198	-0.0994	0.2851	0.3014	2.0907	-0.4056

Appendix 52: Temperature RMS Error vs Year in the TOTO with and without Quality Control of HYCOM data

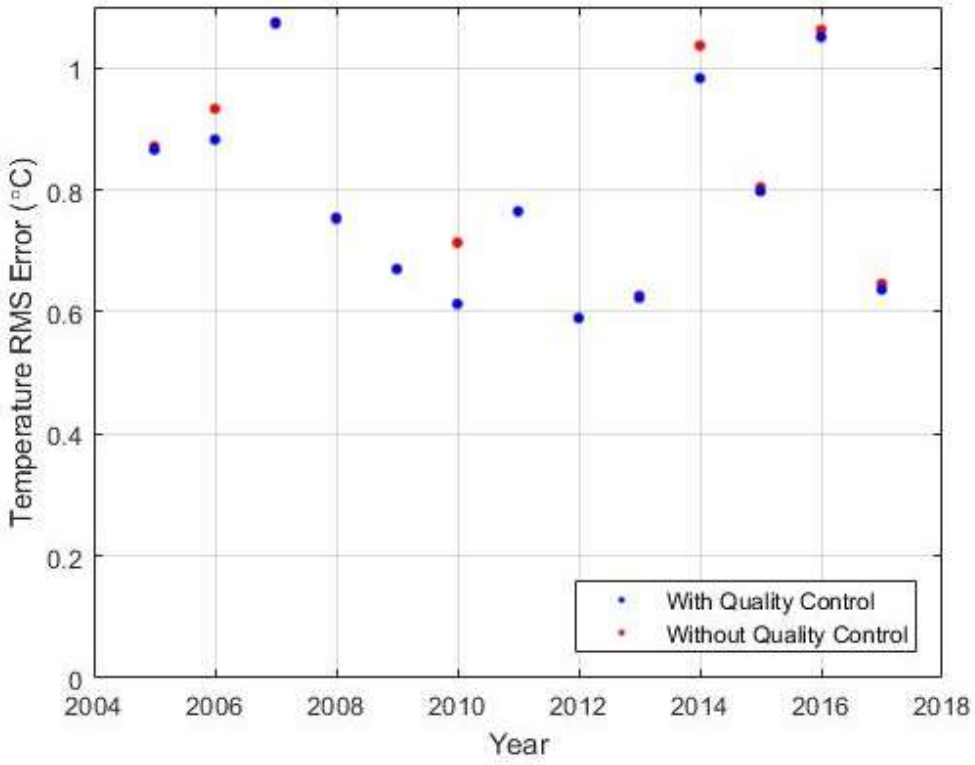

Appendix 53: Salinity RMS Error vs Year in the TOTO with and without Quality Control of HYCOM data

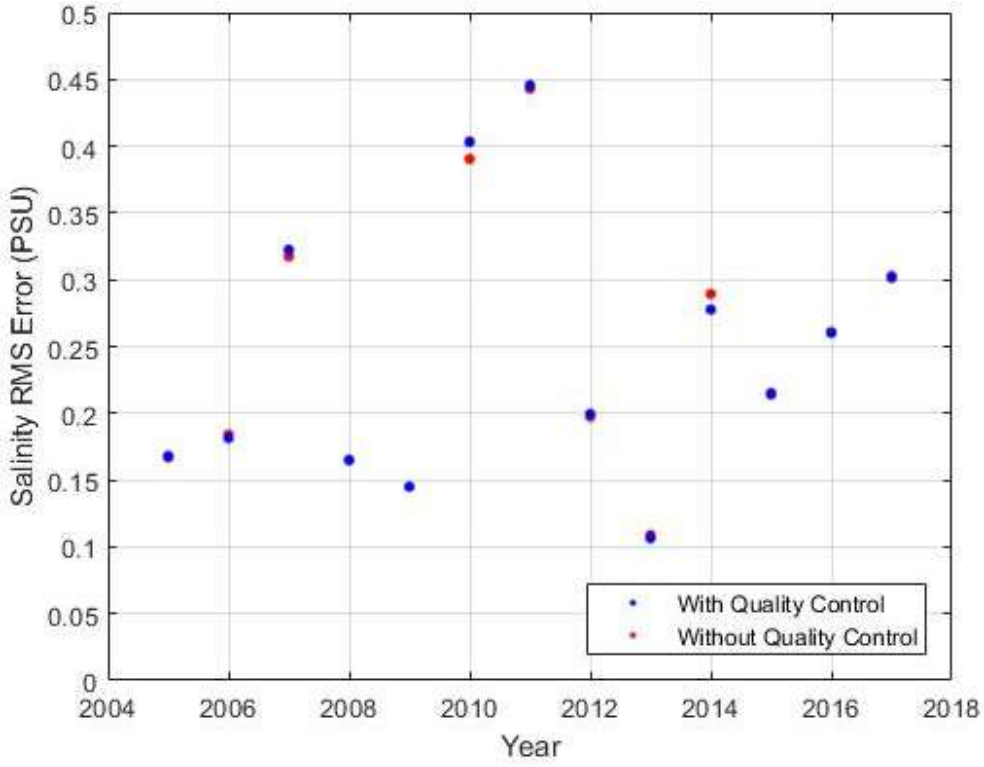

Appendix 54: Statistics Summary of Error as a Function of Experiment in the TOTO without HYCOM Quality Control Checks

Experiment	Number of Casts	Temperature					Salinity				
		Mean	Standard Deviation	RMS Error	Maximum	Minimum	Mean	Standard Deviation	RMS Error	Maximum	Minimum
19.1	**171***	-0.3413	0.8703	0.9347	3.5008	-8.7652	-0.0304	0.2490	0.2509	4.2197	-1.2424
90.9	**6***	-0.2159	0.7274	0.7571	1.7607	-2.9169	-0.0016	0.1890	0.1885	0.4429	-0.4462
91	**5**	0.1484	1.0221	1.0298	4.4187	-1.5755	0.1376	0.2396	0.2757	1.1889	-0.3456
91.1	**29**	-0.0475	0.8609	0.8617	3.2255	-2.9614	0.1005	0.2090	0.2318	1.1017	-0.4318
91.2	**17**	-0.3395	0.9115	0.9719	2.2214	-3.5694	-0.1178	0.2698	0.2942	2.0907	-0.8147

*Four CTD casts overlapped between Experiments 19.1 and 90.9

Appendix 55: Temperature RMS Error vs HYCOM Experiment in the TOTO with and without Quality Control of HYCOM data

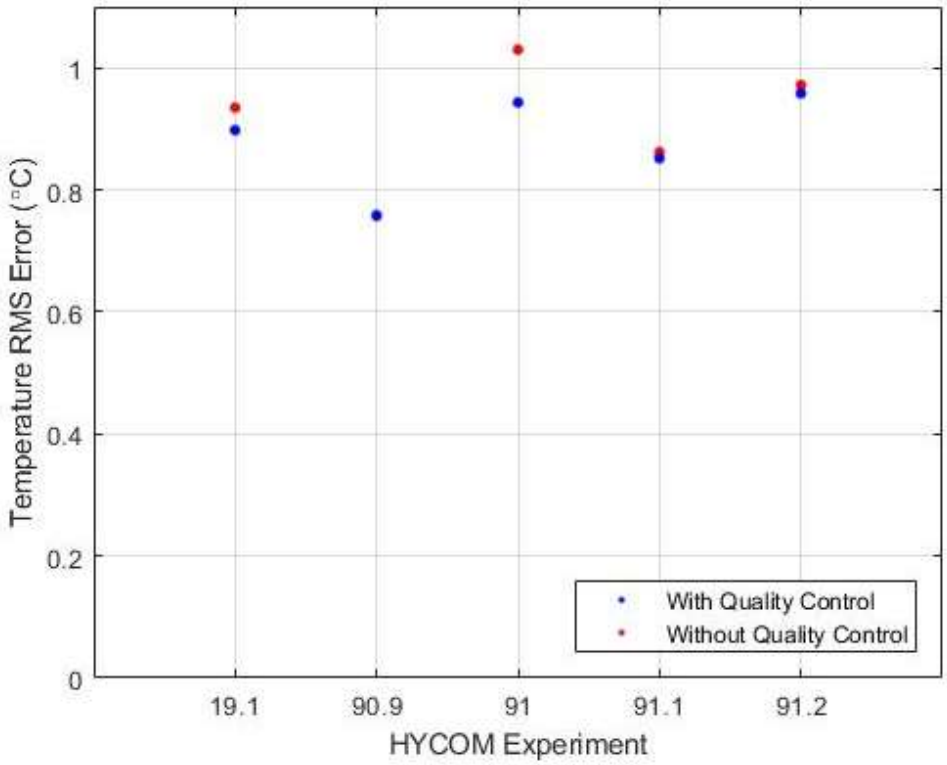

Appendix 56: Salinity RMS Error vs HYCOM Experiment in the TOTO with and without Quality Control of HYCOM data

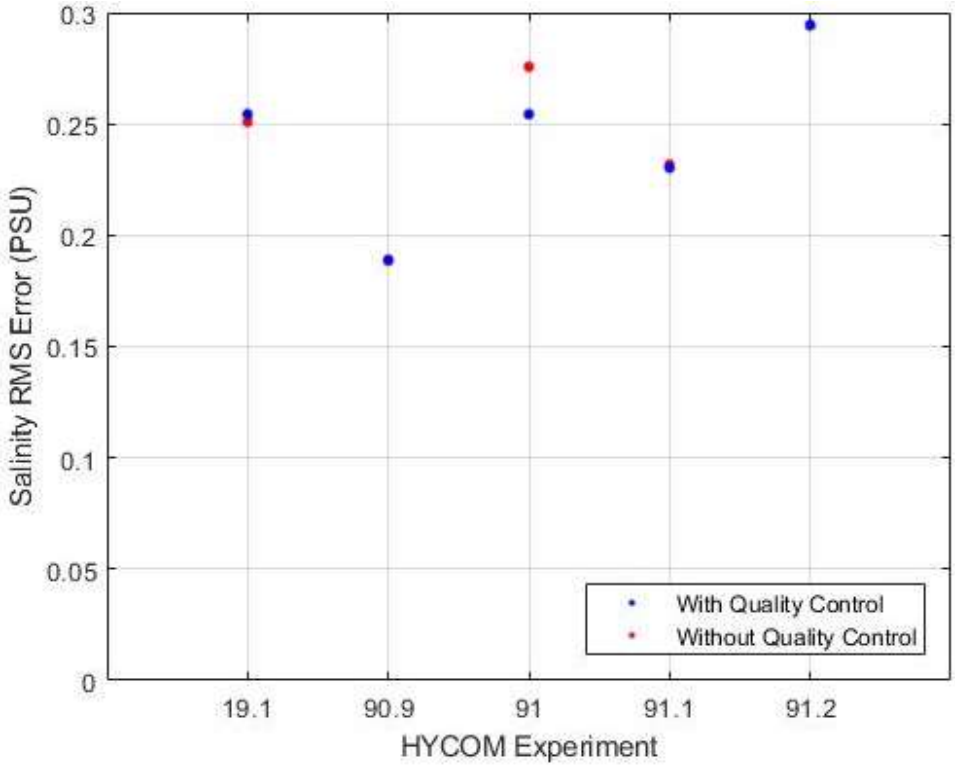

Appendix 57: Comparison of Temperature Difference between Experiments 19.1 and 90.9 of the Global 1/12° HYCOM Model

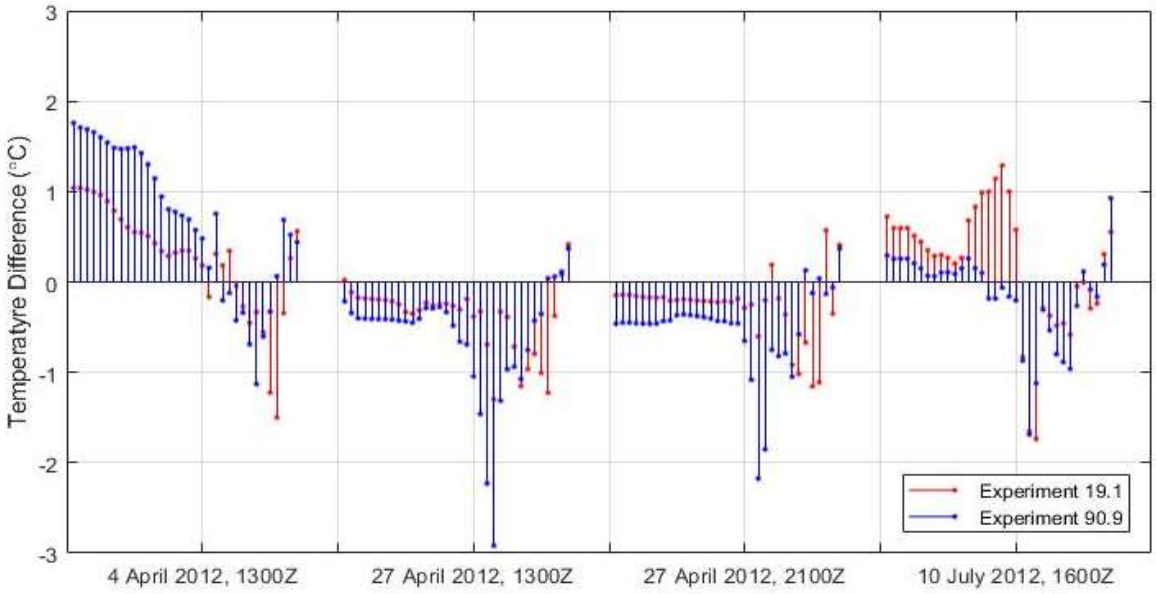

Appendix 58: Comparison of Salinity Difference between Experiments 19.1 and 90.9 of the Global 1/12° HYCOM Model

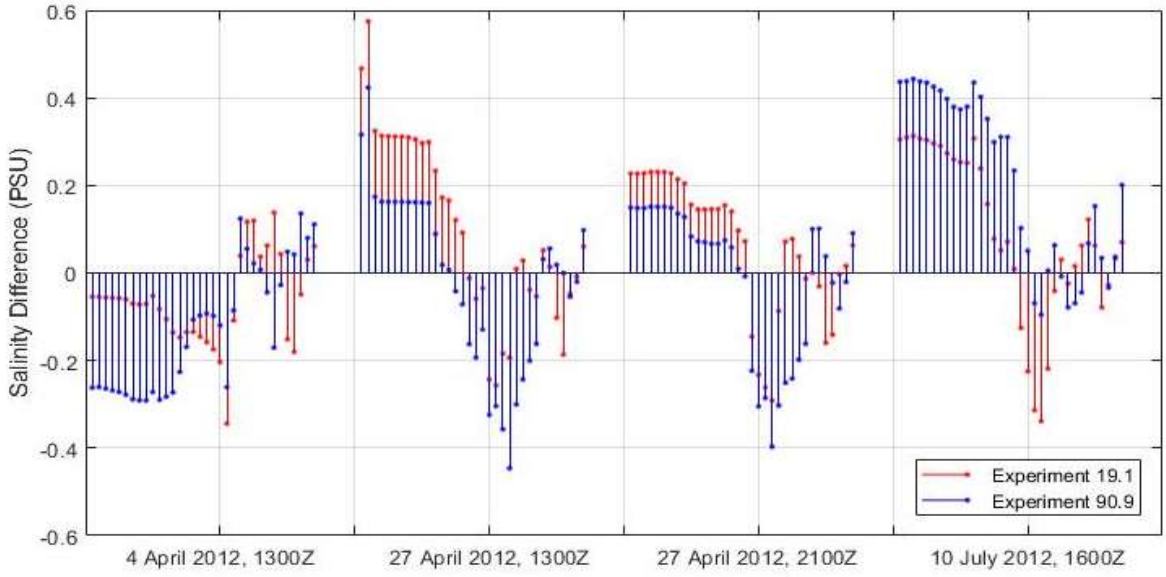

Appendix 59: GAM of Temperature Mean Error as a Function of Depth in the GoM

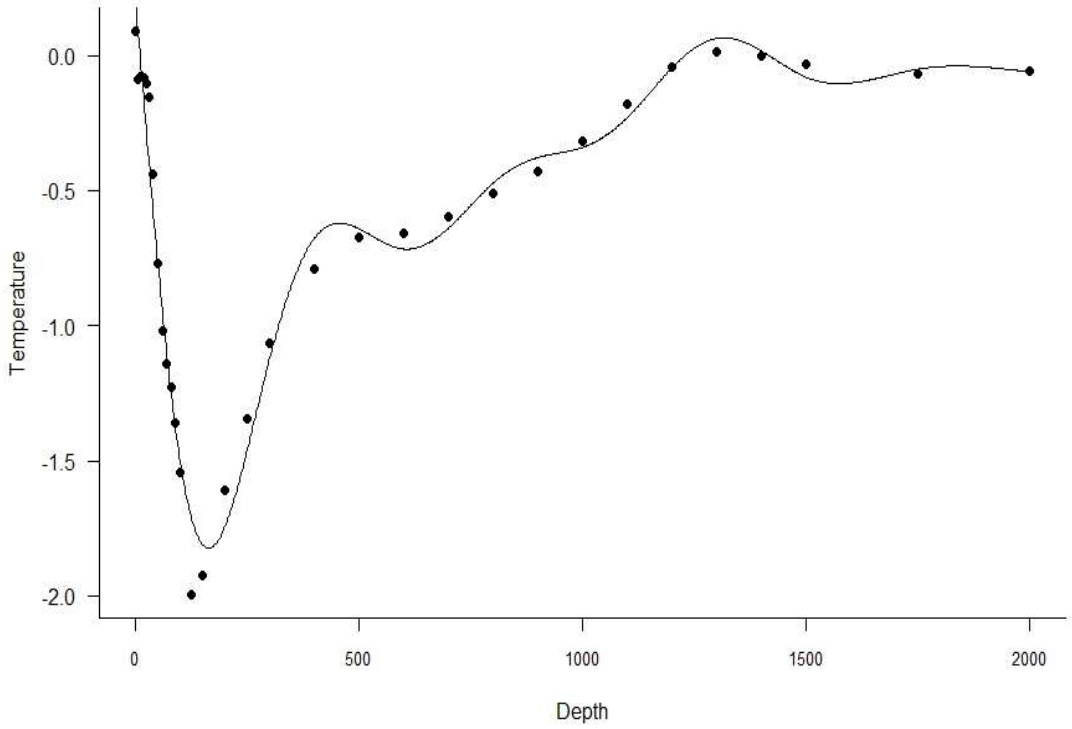

Appendix 60: GAM of Salinity Mean Error as a Function of Depth in the GoM

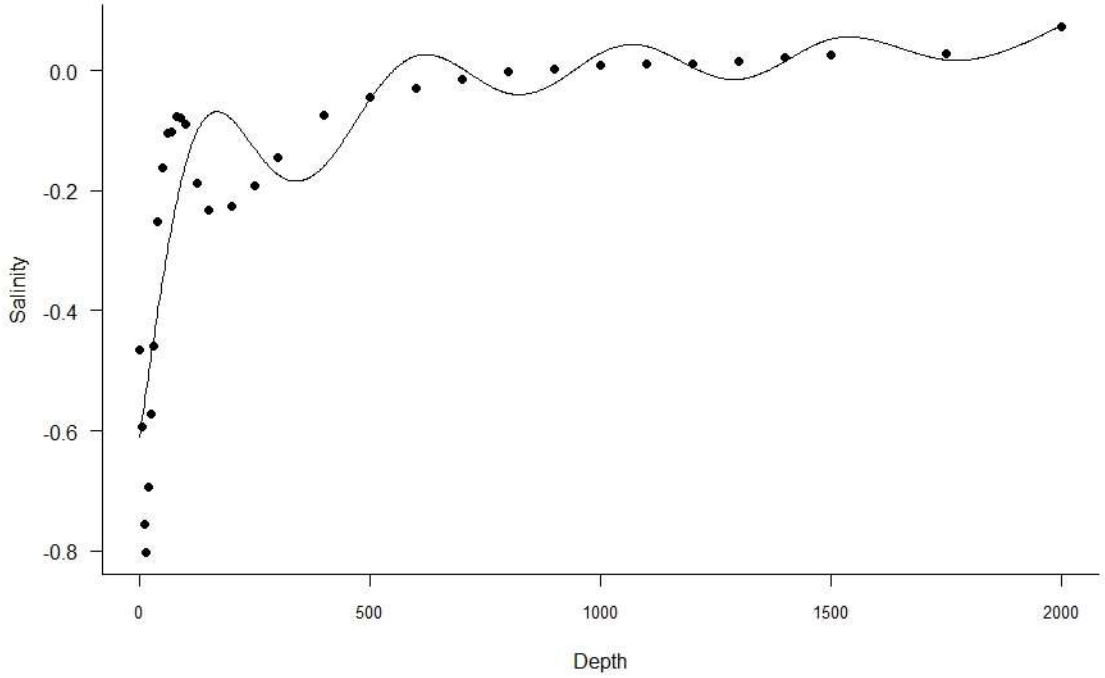

Appendix 61: GAM of Temperature Mean Error as a Function of Depth in the TOTO

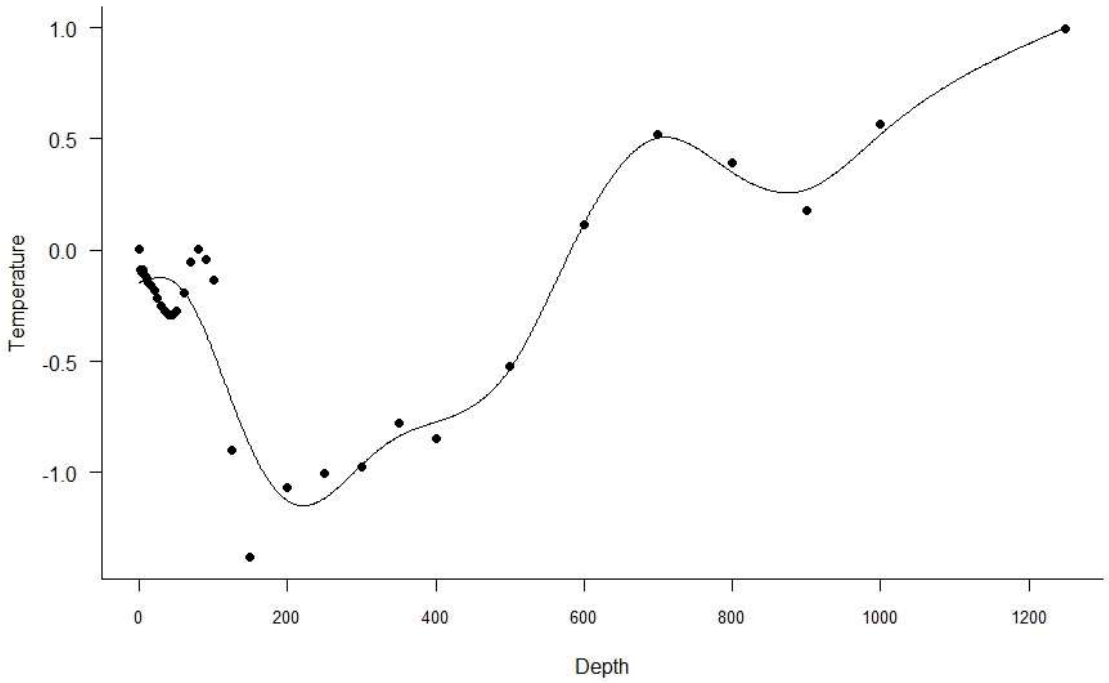

Appendix 62: GAM of Salinity Mean Error as a Function of Depth in the TOTO